

AD-A100 826

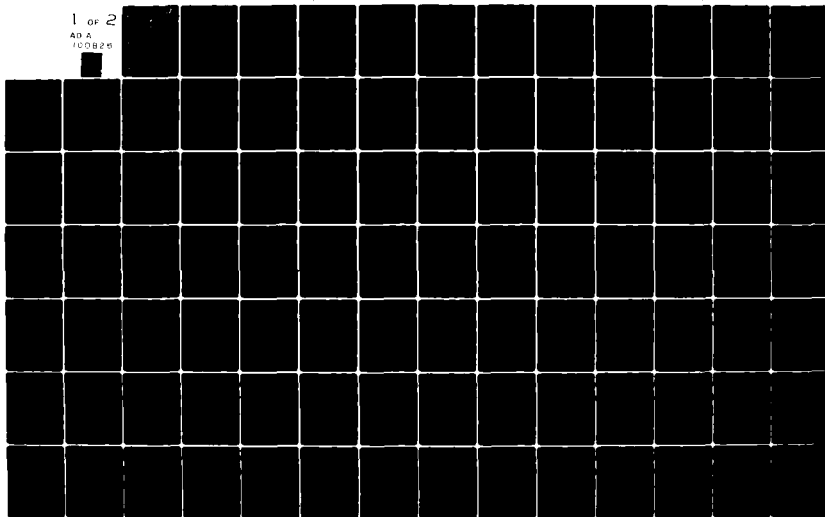
AIR FORCE INST OF TECH WRIGHT-PATTERSON AFB OH SCH00--ETC F/G 17/2.1  
TRANSMISSION LOSS PREDICTION FOR THE AN/TRC-97A OVER A TROPOSPH--ETC(U)  
DEC 80 H S STORY

UNCLASSIFIED AFIT/GE/EE/800-40

NL

1 OF 2

AD A  
100826

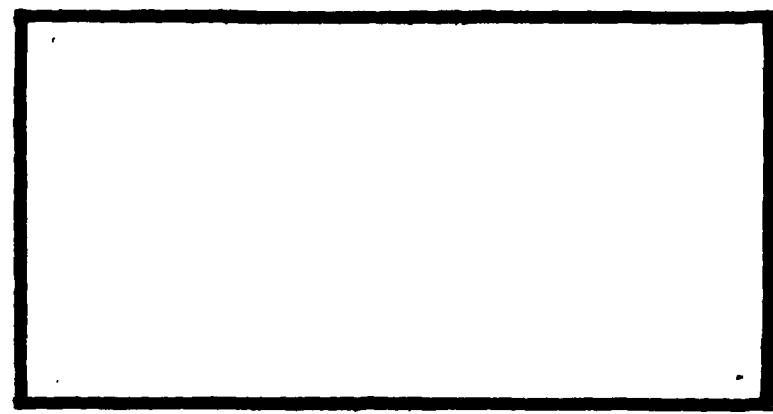


AD 2

AD A100026

0 <sup>BS</sup>

LEVEL II



DTIC FILE COPY

DTIC  
ELECTE  
JUL 1 1981  
S D

DEPARTMENT OF THE AIR FORCE  
AIR UNIVERSITY (ATC)  
**AIR FORCE INSTITUTE OF TECHNOLOGY**

Wright-Patterson Air Force Base, Ohio

DISTRIBUTION STATEMENT A  
Approved for public release;  
Distribution Unlimited

81 6 30 031

AFIT/GE/EE/80D-40

Accession For	
NTIS - COMET	X
DTIC TAB	
Unannounced	
Justification	
By	
DTIC	
AVAIL	
FILE	
A	

TRANSMISSION LOSS PREDICTION  
FOR THE AN/TRC-97A OVER A  
TROPOSPHERIC SCATTER PATH

THESIS

AFIT/GE/EE/80D-40

H. Stephen Story  
Captain USAF

Approved for public release; distribution unlimited

TRANSMISSION LOSS PREDICTION  
FOR THE AN/TRC-97A OVER A  
TROPOSPHERIC SCATTER PATH

THESIS

Presented to the Faculty of the School of Engineering of  
The Air Force Institute of Technology  
Air University  
In Partial Fulfillment of the Requirements for the  
Degree of Master of Science

By

H. Stephen Story, B.S.  
Captain USAF

Graduate Electrical Engineering

December 1980

Approved for public release; distribution unlimited

## PREFACE

-----

This research was motivated by a desire to improve the techniques available to the tactical communicator for predicting the performance of his troposcatter systems. Improving upon the classical prediction techniques was recognized from the outset to be a very broad area of study. Therefore, the first task of this research was to analyze the general troposcatter propagation problem in enough detail to identify specific areas for possible improvement. This initial analysis proved to be much more time consuming than expected but did result in a suitably narrow topic for detailed study: a modified scattering loss model. Subsequent problems with the available path data prevented the evaluation of the coefficients in the model, however. As a result, this research has fallen short of providing an improved prediction algorithm to the engineer in the field. Nevertheless, I believe that the potential for such improvement has been adequately demonstrated and that a promising area for continued research has been identified.

I am indebted to Maj Joseph W. Carl, my advisor, for his guidance throughout this effort. I would like to thank Maj Duane B. Reynolds and Capt Ronnie E. Lesher of the Air Force Communications Command, without whose support this research would not have been possible. I am particularly grateful to the engineers at the 5th Combat Communications Group and the 602d Tactical Air Control Wing for the field

data that they have so willingly provided.

# TABLE OF CONTENTS

	Page
Preface . . . . .	ii
List of Figures . . . . .	vi
List of Tables . . . . .	vii
Notation . . . . .	viii
Abstract . . . . .	xi
I. Introduction . . . . .	1
Background . . . . .	1
Problem . . . . .	2
Scope . . . . .	3
Approach and Presentation . . . . .	4
II. The Troposcatter Path . . . . .	6
III. A General Path Model . . . . .	10
The Algebraic Model . . . . .	11
The Stochastic Model . . . . .	14
IV. The Classical Path Models . . . . .	23
NBS Model . . . . .	24
CCIR Model . . . . .	25
PRC Model . . . . .	26
Norton Model . . . . .	27
Rider Model . . . . .	28
Yeh Model . . . . .	29
AFCSP 100-61 Model . . . . .	29
Collins Model . . . . .	31
V. Comparison of the Classical Models with the General Path Model . . . . .	33
VI. The General Path Model Tailored to the AN/TRC-97A . . . . .	43
Typical Path Model Values for the AN/TRC-97A . . . . .	43
Simplifying Assumptions in the Path Model . . . . .	50
Statistics of the Path Model . . . . .	53

VII.	The Modified Scattering Loss Model . . . . .	59
	Statement of the Regression Problem . . . . .	61
	Evaluation of Available AN/TRC-97A Path Data . . . . .	62
VIII.	Conclusions . . . . .	78
IX.	Recommendations . . . . .	80
	Bibliography . . . . .	82
	Appendix A: AFCSP 100-61 Path Loss Predictions for Eight Hypothetical Path Cases . . . . .	84
	Vita . . . . .	108



# LIST OF FIGURES

Figure -----	Page ----
1 Geometry of the Troposcatter Path . . . . .	8
2 Typical Values in the General Path Model for the AN/TRC-97A . . . . .	44
3 Variation in Path Length with Antenna Elevation . . . . .	54
4 The Received Power Distribution Function, $F(P_r; t)$ . . . . .	69
5 Comparison of Observed Data with the Assumed Power Distribution Function . . . . .	70
6 The Distribution Parameter $ko^2$ as a Function of Path Length . . . . .	75
A1 Case 1 Troposcatter Path Calculation . . . . .	85
A2 Case 2 Troposcatter Path Calculation . . . . .	87
A3 Case 3 Troposcatter Path Calculation . . . . .	89
A4 Case 4 Troposcatter Path Calculation . . . . .	91
A5 Case 5 Troposcatter Path Calculation . . . . .	93
A6 Case 6 Troposcatter Path Calculation . . . . .	95
A7 Case 7 Troposcatter Path Calculation . . . . .	97
A8 Case 3 Troposcatter Path Calculation . . . . .	99
A9 Effective Earth's Radius, $a$ . . . . .	101
A10 Normalized Height of Horizon Ray crossover, $\eta_s$ . . . . .	102
A11 Frequency Gain Function, $H_o$ , for $\eta_s \geq 1$ . . . . .	103
A12 Frequency Gain Asymmetry Function, $\Delta H_o$ . . . . .	104
A13 Frequency Gain Function, $H_o$ , for $\eta_s = 0$ . . . . .	105
A14 Atmospheric Absorption, $A_a$ . . . . .	106
A15 The Climatological Function, $V(d_e)$ . . . . .	107

# LIST OF TABLES

Table	Page
I Classical Path Models in Original Form . . . . .	32
II Classical Path Models Expressed in the Form of the General Path Model . . . . .	42
III Range of Values of Scattering Loss, $L_s$ , for AN/TRC-97A . . . . .	49
IV Observed AN/TRC-97A Troposcatter Paths . . . . .	64

# NOTATION

-----

$a$	Effective earth's radius
$A_a$	Atmospheric absorption loss
$c$	Speed of light
$d$	Path length, total
$d_{lr}$	Path length, receiving station to radio horizon
$d_{lt}$	Path length, transmitting station to radio horizon
$D(t)$	Path length, total
$D_a$	Atmospheric density
$D_a(t)$	Atmospheric density
$E_r(t)$	Received signal voltage
$f$	Frequency
$F_o$	Scattering efficiency
$F(f\theta, l_v)$	Blob size correction factor
$F_v(s)$	Path asymmetry function
$F(\theta d)$	Attenuation function
$G_p$	Effective antenna gain, total
$G_r$	Effective receive antenna gain
$G_{rf}$	Receive antenna gain in free space
$G_t$	Effective transmit antenna gain
$G_{tf}$	Transmit antenna gain in free space
$h_{lr}$	Receive radio horizon altitude
$h_{lt}$	Transmit radio horizon altitude
$h_o$	Horizon ray crossover point altitude
$h_{re}$	Effective receive antenna altitude

$h_{rg}$	Receive station altitude
$h_{rs}$	Receive antenna altitude
$h_{te}$	Effective transmit antenna altitude
$h_{tg}$	Transmit station altitude
$h_{ts}$	Transmit antenna altitude
$H_o$	Frequency gain function
$H_{ot}[(h_{te}/\lambda)\alpha] + H_{or}[(h_{re}/\lambda)\beta]$	Frequency gain function
$L$	System transmission loss
$L_a$	Atmospheric absorption loss
$L_a(t)$	Atmospheric absorption loss
$L_{bms}$	System transmission loss
$L_e$	Equipment loss
$L_{fs}$	Free space loss
$L_{fs}(t)$	Free space loss
$L_{gt}$	Transmit antenna aperture-medium coupling loss
$L_{gt}(t)$	Transmit antenna aperture-medium coupling loss
$L_{gr}$	Receive antenna aperture-medium coupling loss
$L_{gr}(t)$	Receive antenna aperture-medium coupling loss
$L_h$	Ground reflection loss
$L_h(t)$	Ground reflection loss
$L_p$	System transmission loss
$L_s$	Scattering loss
$L_s(t)$	Scattering loss
$L(0.5)$	System transmission loss
$L(50)$	System transmission loss

$N_h$	Path radio refractivity
$N_s$	Surface radio refractivity
$\tilde{N}(t)$	Surface radio refractivity
$P_r$	Received signal power
$\tilde{P}_r(t)$	Received signal power
$P_t$	Transmitted power
$s$	Path asymmetry factor
$s_1$	Path asymmetry factor
$S(t)$	Scattering process
$V(d_e)$	Climatological factor
$\alpha_0$	Effective transmit antenna elevation angle
$\tilde{\alpha}_0(t)$	Effective transmit antenna elevation angle
$\beta_0$	Effective receive antenna elevation angle
$\tilde{\beta}_0(t)$	Effective receive antenna elevation angle
$\Delta H_0$	Frequency gain asymmetry function
$\eta_s$	Normalized horizon ray crossover point altitude
$\theta$	Scatter angle
$\tilde{\theta}(t)$	Scatter angle
$\theta_{er}$	Receive antenna elevation angle
$\theta_{et}$	Transmit antenna elevation angle
$\theta_o$	Scatter angle
$\lambda$	Wavelength

ABSTRACT

-----

This research investigates transmission loss predictions for a short range tactical troposcatter radio system. The analysis is based on the AN/TRC-97A radio set, but the conclusions reached should apply to similar troposcatter systems operating at frequencies from 4.4 to 5.0 GHz and over distances of 160 km or less. A general analysis of the troposcatter path is performed to determine the sensitivity of the transmission loss to the various phenomena which contribute to the loss. That component of the loss which is unique to the scattering process is studied in further detail and a modified scattering loss model is developed. A procedure for determining the coefficients of the scattering loss model based on observed transmission loss is described. A preliminary analysis of the path data available for this research is performed. It is found that the received power probability distribution for the observed paths does not agree with the theoretical distribution in all cases. Further, the available path data is seen to lack sufficiently detailed path geometry information to complete the analysis of the scattering loss model. Recommendations concerning data requirements and continued research are offered.

## I. INTRODUCTION

-----

### Background

-----

Early researchers generally believed that practical radio systems operating at VHF frequencies and above were limited to line of sight applications. Diffraction by the earth's surface was the only mechanism which was recognized to support propagation beyond the horizon at these frequencies, and diffraction theory predicted an exponential decrease in signal strength with distance. With the development of radar during World War II and of television following the war, the body of observed data on such systems expanded rapidly. As the data accumulated a surprising result began to emerge: the signal level beyond the horizon was often much greater than that predicted by diffraction theory alone. The phenomenon which produces this signal enhancement has since come to be known as scatter propagation and may take place in the troposphere, in the ionosphere, or beyond. The subject of this research is scattering within the troposphere, known as tropospheric scatter, or simply troposcatter.

Troposcatter communications systems are now in common use, albeit within a fairly narrow range of applications. They are most suited to situations requiring high quality, multichannel communications beyond the horizon, where intervening terrain is not readily accessible. Distance between ground stations ranges from approximately 80 to 800

km, with typical operating frequencies between 0.1 and 10.0 GHz. Permanently installed troposcatter systems are found in civilian as well as military applications, while transportable troposcatter systems are widely used by today's military forces. Although the fixed and transportable systems share the same basic operating principles, fixed systems are generally characterized by greater transmitted power, larger antennas, and longer radio path distances. Transportable troposcatter systems are designed for rapid deployment in support of tactical ground forces and are generally vehicle mounted. Transportable systems are constrained to less radiated power and smaller antennas, and consequently, shorter communications range.

The ability to accurately predict the performance of a troposcatter system prior to its installation is essential to the effective employment of these systems. The importance of these predictions is particularly acute in the case of tactical systems which must often be installed in unfamiliar terrain in the shortest possible time.

#### Problem

Present troposcatter performance prediction methods produce results which are, in the majority of cases, consistent with observed performance. There remain a significant number of cases, however, where considerable disparity exists between predicted and observed performance. Furthermore, inaccuracies in the predictions seem to be



particularly pronounced for the short transmission paths encountered by tactical systems. The purpose of this research is to investigate the accuracy of present troposcatter performance prediction methods when applied to short range tactical troposcatter systems.

#### Scope

-----

The predominant tactical troposcatter system in the Air Force inventory today is the AN/TRC-97A. This is a 24-channel system using a frequency modulated carrier in the range from 4.4 to 5.0 GHz. The maximum output power is 1000 watts, producing a maximum range of approximately 160 km in the troposcatter mode. The TRC-97A is also capable of operating in line of sight and obstacle gain diffraction modes over shorter distances.

This research is limited to performance prediction for the TRC-97A operating in the troposcatter mode. The alternate line of sight and diffraction modes are not considered. Also, study is limited to "normal" tropospheric scatter propagation; anomalous propagation phenomena such as superrefractive ducting are not considered.

In predicting how a troposcatter system will operate, several parameters may be of interest. Characteristics of the received noise are generally of concern and the delay characteristics of the received signal may be important, particularly for digital systems. In all cases, it is necessary to predict the level of the received signal. This

study is limited to predictions of the received signal level, or alternatively, the transmission loss along the path.

While this research is concerned specifically with the TRC-97A, the results should be applicable to other systems operating in the same frequency range and over similar paths.

#### Approach and Presentation

-----

The stated problem is a very general one: methods of transmission loss prediction presently used to engineer Air Force tactical troposcatter systems are less accurate than desired. How can this very general problem statement be translated into terms specific enough to begin some analysis? Consider some additional facts. The predominant tactical troposcatter system in the Air Force inventory today is the AN/TRC-97A. Two published path prediction methods are used with the TRC-97: Air Force Communications Service Pamphlet 100-61, Volume II, and Technical Order T.O. 31R5-2TRC97-12. Both of these methods were derived from the prediction procedures contained in the National Bureau of Standards (NBS) Technical Note 101. Tactical troposcatter path predictions are therefore based on NBS Technical Note 101.

The technical note presents a somewhat complex model of the troposcatter path. At the time that the model was developed (and still today), theoretical explanations of

troposcatter propagation could not fully account for the transmission loss which was observed over actual paths. Empirical adjustments were incorporated into the model to insure the best agreement with available path data. Note, however, that the TRC-97 operates in the frequency range from 4.4 to 5.0 GHz and with a maximum range of approximately 160 km. The measured path data which influenced the NBS model were predominantly from lower frequencies and/or longer distance paths. It is possible that different empirical adjustments would have resulted if path data more representative of the TRC-97 had been used. If so then two possible approaches come to mind for improving the correlation between the TRC-97 performance and the model: (1) rectify those theoretical deficiencies which made empirical adjustment necessary in the first place, and (2) modify the adjustments so they are tailored to the TRC-97.

The latter approach is adopted in this research. First, the general characteristics of the troposcatter path are described in Section II. Next, a general model of the path is developed in Section III. The "classical" path models are described in Section IV and compared with the general path model in Section V. Section VI tailors the general model to the TRC-97A. Finally, a modified scattering loss model is investigated in Section VII.

## II. THE TROPOSCATTER PATH

-----

The troposphere is the lowest portion of the atmosphere and the region in which virtually all weather phenomena occur. While the boundaries between atmospheric regions are indistinct and highly variable, the troposphere is customarily considered to extend from the surface of the earth to an altitude between 10 and 20 km. The composition of the troposphere is essentially that of the air at ground level, although the density varies with altitude and meteorological conditions. By contrast with the ionosphere (approximately 50 to 500 km), free ions do not exist within the troposphere in sufficient quantities to affect radio wave propagation. Relative to troposcatter radio propagation, the most significant characteristic of the troposphere is its high degree of turbulence.

Present theoretical explanations of the tropospheric scattering phenomenon do not completely account for the observed results. Further, researchers in the area do not fully agree on the underlying physical mechanism, so several theories exist. The earliest, and probably most widely accepted theory is based on turbulent scattering in a medium which is nonhomogeneous in all dimensions (see for example Ref 3). Other theories are based on a scattering medium having a layered structure (nonhomogeneous in two dimensions) or a number of other specialized cases of the nonhomogeneous structure. It is very likely that the true

structure is more complex than that proposed by any of the prominent theories. In any event, this research does not directly depend on a precise statement of the scattering mechanism.

The important geometric parameters in the troposcatter path are illustrated in Figure 1. The smooth earth distance between transmitting and receiving stations is  $d$ . The distance from the transmitting station to its radio horizon is  $d_{lt}$  and the distance from the receiving station to its radio horizon is  $d_{lr}$ .

The altitudes of the transmitting and receiving stations are given by  $h_{tg}$  and  $h_{rg}$  respectively; the altitudes at the center of the transmitting and receiving antennas are  $h_{ts}$  and  $h_{rs}$ . The altitudes at the two radio horizons are given by  $h_{lt}$  and  $h_{lr}$ .

$\theta_{et}$  and  $\theta_{er}$  are the elevation angles (angle relative to the local horizontal) of the transmitting and receiving antennas respectively. The angles  $\alpha_o$  and  $\beta_o$  represent the elevation angles of the transmitting and receiving antennas relative to a straight line between the two antennas. The scattering angle  $\theta_o$  is the angle through which the transmitted signal must be scattered in order for it to reach the receiving antenna. The quantity  $h_o$  is the distance between the straight line between antennas and the horizon ray crossing point. The effective earth's radius,  $a$ , is that imaginary value which would permit the normally curved (because of refraction through the atmosphere) radio

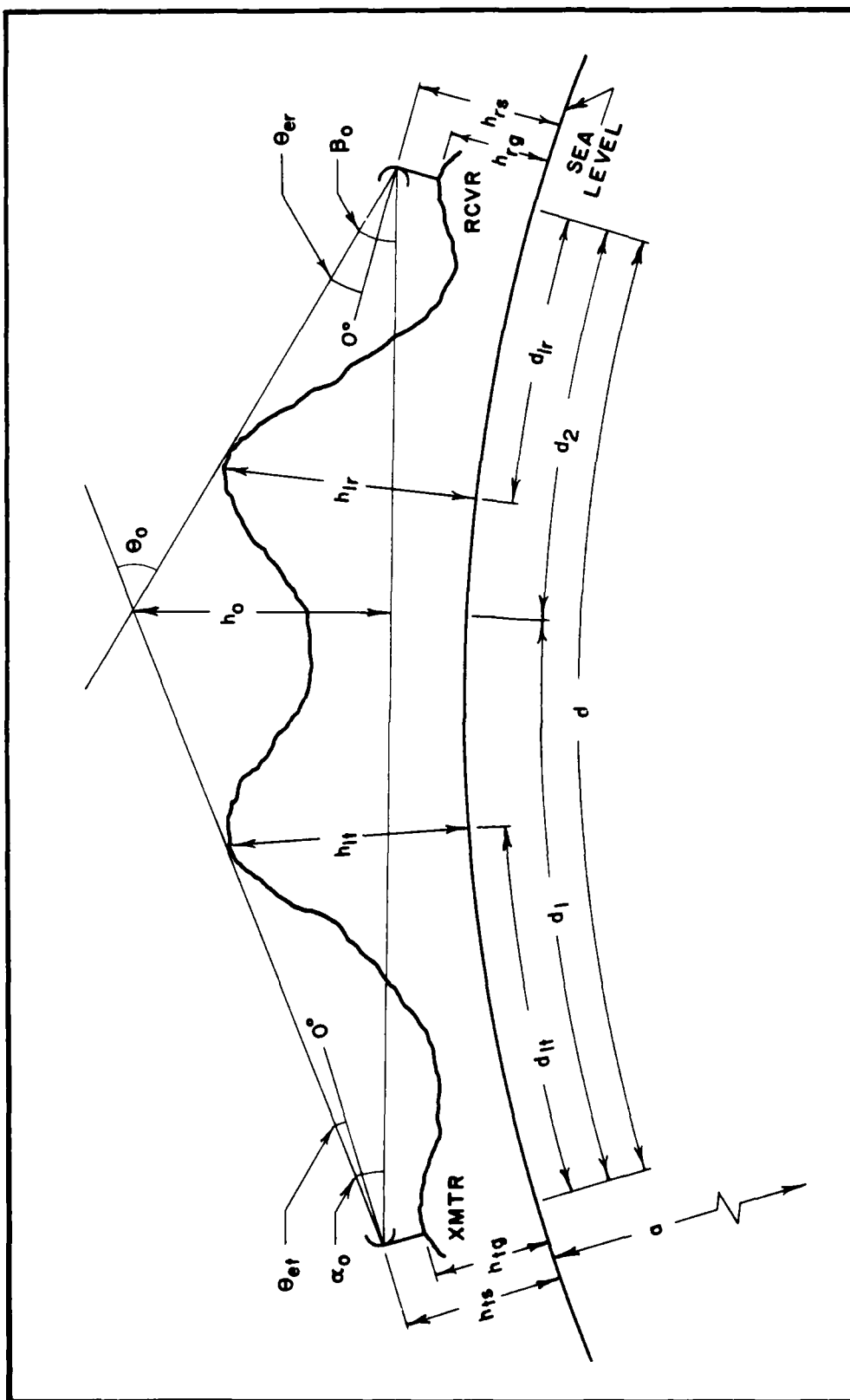


Figure 1. Geometry of the Troposcatter Path

rays to be represented as straight lines, and is a function of the true earth's radius and the radio refractivity.

### III. A GENERAL PATH MODEL

-----

The first major research goal is to obtain a suitable model of transmission loss along the troposcatter path. Ideally, the model will be in a form that can be related to the prediction methods presently employed by Air Force engineers. Ideally, the model will also remain as general as possible in order for the research results to have the widest applicability.

As pointed out in the previous section, the most notable characteristic of the troposcatter path is its great variability in both time and space. Thus, to be fully characterized, the path must be modeled by a stochastic process. The path model developed here begins at an elementary level with an emphasis on the distinct phenomena which influence the path. Initially the model is so general that random influences are not easily distinguished from deterministic influences. Therefore a preliminary algebraic model is developed first. Only at this point is it clear precisely what the path influences are, and whether or not they are random influences. Then the algebraic model is transformed into a stochastic model, taking account of the random influences previously identified.



## The Algebraic Path Model

-----

Beginning in very simple terms, the relation between transmitted power and received power along the path can be expressed as

$$P_r = P_t + G_t + G_r - L \quad (1)$$

where

$P_r$  = received power, dbm

$P_t$  = transmitted power, dbm

$G_t$  = effective transmit antenna gain, db

$G_r$  = effective receive antenna gain, db

$L$  = system loss, db

The effective antenna gains,  $G_t$  and  $G_r$ , can themselves be expressed as

$$G_t = G_{tf} + L_{gt} \quad (2)$$

and

$$G_r = G_{rf} + L_{gr} \quad (3)$$

where

$G_{tf}$  = transmit antenna gain in free space,  
relative to an isotropic radiator, db

$G_{rf}$  = receive antenna gain in free space,  
relative to an isotropic radiator, db

$L_{gt}$  = transmit antenna aperture-medium coupling  
loss, db

$L_{gr}$  = receive antenna aperture-medium coupling  
loss, db

The free space isotropic antenna gains,  $G_{tf}$  and  $G_{rf}$ , are the measures of antenna gain most frequently stated in manufacturers' literature. This measure of gain assumes that all components of the transmitted signal arrive at the receiving antenna from the same direction and in phase coherence, as would be the case if the antennas were operating in free space. When the antennas are in a medium other than free space this coherence of the signal is subject to distortion. Over a troposcatter path components of the transmitted signal may be scattered from any point within the scattering volume. The signal arriving at the receive antenna appears to originate at a large number of points within the scatter volume, all at different angles to the antenna centerline. The gain of the antenna is reduced when the received signal arrives from a direction other than along the antenna's centerline. The net effect of this noncoherent signal on the antenna can be represented as a reduction in its free space gain, and is generally referred to as aperture-to-medium coupling loss, or loss in antenna gain.

The system loss,  $L$ , represents the combined effect of several distinct phenomena on the transmitted signal. For the troposcatter path it appears that all of the loss

components can be accounted for by the expression

$$L = L_{fs} + L_s + L_h + L_a + L_e \quad (4)$$

where

- $L$  = system loss, db
- $L_{fs}$  = free space loss, db
- $L_s$  = scattering loss, db
- $L_h$  = ground reflection loss, db
- $L_a$  = absorption loss, db
- $L_e$  = equipment loss, db

Free space loss,  $L_{fs}$ , is the reduction in power density of an expanding wavefront with distance as it travels through free space. Scattering loss,  $L_s$ , is that loss which is attributable to the scattering phenomena within the troposphere. The ground reflection loss,  $L_h$ , occurs when signal components reflected from the terrain in the near-field of the receive antenna arrive at the antenna out of phase with the direct components to cause partial signal cancellation. The absorption loss,  $L_a$ , results when signal energy is dissipated as heat when the signal interacts with the molecules within the atmosphere. The equipment loss,  $L_e$ , is that loss which occurs between the transmitter and transmit antenna, and between the receiver and receive antenna.

Combining Eqs (1), (2), (3), and (4) gives

$$P_r = P_t + (G_{tf} - L_{gt}) + (G_{rf} - L_{gr}) - (L_{fs} + L_s + L_h + L_a + L_e) \quad (5)$$

Rearranging Eq (5) into the somewhat more mnemonic form

$$(\text{Power Difference}) = (\text{System Gains}) - (\text{System Losses})$$

gives

$$P_r - P_t = G_{tf} + G_{rf} - (L_{gt} + L_{gr} + L_{fs} + L_s + L_h + L_a + L_e) \quad (6)$$

#### The Stochastic Path Model

Discussion to this point has introduced the nondeterministic nature of the troposcatter path. Such a characteristic is not surprising when the variability of the scattering medium is considered. In the previous section, a phenomena-oriented path model is developed without attempting to account for the random characteristics of the path. This approach is appealing from the standpoint of simplicity and emphasis on the general physical phenomena which affect the troposcatter transmission. Indeed, as development of the algebraic model was begun (Eq (1)), received power was characterized simply as a function of transmitted power, antenna gains, and nonspecific system losses. Without some further knowledge of these system losses, discussion of random influences is not very satisfying. Working from Eq (6), however, the losses associated with specific physical phenomena can be isolated

and the randomness appropriate to these phenomena can be introduced.

In attempting to differentiate between random and deterministic influences, one is quickly confronted with a dilemma: if observed in sufficient detail, any physical event can be considered random in some respect. However, the randomness of certain factors may be on such a small scale relative to other factors, that the randomness may be ignored without significant loss of accuracy. This is assumed to be the case for several terms in the troposcatter path model. Following are the notation conventions which are used for random quantities.

The random variable whose possible outcomes are

$$\{\xi_1, \xi_2, \dots, \xi_i\}$$

is given by

$$\tilde{X}(\xi)$$

which is generally simplified to  $\tilde{X}$  when clarity is not compromised. The value which the random variable  $\tilde{X}$  takes on for a specific outcome  $\xi_k$  is represented by the deterministic quantity  $x_k$ , or more simply,  $x$ . The distribution and density functions of the random variable  $\tilde{X}$  are given by

$$\tilde{F}_X(x) \text{ and } \tilde{f}_X(x)$$

respectively, and are generally simplified to  $F(x)$  and  $f(x)$ .

The stochastic process representing a family of time functions of the possible outcomes

$$\{\omega_1, \omega_2, \dots, \omega_n\}$$

is given by

$$\underline{X}(t, \omega)$$

which is generally simplified to  $\underline{X}(t)$ .

Consider, then, the algebraic path model given by Eq (6). The received power,  $P_r$ , is a function of the remaining terms, and derives its randomness from them.

The envelope, or average transmitted power,  $P_t$ , is assumed to be constant for a given radio path. Since frequency modulation is almost universally used as the RF modulation technique in troposcatter systems, envelope power is independent of the modulating signal. Fluctuations in the output power due to varying equipment parameters are considered to be negligible.

The free space antenna gains,  $G_{tf}$  and  $G_{rf}$ , are functions of the size and shape of the antennas, as well as the operating frequency. Thus, for a particular antenna, free space gain depends only upon frequency. Furthermore, the range of possible operating frequencies of a given troposcatter system is normally narrow enough that variation in free space antenna gain is only considered to be negligible (see for example, Ref 1: 5.20); such an assumption is made here.

In the previous section, it is shown that the aperture-medium coupling losses,  $L_{gt}$  and  $L_{gr}$ , are a result of scattering of the transmitted radio energy within the troposphere and the resultant noncoherence of the energy when it reaches the receiving antenna. The scattering mechanism has already been shown to depend on a number of highly variable parameters of the troposphere, such as wind velocity and refractive index gradient. Thus, it is intuitively appealing to consider the scattering mechanism to be represented by a stochastic process, and it will be seen that such a representation is well born out by other researchers. Even if this were not the case, however, no generality is lost by a random process representation. Denoting the scattering mechanism by the stochastic process

$$\tilde{S}(t, \mathbf{r}) \text{ or } \tilde{S}(t)$$

then the aperture-medium coupling losses can be expressed as functions of free space antenna gain and the scattering process:

$$\tilde{L}_{gt}(t) = g_1[G_{tf}, \tilde{S}(t)] \quad (7)$$

and

$$\tilde{L}_{gr}(t) = g_1[G_{rf}, \tilde{S}(t)] \quad (8)$$

The free space loss,  $L_{fs}$ , can be expressed as

$$L_{fs} = \left[ \frac{4\pi d}{\lambda} \right]^2 \quad (9)$$

where

$d$  = path length

$\lambda$  = wavelength of transmitted signal

and  $d$  and  $\lambda$  are in like units. (Ref 5: 101) Making use of the equality

$$\lambda = \frac{c}{f} \quad (10)$$

where

$\lambda$  = wavelength

$f$  = frequency

$c$  = speed of light

an alternate expression of the free space loss is

$$L_{fs} = \left[ \frac{4\pi fd}{c} \right]^2 \quad (11)$$

The speed of light is constant and the frequency is taken as the carrier frequency of the radio system, which is also assumed constant for a given path. The path length, however, clearly varies as a result of the scattering; components of the transmitted radio energy which are scattered from different points within the scattering volume will in general travel different distances to reach the receiving antenna. The sensitivity of  $L_{fs}$  to variations in  $d$  caused by this scattering depends on the geometry of the



radio path. For the present, however, the free space loss is taken to be a function of the operating frequency and effective path length,  $\underline{D}(t)$ :

$$\underline{L}_{fs}(t) = g_2[f, \underline{D}(t)] \quad (12)$$

where the effective path length is in turn a function of horizon ray path distance,  $d$ , and the scattering:

$$\underline{D}(t) = g_3[d, \underline{S}(t)] \quad (13)$$

By definition the scattering loss,  $L_s$ , is that portion of the transmission loss which is directly attributable to the scattering mechanism. As a minimum, then,  $L_s$  would be expected to be a function of  $S(t)$ . As is shown in the next section, other researchers generally agree that  $L_s$  can be expressed in terms of path length, frequency, scattering angle, and refractivity. It is therefore postulated that

$$\underline{L}_s(t) = g_4[f, \underline{D}(t), \underline{\theta}(t), \underline{N}(t)] \quad (14)$$

where

$f$  = frequency

$\underline{D}(t)$  = path length

$\underline{\theta}(t)$  = scattering angle

$\underline{N}(t)$  = radio refractivity

$\underline{D}(t)$  can in turn be expressed as a function of the horizon ray path length,  $d$ , and the scattering process, as given by Eq (13).

Similarly,  $\theta(t)$  is a function of horizon ray scattering angle,  $\theta$ , and scattering:

$$\theta(t) = g_6[\theta, S(t)] \quad (15)$$

and  $N(t)$  is a function of radio refractivity along the horizon ray,  $N_h$ , and the scattering:

$$N(t) = g_7[N_h, S(t)] \quad (16)$$

The ground reflection loss,  $L_h$ , is basically a function of frequency and the geometry of the path. As has already been seen, however, the path geometry is dependent upon the random variations in the scattering process. As a minimum, then, it appears justified to treat the ground reflection loss as a random process itself,  $L_h(t)$ . Rice, et al. (Ref 9: 9.3-9.4) have derived an expression for this loss expressed in terms of frequency, path length, scattering angle, antenna heights, and antenna elevation angles. Based on these results,  $L_h(t)$  can be expressed as

$$L_h(t) = g_8[f, D(t), \theta(t), \alpha(t), \beta(t), h_{te}, h_{re}] \quad (17)$$

where

$f$  = frequency

$D(t)$  = path length

$\theta(t)$  = scattering angle

$\alpha(t)$  = radio wave departure angle

$\beta(t)$  = radio wave arrival angle

$h_{te}$  = effective transmit antenna height

$h_{re}$  = effective receive antenna height

In this expression,  $\underline{D}(t)$  and  $\underline{\theta}(t)$  are as given above and arrival angles depend upon the scattering mechanism and the center-ray elevation angles of the transmit and receive antennas,  $\alpha_0$  and  $\beta_0$ , respectively:

$$\underline{g}(t) = g_9[\alpha_0, \underline{S}(t)] \quad (18)$$

$$\underline{g}(t) = g_{10}[\beta_0, \underline{S}(t)] \quad (19)$$

Atmospheric absorption loss depends upon frequency (certain frequencies are more readily absorbed than others), path length, and density of the atmosphere along the path. As above, path length depends upon the scattering process (Eq (13)). The atmospheric density,  $D_a$ , is similarly influenced by many of the same factors which produce the scattering phenomenon. The absorption loss then can be expressed as

$$\underline{L}_a(t) = g_{11}[f, \underline{D}(t), \underline{D}_a(t)] \quad (20)$$

where

$f$  = frequency

$\underline{D}(t)$  = path length

$\underline{D}_a(t)$  = atmospheric density

and  $\underline{D}_a(t)$  is itself a function of the scattering process:

$$\underline{D}_a(t) = g_{12}[\underline{S}(t)] \quad (21)$$

The equipment loss,  $L_e$ , represents losses within the transmitting and receiving equipment, and is composed principally of waveguide losses. It is assumed that for a given equipment configuration, this loss is constant.

Combining the above results gives the following stochastic model, which parallels the algebraic model in Eq (6):

$$P_r(t) - P_t = G_{tf} + G_{rf} - [L_{gt}(t) + L_{gr}(t) + L_{fs}(t) + L_s(t) + L_h(t) + L_d(t) + L_e] \quad (22)$$

Nothing has been said thus far concerning the statistics of the various random quantities discussed above. This is the subject of further discussion in Section VI as the general model of Eq (22) is tailored to the TRC-97. Based on the functional relationships described above, however, one would expect the statistical dependence among the terms of Eq (22) to be rather complex.

#### IV. THE CLASSICAL PATH MODELS

---

Several path models have been mentioned so far. The model in AFCSP 100-61 (Vol II) is primarily derived from the NBS model, but it contains an additional term taken from another model published by the International Radio Consultative Committee (CCIR). The model in T.O. 31R5-2TRC97-12, also known as the Collins model, is also based on the NBS model, but it contains additional terms derived directly from experiments with the TRC-97. In fact there is a small family of models which are similar in form, yet are considered in the literature to be more or less distinct models.[1]

Following is a brief description of these models, with a summary appearing in Table I on page 31. The models are stated using the notation in which they were originally published.

---

[1] Other models exist which differ sufficiently in form as to be excluded from this 'family'. Notable is the model published by Pusone (Ref 7: 67-69).

# NBS Model -----

$$L(0.5) = 30 \log f - 20 \log d + F(\theta d) + F_o + H_o + A_a - V(d_e) \quad (23)$$

where

$L(0.5)$  = long-term median transmission loss, db

$f$  = frequency, MHz

$d$  = path length, km

$F(\theta d)$  = attenuation function, db

$F_o$  = scattering efficiency, db

$H_o$  = frequency gain function, db

$A_a$  = atmospheric absorption, db

$V(d_e)$  = climatological factor, db

This model was developed at the Central Radio Propagation Laboratory of the National Bureau of Standards (NBS) and is probably the most widely known and used model today. It is the basis for NBS Technical Note 101 (Ref 9, 10), published in 1965, which provides detailed procedures for predicting the path loss over a troposcatter path. The NBS model is the basis for the prediction methods in both AFCSP 100-61, Vol II (Ref 11) and F.O. 31R5-2TRC97-12 (Ref 12).

#### CCIR Model

-----

$$L(50) = 30 \log f - 20 \log d + F(\theta d) - G_p - V(d_e) \quad (24)$$

where

$$G_p = G_t + G_r - .07 \exp \{ .055 (G_t + G_r) \}$$

and

$L(50)$  = long-term median transmission loss, db

$f$  = frequency, MHz

$d$  = path length, km

$F(\theta d)$  = attenuation function, db

$G_p$  = effective antenna gain, db

$V(d_e)$  = climatological factor, db

$G_t$  = transmit antenna free space gain, db

$G_r$  = receive antenna free space gain, db

The model published by the International Radio Consultative Committee (CCIR) (Ref 8: 200) was adapted largely from the NBS model. The CCIR simplified the NBS model by eliminating the terms  $F_o$ ,  $H_o$ , and  $A_a$ , which were felt by the CCIR to be of only minor significance. They also added a term for the aperture-medium coupling loss, which was not explicitly included in the NBS work.

PRC Model

$$L(50) = 124.6 + 30 \log f + 30 \log \theta + 10 \log d + f(H) - .08 (N_s - 323) - G_p \quad (25)$$

where

$$f(H) = 20 \log (5 + .3H) + .65H$$

$$H = (S\theta d/4)$$

$$S = (4S_1)/(1 + S_1)^2$$

$$S_1 = d_1/d_2$$

$$G_p = G_t + G_r - .07 \exp [.055 (G_t + G_r)]$$

and

$L(50)$  = long term median transmission loss, db

$F$  = frequency, MHz

$d$  = path length, km

$N_s$  = surface radio refractivity

$G_p$  = effective antenna gain, db

$\theta$  = scatter angle, radians

$d_1$  = distance from the horizon ray crossing point to the transmitting antenna, km  
(see figure 1)

$d_2$  = distance from the horizon ray crossing point to the receiving antenna, km  
(see figure 1)

$G_t$  = transmit antenna free space gain, db

$G_r$  = receive antenna free space gain, db



This model has been developed by the People's Republic of China (PRC) and is published by the CCIR (Ref 3: 201) as an alternate method of transmission loss prediction.

#### Norton Model

$$\begin{aligned}
 L_{bms} = & 30 \log f + 30 \log d + 50 \log \theta - F_v(s) \\
 & + F(f\theta, l_v) + H_{ot}[(h_{te}/\lambda)^\alpha] + H_{or}[(h_{re}/\lambda)^\beta] \\
 & - .156 (N_s - 308) + 126 \quad (26)
 \end{aligned}$$

where

$L_{bms}$  = long-term median transmission loss, db

$f$  = frequency, MHz

$d$  = path length, statute miles

$\theta$  = scatter angle, radians

$F_v(s)$  = asymmetry function, db

$F(f\theta, l_v)$  = blob size correction factor, db

$H_{ot}[(h_{te}/\lambda)^\alpha] + H_{or}[(h_{re}/\lambda)^\beta]$

= frequency gain function, db

$N_s$  = surface refractivity

The Norton model (Ref 4: 44) is the earliest of this group of models and has had considerable influence on the others.

Note that in Norton's notation,  $H_{ot}[(h_{te}/\lambda)^\alpha]$  denotes " $H_{ot}$ , a function of  $[(h_{te}/\lambda)^\alpha]$ " rather than an algebraic expression involving  $H_{ot}$ ; similarly  $H_{or}[(h_{re}/\lambda)^\beta]$  represents " $H_{or}$ , a function of  $[(h_{re}/\lambda)^\beta]$ ." For ease of notation we will define

$$H_o = H_{ot} [(h_{te}/\lambda)^\alpha] + H_{or} [(h_{re}/\lambda)^\beta]$$

This appears to be precisely the substitution made by the authors of Technical Note 101.

#### Rider Model

$$\begin{aligned} L_{bms} = & 30 \log f + 30 \log d + 50 \log \theta - F_v(s) \\ & + F(f\theta, l_v) + H_{ot} [(h_{te}/\lambda)^\alpha] + H_{or} [(h_{re}/\lambda)^\beta] \\ & - .43 (N_s - 308) + 126 \end{aligned} \quad (27)$$

where

$L_{bms}$  = long-term median transmission loss, db

$f$  = frequency, MHz

$d$  = path length, statute miles

$\theta$  = scatter angle, radians

$F_v(s)$  = asymmetry function, db

$F(f\theta, l_v)$  = blob size correction factor, db

$H_{ot} [(h_{te}/\lambda)^\alpha] + H_{or} [(h_{re}/\lambda)^\beta]$

= frequency gain function, db

$N_s$  = surface refractivity

Although this is referred to as the Rider model in some of the literature it is more accurately described as Rider's modification to the Norton model. Rider, working with a different set of experimental data than that which Norton had used, found that better agreement between his data and the model could be achieved if the coefficient of the refractivity term,  $(N_s - 308)$ , were changed from .156 to

.43. (Ref 11: 203-210).

Yeh Model

-----

$$L_p = 57 + 10\theta + 20 \log d + 30 \log f - .2 (N_s - 310) \quad (28)$$

where

$L_p$  = long-term median transmission loss, db

$\theta$  = scatter angle, degrees

$d$  = path length, statute miles

$f$  = frequency, MHz

$N_s$  = surface refractivity

Yeh developed his model (Ref 14: 193-198) to provide a reasonably accurate yet simple alternative to the more cumbersome methods, such as the NBS model. This method has the most pronounced empirical basis of those considered here, and its simplicity appears to be gained at the expense of some potential accuracy.

AFCSP 100-61 Model

-----

$$L = 30 \log f - 20 \log d + F(\theta d) + H_o + A_a + 90 - V(d_e) - .07 \exp [1.055 (G_t + G_r)] \quad (29)$$

where

$L$  = long term transmission loss, db

$f$  = frequency, GHz

$d$  = path length, km  
 $f(\theta d)$  = attenuation function, db  
 $H_0$  = frequency gain function, db  
 $A_a$  = atmospheric absorption, db  
 $V(d_e)$  = climatological factor, db  
 $G_t$  = transmit antenna free space gain, db  
 $G_r$  = receive antenna free space gain, db

This model appears in AFCSP 100-61 (Ref 1) where it is presented in a tabular worksheet form. The algebraic expression of Eq (29) is not specifically stated but rather incorporated into the worksheet. The model is essentially a combination of the NBS and CCIR models. The AFCSP 100-61 model incorporates all of the terms of the NBS work except  $F_0$ , which is omitted. To this is added an aperture-medium coupling loss term

$$.07 \exp [.055 (G_t + G_r)]$$

which is taken from the CCIR model. The constant term, 90 db, results from expressing the frequency in GHz rather than MHz, i.e.

$$30 \log f_{\text{MHz}} = 30 \log f_{\text{GHz}} + 90$$

AFCSP 100-61 (Vol II) is intended for use by Air Force engineers in designing all types of troposcatter systems. The method it presents is considerably more complex than that given in T.O. 31R5-2TRC97-12 specifically for the TRC-97A.

#### Collins Model

-----

The Collins model is that which is incorporated into the AN/TRC-97 technical orders (Ref 12). It is the most specialized of these models, having been tailored to a particular radio set. As it appears in the technical order it is entirely a graphical method. The underlying analytical basis, however, is the NBS model.

NBS Model	$L(0.5) = 30 \log f_{MHz} - 20 \log d_{KM} + F(0d) + F_o + H_o + A_a - V(d_o)$			
CCIR Model	$L(50) = 30 \log f_{MHz} - 20 \log d_{KM} + F(0d) - G_p - V(d_o)$			
PRC Model	$L(50) = 124.6 + 30 \log f_{MHz} + 30 \log 0 + 10 \log d_{KM} + f(H) - .08(f_s - 323) - G_p$			
Norton Model	$I_{rms} = 30 \log f_{MHz} + 30 \log d_{mi} + 50 \log 0 - F_v(s) + F(f_o, l_v)$ $+ H_o [(h_{te}/\lambda)\alpha] + H_o [(h_{re}/\lambda)\rho] - .156(f_s - 308) + 126$			
Rider Model	$I_{rms} = 30 \log f_{MHz} + 30 \log d_{mi} + 50 \log 0 - F_v(s) + F(f_o, l_v)$ $+ H_o [(h_{te}/\lambda)\alpha] + H_o [(h_{re}/\lambda)\rho] - .43(f_s - 308) + 126$			
Yeh Model	$I_p = 57 + 10 0 + 20 \log d_{mi} + 30 \log f_{MHz} - .2(f_s - 310)$			
AFCSF 100-61 Model	$I = 30 \log f_{MHz} - 20 \log d_{KM} + F(0d) + H_o + A_a + 90 - V(d_o) - .07 \exp[.055(G_t + G_p)]$			
CCIR Model	TOTAL PROPAGATION LOSS	BASIC LOSS	HORIZONTAL ANGLE LOSS	APERTURE MEDIUM CORRECTING LOSS

Table 1. Classical Path Models in Original Form

## V. COMPARISON OF THE CLASSICAL MODELS WITH

### THE GENERAL PATH MODEL

The previous section describes a family of classical path models expressed as they were originally published. Looking at the summary of these models in Table I some similarity in the form of the models is apparent, yet the models are sufficiently different to make direct comparison difficult. Also it is not clear which terms in the models correspond to the various loss phenomena discussed in Section III. Anticipating that such comparisons may shed further light on the path modeling problem, the classical models will be transformed, as closely as possible, into the form of the algebraic path model given by Eq (5).

Consider first the NBS model (Eq (23)). Neither the aperture-medium coupling loss nor the equipment loss are included in this model. The ground reflection loss and atmospheric absorption loss are represented by  $H_0$  and  $A_a$  respectively. The remaining terms of the model

$$30 \log f_{\text{MHz}} - 20 \log d_{\text{km}} + F(\theta d) - F_0 - V(a_m) \quad (30)$$

represent the sum of the free space and scattering losses.

Using Eq (11) the free space loss can be expressed as

$$L_{fs} = 20 \log f_{\text{MHz}} + 20 \log d_{\text{km}} + 32.4 \quad (31)$$

or alternatively

$$L_{fs} = 20 \log f_{\text{GHz}} + 20 \log d_{\text{km}} + 92.4 \quad (32)$$

or

$$L_{fs} = 20 \log f_{\text{MHz}} + 20 \log d_{\text{mi}} + 36.6 \quad (33)$$

Subtracting the free space loss from Eq (30) then gives

$$L_s = 10 \log f_{\text{MHz}} - 40 \log d_{\text{km}} + F(\theta d) - F_0 - V(d_e) - 32.4 \quad (34)$$

Stating the attenuation function,  $F(\theta d)$ , in analytic terms provides further insight into the basis of  $L_s$ . Defining the path asymmetry factor as

$$s = \alpha_c / \beta_0$$

where the angles  $\alpha_0$  and  $\beta_0$  are as given in Figure 1,  $F(\theta d)$  can be expressed as follows: (Ref 9: Section 9.1 and Ref 10: Section III.5)

For  $0.01 \leq \theta d \leq 10$ ,  $N_s = 301$ :

$$F(\theta d) = 30 \log (\theta d) + .33 \theta d + 135.8 \quad (35)$$

For  $10 \leq \theta d \leq 70$ ,  $N_s = 301$ ,  $0.7 < s < 1.0$ :

$$F(\theta d) = 37.5 \log (\theta d) + .212 \theta d + 129.5 \quad (36)$$

For  $\theta d \geq 70$ ,  $N_s = 301$ ,  $0.7 < s < 1.0$ :

$$F(\theta d) = 45 \log (\theta d) + .157 \theta d + 119.2 \quad (37)$$

Further, for values of  $N_s$  other than 301, the function  $F(\theta d)$



is given by

$$F(\theta d, N_s) = F(\theta d, N_s = 301) - [.1 (N_s - 301) \exp (-\theta d/40)] \quad (38)$$

It can be shown that the value of the product  $\theta d$  for a practical TRC-97A path will not exceed 10. Experience has shown that antenna elevation angles ( $\theta_{et}, \theta_{er}$ ) in excess of 1.0 deg will not generally support usable communications with this system. Using the procedure in Appendix A with  $\theta_{et} = \theta_{er} = 1.0$  deg (.0175 rad) and  $N_s = 290$  [2] gives the maximum value of the scatter angle,  $\theta$ , as .0542 rad. With the maximum range of the TRC-97A taken as 160 km, the maximum value of the product  $\theta d$  is then

$$\text{MAX } (\theta d) = (.0542 \text{ rad})(160 \text{ km}) = 8.67 \text{ rad-km}$$

For the TRC-97A, therefore, Eqs (35) and (36) are combined to give an expression for  $F(\theta d)$  which is valid for all values of  $s$  and  $N_s$ :

$$F(\theta d) = 30 \log (\theta d) + .33 \theta d + 135.8 - [.1 (N_s - 301) \exp (-\theta d/40)] \quad (39)$$

Combining this last result with Eq (34) then gives

-----

[2] Scattering angle,  $\theta$ , varies inversely with the refractivity.

$$\begin{aligned}
L_3 = 10 \log 4_{\text{MHz}} - 10 \log d_{\text{KE}} + 30 \log \Theta \\
+ .33 \Theta d - .1 (\Omega_s - 301) \exp (-\Theta d) + 0 \\
+ 103.4 - F_0 - V(d_0) \quad (40)
\end{aligned}$$

The scattering efficiency,  $F_0$ , can also be expressed analytically: (Ref 9: 9-5)

$$\begin{aligned}
F_0 = 1.086 \left[ \frac{r}{h_0} \right] \\
\times \left[ h_0 - \frac{s(d - d_{lt} - d_{lr})}{(1 + s)^2} - d_{lt} - d_{lr} \right] \quad (41)
\end{aligned}$$

This is a rather cumbersome expression, and it will be seen in the next section that  $F_0$  is negligible for the short-range troposcatter path. In the interest of clarity, therefore, Eq (41) is not incorporated into  $L_3$  (Eq 40) at this time.

The climatological factor,  $V(d_0)$ , is a correction for different geographic regions and was derived from analysis of experimental observation.  $V(d_0)$  can also be expressed analytically as: (Ref 10: III-66)

$$V(d_0) = 10 d_0^{\alpha_1} + \alpha_2 d_0 \exp(-\alpha_3 d_0^{\alpha_4}) + \alpha_5 d_0^{\alpha_6} + \alpha_7 d_0^{\alpha_8}$$

where

$$\alpha_2 V(d_0) = 1 + \alpha_1 d_0 + \alpha_4 \exp(-\alpha_3 d_0^{\alpha_4})$$

and the constants  $\alpha_1, \alpha_2, \alpha_3, \alpha_4, \alpha_5, \alpha_6, \alpha_7, \alpha_8, \alpha_9$  are given in Table III.2 of Ref 10. When incorporated into

does not appear to be of any immediate benefit to the present analysis, and therefore is not used. Instead, values of  $V(a_g)$  are obtained from Figure A15, which graphically represents Eq (42).

For the NBS model then, Eq (40) is taken to represent the scattering loss. Table II summarizes the above results as well as similar results for the remaining classical models. Displayed in this manner the relationships between the models and the underlying loss phenomena become more clear, and comparison between models is facilitated.

The CCIR model is similar to the NBS model. The CCIR model adds an aperture-medium coupling loss term

$$.07 \exp [1.055 (G_t + G_r)]$$

and deletes the terms  $F_a$ ,  $H_a$ , and  $A_d$ .

The PRU model uses the same aperture-medium coupling loss as appears in the CCIR model. Subtracting  $(L_{gt} + L_{gr})$  and the free space loss (Eq (31)) from the PRU model

$$\begin{aligned} L_{PRU} &= L_{gt} + L_{gr} + L_{fs} = 10 \log (100 \text{ MHz}) + 10 \log (4 \text{ km}) \\ &\quad + 10 \log (H) + 10 \log (N_s) = 32.3 + 12.2 + 10 \log (H) \end{aligned} \quad (43)$$

which

$$10 \log (H) = 20 \log (f) + 1.3 \text{ dB} + 10 \log (H)$$

$$L_{PRU} = \frac{100}{f}$$

$$S = \frac{4S_1}{(1 + S_1)^2}$$

$$S_1 = d_1/d_2$$

It can be shown that for a reasonably symmetric path  $r(H)$  is relatively insensitive to the asymmetry function  $S_1$ . Specifically for  $0.75 \leq S_1 \leq 1.0$  (which includes the majority of practical paths)  $r(H)$  can be very closely approximated by assuming  $S_1 = 1$  which gives

$$r(H) = 20 \log [5 + .075 \theta d] + .16 \theta d_{km} \quad (44)$$

Substituting this result into Eq (43) gives

$$\begin{aligned} L(50) - (L_{gt} + L_{gr} + L_{fs}) &= 10 \log f_{MHz} - 10 \log d_{km} \\ &+ 30 \log \theta + .16 \theta d - .03 (N_s - 323) \\ &+ 92.2 + 20 \log [5 + .075 \theta d] \end{aligned} \quad (45)$$

At this point, the limited information on the derivation of the PRC model makes further conclusions somewhat speculative. Eq (45) contains no apparent equipment loss term. By comparison with the other models, it seems safe to conclude that all but the last term of Eq (45) are components of the scattering loss,  $L_s$ . The origin of the remaining term

$$20 \log [5 + .075 \theta d]$$

is not at all obvious. Lacking further information then Eq (45) will be taken as the sum of  $L_s$ ,  $L_{gt}$ , and  $L_{gr}$ , as is shown in Table II.

In the Norton model given by Eq (26) the ground reflection loss

$$H_o = H_{ot}[(h_{te}/\lambda)\pi] + H_{or}[(h_{re}/\lambda)\pi]$$

can be clearly identified. Subtracting the free space loss (Eq (32)) and the ground reflection loss from Eq (26) gives

$$\begin{aligned} L_{bms} - L_{fs} - L_h = & 10 \log f_{MHz} + 10 \log d_{mi} \\ & + 50 \log \theta - .156 (N_s - 308) \\ & + 89.4 - F_v(s) + F(f\theta, l_v) \end{aligned} \quad (46)$$

When Norton published this model, analytic expressions for the asymmetry function  $F_v(s)$  and the blob size correction factor  $F(f\theta, l_v)$  were not explicitly given; instead they were shown graphically (Ref 4: Figures 2 and 4). Applying the parameters of a practical TRC-97A path to these graphs, however, both  $F_v(s)$  and  $F(f\theta, l_v)$  can be shown to be negligible. Therefore, no further attempt is made here to derive the analytic expressions for these two terms. Norton does indicate that these terms result from the scattering process, so Eq (46) is taken to represent the scattering loss,  $L_s$ , as given by the Norton model.

As pointed out in the previous section, the Rider model is more correctly a modification of Norton's model, the only difference being the constant associated with the refractivity term. The derivation of the Rider model as it appears in Table II is therefore identical to that for the Norton model.

The Yeh model makes no attempt to account for losses due to ground reflection, atmospheric absorption, or losses within the equipment. Also, while aperture-medium coupling loss was addressed by Yeh, it was not explicitly included in his model. The model given by Eq (28) therefore represents only the sum of the free space and scattering losses. Subtracting  $L_{fs}$  (Eq (32)) from Eq (28) thus gives

$$L_s = 10 \log f_{MHz} + 10 \theta - .2 (N_s - 310) + 20.4 \quad (47)$$

where  $\theta$  is in degrees. This is equivalently expressed as

$$L_s = 10 \log f_{MHz} + 573 \theta - .2 (N_s - 310) + 20.4 \quad (48)$$

where  $\theta$  is in radians.

As described in the last section, the model in AFCSP 100-61 is a composite of the NBS and CCIR models. The aperture-medium coupling loss is from the CCIR model and is given by

$$L_{gt} + L_{gr} = .07 \exp \{ .055 (G_t + G_r) \}$$

The remaining terms are from the NBS model. The ground reflection loss and atmospheric absorption loss are represented by  $H_o$  and  $A_a$  respectively. Subtracting  $L_{gt}$ ,  $L_{gr}$ ,  $L_{fs}$  (Eq (32)),  $L_h$ , and  $L_a$  from Eq (29) gives

$$L_s = 10 \log f_{GHz} - 40 \log d_{km} + F(\theta d) - V(d_e) - 2.4$$

and substituting Eq (33) for  $F(\theta d)$  produces the result

$$\begin{aligned}
L_s = & 10 \log f_{\text{GHz}} - 10 \log d_{\text{km}} + 30 \log \theta \\
& + .33 \theta d - .1 (N_s - 301) \exp (-\theta d/40) \\
& + 133.4 - V(d_e) \quad (49)
\end{aligned}$$

The Collins model is presented graphically. The aperture-medium coupling loss and equipment loss are tabulated for various equipment configurations. The combination of free space and scattering losses is taken from two graphs. The first graph gives a basic loss for transmission over a smooth earth, while the second graph gives an additional loss to compensate for the effects of irregular terrain. No attempt is made here to derive the analytic expressions from which these graphs are constructed.

		ANTENNA GAIN	ATMOSPHERE-MEDIUM COUPLING LOSS	FREE SPACE LOSS	SCATTERING LOSS	REFLECTED FIELD LOSS	ATTEN. LOSS	ATTEN. LOSS
GENERAL EQUATION	$P_r - P_t -$	$G_{eff} + G_{eff}$	$- I_{gr} + I_{gr}$	$+ I_{fs}$	$+ I_{sc}$	$+ I_{h}$	$+ I_{r}$	$+ I_{r}$
2000 MILES				$+ 20 \log f_{MHz}$ $+ 20 \log d_{km}$ $+ 32.4$	$+ 10 \log f_{MHz} - 10 \log d_{km} + 30 \log \rho + .13 \log$ $- .1 \log S - 30.1 \exp (-\rho d / 400) + 103.5 - F_0 - \sqrt{d_{km}}$	$+ H_0$	$+ A_0$	
2000 MILES			$.07 \exp$ $.055(G_t + G_r)$	$+ 20 \log f_{MHz}$ $+ 20 \log d_{km}$ $+ 32.4$	$+ 10 \log f_{MHz} - 10 \log d_{km} + 30 \log \rho + .13 \log$ $- .1 \log S - 30.1 \exp (-\rho d / 400) + 103.5 - \sqrt{d_{km}}$			
2000 MILES			$.07 \exp$ $.055(G_t + G_r)$	$+ 20 \log f_{MHz}$ $+ 20 \log d_{km}$ $+ 32.4$	$+ 10 \log f_{MHz} - 10 \log d_{km} + 30 \log \rho + .16 \log S - .09 \log S - 32.0$ $+ 92.2 + 20 \log (S + .075 \log)$			
2000 MILES				$+ 20 \log f_{MHz}$ $+ 20 \log d_{mi}$ $+ 36.6$	$+ 10 \log f_{MHz} + 10 \log d_{mi} + 50 \log \rho$ $- .156 \log S - 30.8 + 89.5 - F_0 (S) + F_0 (4.3 \sqrt{S})$	$+ H_0$		
2000 MILES				$+ 20 \log f_{MHz}$ $+ 20 \log d_{mi}$ $+ 36.6$	$+ 10 \log f_{MHz} + 10 \log d_{mi} + 50 \log \rho$ $- .156 \log S - 30.8 + 89.5 - F_0 (S) + F_0 (4.3 \sqrt{S})$	$+ H_0$		
2000 MILES				$+ 20 \log f_{MHz}$ $+ 20 \log d_{mi}$ $+ 36.6$	$+ 10 \log f_{MHz} + 57.3 \rho - .2 \log S - 31.0 + 20.5$			
2000 MILES			$.07 \exp$ $.055(G_t + G_r)$	$+ 20 \log f_{MHz}$ $+ 20 \log d_{km}$ $+ 92.4$	$+ 10 \log f_{MHz} - 10 \log d_{km} + 30 \log \rho + .13 \log$ $- .1 \log S - 30.1 \exp (-\rho d / 400) + 103.5 - \sqrt{d_{km}}$	$+ H_0$	$+ A_0$	
2000 MILES			$.07$		$+ f(0) + f(0, d) + \text{constant}$			$+ A_0$

Table II. Classical Path Models Expressed in the Form of the General Path Model



## VI. THE GENERAL PATH MODEL TAILORED

### TO THE AN/TRC-97A

Eq (22) gives a model of the troposcatter path which attempts to account for all the significant random influences on the path. It is also general enough to encompass all of the more specific classical models which have been examined. As stated previously, the primary goal of this research is to examine empirical adjustments which are necessary to bridge the gap between the theoretical model and experimental evidence. To do so will require some numerical analysis of the model in Eq (22), a task which appears to be quite formidable, given the complex statistical dependence among the terms in this model. If it turned out that some of the terms in Eq (22) were far less sensitive than others to the random variations in the scattering process, some simplification of the model may be justified prior to numerical analysis. Thus one could, as a first approximation, sacrifice some generality and accuracy in the model for the sake of narrowing the complexity of further analysis to manageable limits.

#### Typical Path Model Values for the AN/TRC-97A

First it is instructive to examine typical values which one would expect of the terms in Eq (22). Figure 2 shows these values for the TRC-97A, as calculated using the classical models.

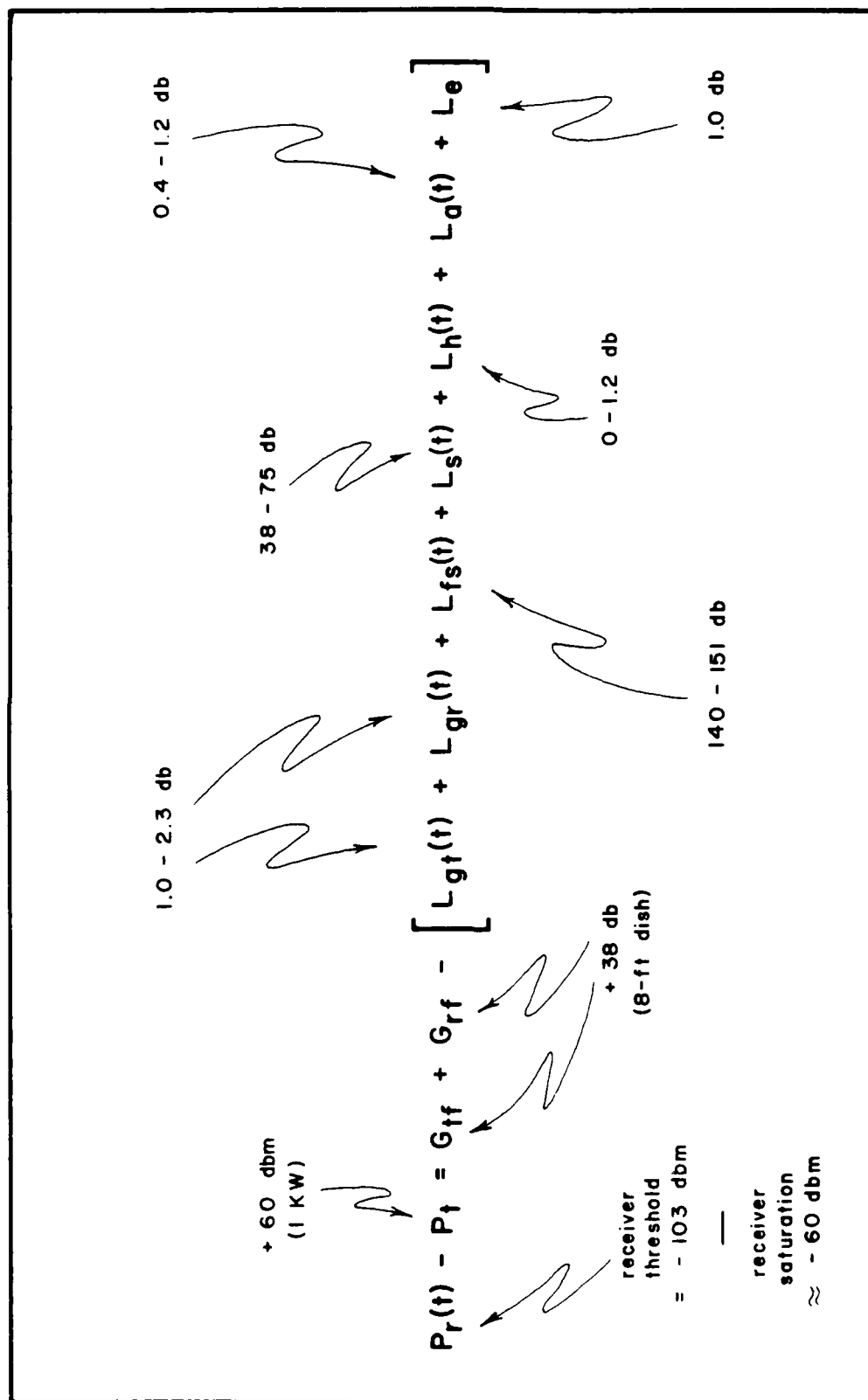


Figure 2. Typical Values in the General Path Model for the AN/TRC-97A

One kilowatt is the nominal maximum output power of the TRC-97A, and that which is normally used in the troposcatter propagation mode. The free space gain of the antenna with which this equipment is primarily configured, an 8-foot parabolic antenna, is specified by the manufacturer as 38 db (each antenna).

The value of the aperture-medium coupling loss,  $L_{gt}$  and  $L_{gr}$ , given by the technical order and AFCSP 100-61 are not in agreement, so both values are given. Table 9-5 of the technical order (Ref 12: 9.10) gives the aperture-medium coupling loss as 1.0 db for each antenna. AFCSP 100-61 calculates the aperture-medium coupling loss for the pair of antennas as

$$\begin{aligned} L_{gt} + L_{gr} &= .07 \exp [.055 (G_{tf} + G_{rf})] \\ &= .07 \exp [.055 (38 + 38)] \\ &= 4.58 \text{ db} \end{aligned}$$

or equivalently, 2.29 db for each antenna.

The free space loss shown represents the range of values possible depending upon the choice of operating frequency and path length, and is calculated from Eq (31). For the TRC-97A's minimum operating frequency (4.4 GHz) and a path length approximating the minimum range in the troposcatter mode (60 km), [3] the free space loss is

$$\begin{aligned}
L_{fs} &= 20 \log f_{\text{MHz}} + 20 \log d_{\text{km}} + 32.4 \\
&= 20 \log (4400) + 20 \log (60) + 32.4 \\
&= 140.8 \text{ db}
\end{aligned}$$

For the TRC-97A's maximum operating frequency (5.0 GHz) and nominal maximum range (160 km), the free space loss is

$$\begin{aligned}
L_{fs} &= 20 \log (5000) + 20 \log (160) + 32.4 \\
&= 150.5 \text{ db}
\end{aligned}$$

Computing the range of values for the scattering loss is less straight forward because of the interdependence of several factors and the need for specific terrain information. The basis for calculating typical values of  $L_s$  for the TRC-97A is Eq (40):

$$\begin{aligned}
L_s &= 10 \log f_{\text{MHz}} - 10 \log d_{\text{km}} + 30 \log \theta \\
&\quad + .33 \theta d - .1 (N_s - 301) \exp (-\theta d/40) \\
&\quad + 103.4 - F_o - V(d_e) \quad (40)
\end{aligned}$$

Calculation of the scattering angle requires detailed information about the terrain which the path traverses. Accounting for every possible variation in the terrain would be a formidable task, and the goal at this point is simply to estimate the range of values for the scattering loss.

-----

[3] This is actually well below the minimum distance at which the troposcatter mode is normally dominant.

Therefore, for the purpose of bounding  $L_s$ , a path over a smooth earth will be assumed. Antenna information is also required: use of an 8-foot parabolic antenna will continue to be assumed.

It will be seen that in Eq (40),  $\theta$  depends upon the choice of both  $d$  and  $N_s$ . Furthermore,  $V(d_e)$  is a function of frequency, path geometry (to include  $d$ ), and the climatic region. Therefore, care must be exercised when evaluating Eq (40) lest the effect of these relationships be distorted.

Consider first the scattering efficiency correction,  $F_0$ . Rice, et al. (Ref 9: 9.5) state that  $F_0$  allows for the reduction of scattering efficiency at great heights in the atmosphere. Over a typical short range path, the scattering takes place at relatively low altitudes, and one would expect that  $F_0$  would have little influence. The small magnitude of  $F_0$  will be confirmed shortly; for the purpose of the present discussion, it is assumed to be negligible.

For the remaining terms, consider eight cases which represent the various combinations of minima and maxima of the independent variables  $f$ ,  $d$ , and  $N_s$ . As before, the frequency range of this equipment is 4.4 - 5.0 GHz and the path length is assumed to lie between 60 and 160 km. In addition, the range of possible values of  $N_s$  is assumed to be between 290 and 390 (Ref 9: 4.3). For each case,  $\theta$  is evaluated using Data Sheet B-5, items 1-24, of Ref 1. The effective distance,  $d_e$ , is then calculated using items 18, 19, 23, and 47-49 of this same data sheet. With the

resulting values of  $d_e$ , the range of possible values of  $V(d_e)$  is read from Figure A15 for each of the eight cases.

Figure A1 shows the evaluation of  $\theta$  and  $d_e$  for the case where  $f = 4.4$  GHz,  $d = 60$  Km, and  $N_s = 290$ . The remaining seven cases are shown in Figures A2 through A8.

All the information necessary to evaluate the minimum and maximum values of  $L_s$  is now at hand. For ease of presentation, define

$$L_s' = 10 \log f_{\text{MHz}} - 10 \log d_{\text{km}} + 30 \log \theta + .33 \theta d - .1 (N_s - 301) \exp (-\theta d / 40) + 103.4 \quad (50)$$

so that

$$L_s = L_s' - V(d_e) \quad (51)$$

The results of evaluating Eq (40) for each of the eight cases are summarized in Table III. The value of  $L_s$  for these eight paths is seen to range between 38 and 74 db. Furthermore, the minimum value of  $L_s$  corresponds to minimum frequency, minimum path length, maximum refractivity, and a desert climatic region.  $L_s$  is maximum for maximum frequency, maximum path length, minimum refractivity, and an overwater path in a temperate climate.

The ground reflection loss,  $L_h$ , is similarly calculated using Data Sheet B-5 (items 29-44), with the results for the same eight path cases considered above appearing in Figures A1 through A8. Graphs of the required intermediate functions,  $\gamma_s$ ,  $H_0$ , and  $\Delta H_0$  are given in Figures A10 through

	CASE 1	CASE 2	CASE 3	CASE 4	CASE 5	CASE 6	CASE 7	CASE 8
$f$ (MHz)	4400	4400	4400	4400	5000	5000	5000	5000
$d$ (KM)	60	60	160	160	60	60	160	160
$r_s$	290	390	290	390	290	390	290	390
$\theta$ (Radians)	.005016	.003619	.017035	.012861	.005016	.003619	.017035	.012861
$d_s$ (KM)	153	153	253	253	153	153	253	253
$10 \log f$	36.43	36.43	36.43	36.43	36.99	36.99	36.99	36.99
$10 \log d$	-17.78	-17.78	-22.04	-22.04	-17.78	-17.78	-22.04	-22.04
$30 \log r_s$	-68.99	-73.24	-53.06	-56.72	-68.99	-73.24	-53.06	-56.72
$33 \log d_s$	.10	.07	.90	.68	.10	.07	.90	.68
$-4.1 \log \frac{r_s - 30}{\exp(-0.40)}$	41.09	-8.85	41.03	-8.45	41.09	-8.85	41.03	-8.45
$103.4$	103.4	103.4	103.4	103.4	103.4	103.4	103.4	103.4
$s$	54.25	40.03	66.66	53.30	54.81	40.59	67.22	53.86
$3 \log d_s$	-1.9 to 4.1	-1.9 to 4.1	-5.9 to 7.0	-5.9 to 7.0	-1.9 to 4.1	-1.9 to 4.1	-5.9 to 7.0	-5.9 to 7.0
$r$	52.35 to 58.35	38.13 to 44.13	60.76 to 73.66	47.4 to 60.30	52.91 to 58.91	38.69 to 44.69	61.32 to 74.22	47.96 to 60.86

Table III. Range of Values of Scattering Loss,  $L_s$ , for AN/TRC-97A

A13. Thus, within the constraints of the paths chosen,  $L_h$  is seen to range between 0 and 1.2 db.

The loss from atmospheric absorption,  $L_a$ , is only considered in two of the classical models: those of the NBS and AFCSP 100-61. In both models, the value of absorption loss is taken from the graph appearing in Figure A14, and that method is used here. Note, however, that this graph displays data from a specific location and month of the year. It is not readily clear how representative this data is of other locations and seasons. In any event, using Figure A14, it is seen that for a path varying between 60 and 160 km, with an operating frequency between 4.4 and 5.0 GHz,  $L_s$  is expected to lie within the range from approximately .4 to 1.2 db.

The equipment loss is addressed only by the Collins method, and is given by the technical order (Ref 12: Table 9-7) as 1 db for a TRC-97A system using parabolic antennas.

#### Simplifying Assumptions in the Path Model

Several conclusions can be drawn from Figure 2. It was previously determined (Section III) that the transmitted power, free space antenna gains, and equipment loss would be considered to be constant for a given path. Among the loss terms, there appear to be two distinct groups based on magnitude. The aperture-medium coupling loss, ground reflection loss, absorption loss, and equipment loss each have maximum values less than 2.5 db. By contrast, the free



space loss and scattering loss are each at least an order of magnitude larger than the other loss terms. Also, the mean values of  $\underline{L}_{fs}(t)$  and  $\underline{L}_s(t)$  display considerably more variability than do the means of  $\underline{L}_{st}(t)$ ,  $\underline{L}_{gr}(t)$ ,  $\underline{L}_h(t)$ , or  $\underline{L}_d(t)$ . To draw firm conclusions about the relative significance of all of the loss terms, one would need to have more knowledge of the statistics of the random terms (only mean values are considered in Figure 2). It has been shown, however, that the randomness in the loss terms stems from the same source: the random scattering process. In other words, all of the loss terms, except  $\underline{L}_s$ , are functions of the scattering process,  $\underline{S}(t)$ . Further, it has been stated that  $\underline{L}_s$  is by definition that term which attempts to account for the losses uniquely associated with the scattering mechanism. If  $\underline{L}_s$  does in fact represent the primary loss due to  $\underline{S}(t)$ , one would expect that in the remaining terms, the influence of  $\underline{S}(t)$  would be less pronounced. Thus, it would be appealing to discount the random influence on the terms  $\underline{L}_{st}(t)$ ,  $\underline{L}_{gr}(t)$ ,  $\underline{L}_h(t)$ , and  $\underline{L}_d(t)$ , thereby considerably simplifying the statistical interdependence of the terms in Eq (22). To do so would also be consistent with the approach most commonly taken by other researchers.

Thus, as a first approximation, the effect of  $\underline{S}(t)$  on  $\underline{L}_{st}(t)$ ,  $\underline{L}_{gr}(t)$ ,  $\underline{L}_h(t)$ , and  $\underline{L}_d(t)$  are considered to be negligible and Eq (22) is rewritten as

$$\begin{aligned} P_r(t) - P_t = G_{ti} + G_{rf} - [L_{gt} + L_{gr} \\ + L_{fs}(t) + L_s(t) + L_h + L_a + L_e] \end{aligned} \quad (52)$$

Consider next the sensitivity of  $L_{fs}(t)$  to  $S(t)$ . Because of the scattering phenomenon, different components of the transmitted signal are returned to the receiving antenna via different scattering points within the common volume, and thus travel different distances between transmitting and receiving stations. Consider the path geometry shown in Figure 3. Antenna elevation angles for a practical TRC-97A system in the troposcatter mode seldom fall beyond the range of -0.5 to +1.0 deg. The center ray for elevation angles of -0.5 and +1.0 deg is shown as lines TAR and TBR of Figure 4. The 3-db beamwidth of the 3-foot parabolic antenna used with the TRC-97A is 2 deg. Thus, the majority of the received signal components arrive via a path which lies in the region between TCR and TDR, where the angle  $DTC = DRC = 3.5$  deg. For the case where elevation angles are +1.0 deg, the scattering angle  $\theta$  can be shown to be approximately 3.1 deg.[4] For the case where elevation angles equal -0.5 deg,  $\theta$  is clearly less than  $\theta$ , and approaches 0 deg in the limit. The worst case difference in path length occurs when  $\theta = 0$ , thereby making angle TCD = 90 deg. In this case the ratio of TC to TD equals the

-----

[4] Using Data Sheet B-5 with  $\theta_{et} = \theta_{er} = +1.0$  deg,  $L_{gt} = 290$ ,  $d = 160$  km, and smooth earth.

cosine of the angle CTD, or

$$\frac{TC}{TD} = \cos 3.5 \text{ deg} = .9981$$

or alternately

$$DT = 1.0019 \times CT$$

which is to say that the maximum distance the signal must travel (DT) is greater than the minimum distance it must travel (CT) by only .19 percent. Thus,  $\tilde{S}(t)$  causes negligible variation in the distance the signal travels and the path length can be treated as a constant.  $L_{fs}(t)$  is therefore given by the previously derived expression:

$$L_{fs} \approx 20 \log f_{\text{MHz}} + 20 \log d_{\text{km}} + 32.4 \quad (31)$$

The result is that Eq (52) can now be further simplified to

$$\begin{aligned} P_r(t) - P_t = G_{tr} + G_{rr} - [L_{jt} + L_{jr} \\ + L_{fs} + L_s(t) + L_h + L_a + L_o] \end{aligned} \quad (53)$$

where  $L_s(t)$  is the only random quantity upon which  $P_r(t)$  depends.

#### Statistics of the Path Model

---

Previous experimental work has lead to the conclusion that for short time intervals the received signal voltage over a troposcatter path can be characterized as a Gaussian process, while the envelope of the received signal voltage

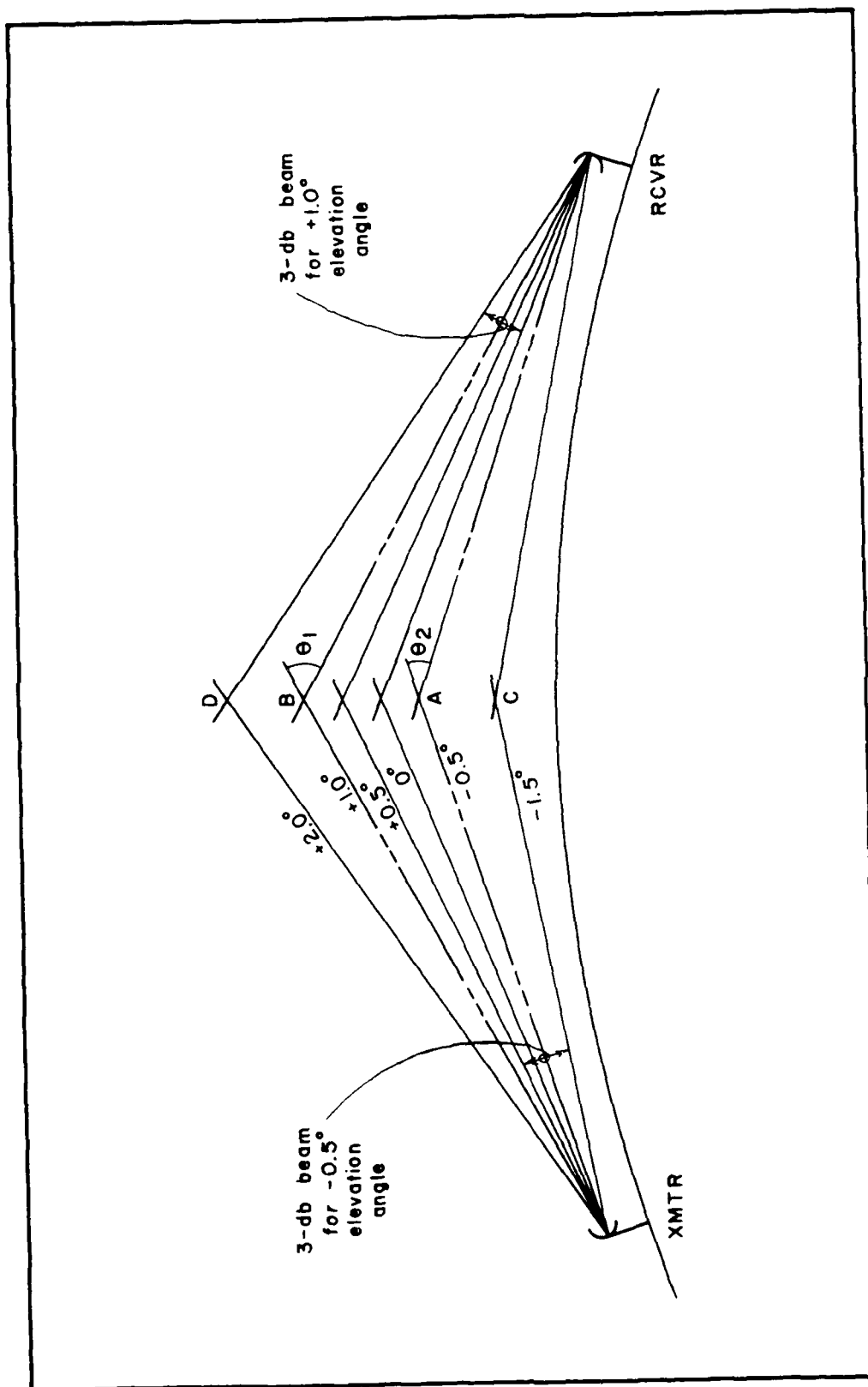


Figure 3. Variation in Path Length with Antenna Elevation

tends to a Rayleigh process (Ref 2: 467). Insofar as these conclusions are valid, then the first-order Rayleigh density of the received signal envelope,  $E_r(t)$ , can be expressed as (Ref 13: 47)

$$f(E_r; t) = \frac{E_r}{2} \exp \left[ -\frac{E_r^2}{2\sigma^2} \right] \quad (54)$$

where  $E_r$  and  $\sigma^2$  are in watts. The corresponding first-order Rayleigh distribution is given by

$$F(E_r; t) = 1 - \exp \left[ -\frac{E_r^2}{2\sigma^2} \right] \quad (55)$$

where  $E_r$  and  $\sigma^2$  are in watts.

The path models considered here are in terms of the power of the received signal rather than its envelope voltage. Also, the data used for this research generally includes recorded values of received signal power rather than signal voltage. The received signal power  $P_r(t)$  can be related to the magnitude of the received voltage  $E_r(t)$  by

$$P_r(t) = k \left[ E_r(t) \right]^2 \quad (56)$$

where  $k$  is the reciprocal of the effective impedance presented to the incoming signal by the radio receiver, and is assumed to be constant for a given type of radio.

It can be shown (Ref 6: 129) that if

$$Y = f(X) = aX^2$$

with  $a, x, y \geq 0$ , then

$$f_{\tilde{y}}(y) = \frac{1}{2\sqrt{ay}} f_{\tilde{x}}(\sqrt{y/a}) \quad (57)$$

and

$$F_{\tilde{y}}(y) = F_{\tilde{x}}(\sqrt{y/a}) \quad (58)$$

Since  $P_r(t)$ ,  $E_r(t)$  and  $k$  can only assume nonnegative values, Eqs (54), (56), and (57) can be combined to give the first order density of the received power as

$$f(P_r; t) = \frac{1}{2k^2} \exp \left[ -\frac{P_r}{2k^2} \right] \quad (59)$$

where  $P_r$  and  $k^2$  are in watts. Similarly the combination of Eqs (55), (56), and (58) gives the first order distribution of the received power as

$$F(P_r; t) = 1 - \exp \left[ -\frac{P_r}{2k^2} \right] \quad (60)$$

where  $P_r$  and  $k^2$  are in watts.

While the received power is directly observable, the other random quantity in Eq (53), the scattering loss, is not. Eq (53), in which the power terms are expressed in dbm and the gain and loss terms in db can also be written as

$$\underline{P}_r(t) = \frac{P_t G_{tf} G_{rf}}{L_{gt} L_{gr} L_{fs} \underline{L}_s(t) L_h L_a L_e} \quad (61)$$

where the power terms are in watts and the gain and loss terms are ratios. For a given path, each of the deterministic quantities on the right side of Eq (61) is assumed to be a constant, making it possible to write Eq (61) as

$$\underline{L}_s(t) = \frac{b}{\underline{P}_r(t)} \quad (62)$$

where

$$b = \frac{P_t G_{tf} G_{rf}}{L_{gt} L_{gr} L_{fs} L_h L_a L_e} \quad (63)$$

It can be shown (Ref 6: 128) that if

$$\underline{Y} = g(\underline{X}) \approx a/\underline{X}$$

then

$$f_y(y) = (|a|/y^2) f_x(a/y)$$

Combining this last result with Eqs (59) and (62) gives the first-order density of the scattering loss as

$$f(L_s; t) = \frac{|b|}{L_s^2} \times \frac{1}{2k^2} \exp \left[ -\frac{b/L_s}{2k^2} \right]$$

Since all the terms on the right side of Eq (63) are nonnegative, b is also nonnegative. Therefore

$$f(L_s; t) = \frac{b}{2k \cdot^2 L_s^2} \exp \left[ - \frac{b}{2k \cdot^2 L_s} \right] \quad (64)$$

where  $b$  and  $k \cdot^2$  are in watts and  $L_s$  is a ratio. The first-order distribution of the scattering loss is found by integrating the density:

$$\begin{aligned} F(L_s; t) &= \int_0^{L_s} \frac{b}{2k \cdot^2 L_s^2} \exp \left[ - \frac{b}{2k \cdot^2 L_s} \right] dL_s \\ &= \exp \left[ - \frac{b}{2k \cdot^2 L_s} \right] \end{aligned} \quad (65)$$

where  $b$  and  $k \cdot^2$  are in watts and  $L_s$  is a ratio.



## VII. THE MODIFIED SCATTERING LOSS MODEL

---

Recall from the Introduction the proposed approach of modifying the empirical adjustments in the existing path models to obtain better correlation with observed performance for the short range tactical troposcatter path. Given that the assumptions in the analysis to this point are valid, Eq (53) shows the scattering loss to be the only random independent variable in the path model. Further, Eqs (64) and (65) give the first-order density and distribution of the scattering loss. The preceeding analysis has also shown that of all the factors in the general path model, the scattering loss has the greatest potential for causing large variations in the received power for a given path. As a first approximation then, assume that the deterministic quantities in Eq (53) are correctly accounted for in the present path models, and that any variation between predicted and observed path loss results from the scattering loss alone.

Recalling that the present predictions use the AFCSP 100-61 and Collins models, which are both based on the NBS model, consider then the model

$$\begin{aligned}
 P_r(t) = & P_t + G_{tf} + G_{rf} - .07 \exp [1.055 (G_{tf} + G_{rf})] \\
 & - 20 \log f_{\text{MHz}} - 20 \log d_{\text{km}} - 32.4 \\
 & - L_h - L_a - L_e - L_s(t)
 \end{aligned} \tag{66}$$

This is the general model of Eq (53) with the deterministic

quantities assumed to be as given by the AFCSP 100-61 and Collins models. This model can also be expressed as

$$P_r(t) = b' - L_s(t) \quad (67)$$

where

$$\begin{aligned} b' = & P_t + G_{tf} + G_{rf} - .07 \exp [1.055 (G_{tf} + G_{rf})] \\ & - 20 \log f_{\text{MHz}} - 20 \log d_{\text{km}} - 32.4 \\ & - L_h - L_a - L_e \end{aligned} \quad (68)$$

Given the operating frequency, antenna gains, and sufficient information about the path geometry,  $b'$  can be readily computed using the combined procedures in AFCSP 100-61 and T.O. 31R5-2TRC97-12.

Consider next the treatment of the scattering loss in the presently used models. Eq (49) gives the scattering loss used in the AFCSP 100-61 model as

$$\begin{aligned} L_s = & 10 \log f_{\text{GHz}} - 10 \log d_{\text{km}} + 30 \log \theta + .33 \theta d \\ & - .1 (N_s - 301) \exp (-\theta d/40) + 133.4 - V(d_e) \end{aligned} \quad (49)$$

This is identical to the NBS expression for  $L_s$  given that the term  $F_0$  is negligible for this type of path (as shown in Section VI). The problem now is one of deriving an alternate expression for the scattering loss which is more accurate for a typical TRC-97A path. The most obvious way to do this is to assume that the form of Eq (49) is correct and that a different choice of coefficients would better match the model to the TRC-97A path. Note that

$L_s$  represents the expected value of  $L_s(t)$  which will be denoted by  $\overline{L_s(t)}$ . Consider then the expression

$$\begin{aligned} \overline{L_s(t)} = & a_1 \log f_{\text{GHz}} - a_2 \log d_{\text{km}} + a_3 \log \theta + a_4 \theta d \\ & - a_5 (N_s - 301) \exp(-\theta d/a_6) + a_7 - V(d_0) \end{aligned} \quad (69)$$

which expresses the scattering loss in the same form as that derived by the NBS, but with most of the coefficients undetermined. As pointed out previously, the analytic expression for  $V(d_0)$  (Eq (42)) is rather complex and based on data collected in a large number of locations throughout the world. Attempting to modify  $V(d_0)$  at this point would complicate Eq (69) to the extent that any further analysis would be extremely difficult. Also, modifying  $V(d_0)$  to more accurately represent the TRC-97A path would require a large data base of TRC-97A performance in all climatic regions of interest; such a data base is not presently available. Assume then that  $V(d_0)$ , as expressed by Eq (42), is correct.

#### Statement of the Regression Problem

A very specific analytic problem can now be stated. Solution of this problem should produce a scattering loss model which better represents a typical TRC-97A path. The problem is as follows:

Given sufficient information about the equipment and path geometry for a number of TRC-97A troposcatter paths, a value of  $b'$  can be computed for each path using Eq (68).

Given experimental observations of received power over these paths, and a value of  $b'$  for each path, a value of  $L_s$  corresponding to each observed value of  $P_r$  can be obtained using Eq (67). Thus a data base of scattering loss values over a number of TRC-97A paths is constructed.

Given this scattering loss data, an expression of  $V(d_e)$  (Eq (42)), and the probability distribution of  $L_s(t)$  given by Eq (65), a nonlinear multivariate regression analysis of Eq (69) can be performed to evaluate the coefficients  $\{a_1, a_2, \dots, a_7\}$ .

The resulting expression for  $\overline{L_s(t)}$  should more accurately reflect the scattering loss for a TRC-97A path and can be used with the AFCSP 100-61 model for future transmission loss predictions.

#### Evaluation of Available AN/TRC-97A Path Data.

-----

Data on the actual performance over TRC-97A paths has been collected from a number of Air Force units which use this equipment. The data is that which is routinely recorded by these units and does not reflect any data collected specifically for this research. Although the content of the data varies, typically included are recorded values of received power and information on the geometry of the path. The paths represented are from training exercises over the past several years in different locations within the continental United States. Duration of each exercise is not very long, ranging from two days to approximately two

weeks. Table IV identifies those paths for which some data is available and which fall within the scope of this study.

Because of the relatively small amount of available data, and particularly the short duration of the paths, it is desirable to evaluate the usefulness of the data. If the data is too limited to accurately represent a wide range of TRC-97A paths, then any analysis based on this data is meaningless.

It has been shown that a possible characterization of the received power over a troposcatter path is given by the density and distribution functions of Eqs (59) and (60). These in turn are the basis for the density and distribution of  $L_s(t)$  which are given by Eqs (64) and (65) and are central to the regression analysis just described. It is reasonable then to require the received power data which is used in the regression analysis to at least approximate the density and distribution in Eqs (59) and (60). Next one would expect to see some dependence of the mean scattering loss upon the parameters of the regression equation (i.e.,  $f$ ,  $d$ ,  $\theta$ , and  $N_s$ ). Were this not the case, no prediction of  $\overline{L_s(t)}$  based on these parameters would be possible. While the scattering loss is not directly observable, it is directly related to the distribution parameter  $k^{-2}$ ; therefore,  $k^{-2}$  must also be dependent upon  $f$ ,  $d$ ,  $\theta$ , and  $N_s$ . Furthermore,  $k^{-2}$  can be readily determined from observation of the received power.

TROPICAL LOCATIONS		DATE	EXERCISE	CIRCUIT	EQUIP- MENT	PATH LENGTH (KM)	RCA TERMINAL	RECEIVER	K <sub>0</sub> <sup>2</sup> (dbm)
A	B								
Fort Myer	Lyndall AFB FL	1 - 17 Oct 76	Brave Shield XV	OP-11	TRC-97A	103	A	----	82
"	"	"	"	"	"	"	B	----	65
Fort Myer	Radio Island SC	30 Apr - 22 May 77	Solid Shield 77	AF-522	TRC-97A	138	A	----	64
"	"	"	"	"	"	"	B	----	66
Fort Myer	Wallace SC	"	"	AF-551A	TRC-97A	100	A	1	85
"	"	"	"	"	"	"	A	2	79
"	"	"	"	"	"	"	B	1	74
"	"	"	"	"	"	"	B	2	70
Fort Myer	Fort Bragg SC	"	"	AF-551B	TRC-97A	90	A	1	71
"	"	"	"	"	"	"	A	2	69
"	"	"	"	"	"	"	B	1	79
"	"	"	"	"	"	"	B	2	68

Table IV. Observed AN/TRC-97A Troposcatter Paths (Sheet 1 of 4)

TERMINAL LOCATIONS		DATE	EXERCISE	CIRCUIT	EQUIPMENT	PATH LENGTH (KM)	RCV TERMINAL	RECEIVER	K <sub>a</sub> <sup>2</sup> (dbm)
A	B								
14, Ridge St	Seymour-Johnson AFB SC	30 Apr - 22 May 77	Solid State 77	AF-502	TRC-97A	140	A	1	72
"	"	"	"	"	"	"	A	2	69
"	"	"	"	"	"	"	B	1	75
"	"	"	"	"	"	"	B	2	75
14, Ridge St	W. Vernon GA	8 - 12 Sep 77	Local	-----	TRC-97A	114	A	-----	85
"	"	"	"	"	"	"	B	-----	86
14, Ridge St	W. Vernon GA	"	"	"	TRC-97A	104	A	-----	70
"	"	"	"	"	"	"	B	-----	72
14, Ridge St	14, Ridge St AFB FL	2 - 30 Oct 77	Solid State 78	AF-15	TRC-97A	103	A	1	65
"	"	"	"	"	"	"	A	2	68
"	"	"	"	"	"	"	B	1	68
"	"	"	"	"	"	"	B	2	67

Table IV. Observed AN/TRC-97A Troposcatter Paths (Sheet 2 of 4)

TERMINAL LOCATIONS		DATE	EXERCISE	CIRCUIT	EQUIPMENT	PATH LENGTH (KM)	RCV TERMINAL	RECEIVER	K <sub>0</sub> <sup>2</sup> (dbm)
A	B								
3rd Lt. Boudin AFB #11	1st Lt. Boudin AFB #11	10 - 30 Oct 77	Bold Eagle 78	AF-22	TRC-97A	101	B	----	77
1st Lt. Boudin AFB #11	1st Lt. Boudin AFB #11	11 - 13 Jan 78	Local	----	TRC-97A	114	A	2	87
"	"	"	"	"	"	"	B	2	79
1st Lt. Boudin AFB #11	1st Lt. Boudin AFB #11	"	"	----	TRC-97A	104	B	2	84
1st Lt. Boudin AFB #11	1st Lt. Boudin AFB #11	Aug 78	Brave Shield XVIII	AF-21	TRC-97A	64	----	----	68
1st Lt. Boudin AFB #11	1st Lt. Boudin AFB #11	15 Oct - 15 Nov 78	Gallant Eagle 79	AF-20	TRC-97A	97	A	----	78
"	"	"	"	"	"	"	B	----	80
1st Lt. Boudin AFB #11	1st Lt. Boudin AFB #11	3 - 24 May 79	Solid Shield 79	AF-21	TRC-97A	138	A	----	80
"	"	"	"	"	"	"	B	----	79

Table IV. Observed AN/TRC-97A Troposcatter Paths (Sheet 3 of 4)



TERMINAL LOCATIONS		DATE	EXERCISE	CIRCUIT	EQUIPMENT	PATH LENGTH (KM)	TERMINAL	RECEIVER	K <sub>2</sub> <sup>2</sup> (dBm)
A	B								
Yakima Ridge, WA	Statue Pass, WA	8 - 17 Apr 79	Bravo Shirley 20	AF-11C	TRC-97A	67	A	1	67
"	"	"	"	"	"	"	A	2	67
"	"	"	"	"	"	"	B	1	69
"	"	"	"	"	"	"	B	2	65
Yakima Ridge, WA	Statue Pass, WA	"	"	AF-11B	TRC-97A	81	B	1	71
"	"	"	"	"	"	"	B	"	77
Yakima Ridge, WA	Rooster Creek, WA	"	"	AF-12C	TRC-97A	78	A	-----	70
"	"	"	"	"	"	"	B	-----	72
Rooster Creek, WA	Statue Pass, WA	"	"	AF-11	TRC-97A	135	A	-----	77
"	"	"	"	"	"	"	B	-----	76

Table IV. Observed AN/TRC-97A Troposcatter Paths (Sheet 4 of 4)

Consider first the received power distribution for the observed TRC-97A paths. The distribution function is chosen because it simplifies the subsequent curve fitting. The power density and distribution functions (Eqs (59), (60)) are both single parameter functions, that parameter being  $k^{-2}$ . (Recall that  $k$  is a constant for a given type of radio set). As  $k^{-2}$  is varied, both the shape and position of the density function change. The distribution function varies only in relative position as  $k^{-2}$  is varied; its shape is independent of the choice of the parameter  $k^{-2}$ . Figure 4 shows a plot of  $F(P_r; t)$  vs  $P_r$  for an arbitrary value of  $k^{-2}$ . When  $P_r$  and  $k^{-2}$  are equal ( $P_r = 0$  db relative to  $k^{-2}$ ),  $F(P_r; t)$  has a value of approximately 0.4. When  $P_r$  exceeds  $k^{-2}$  by more than about 12 db,  $F(P_r; t)$  remains at a constant value of 1.0. When  $P_r$  is smaller than  $k^{-2}$  by more than about 20 db,  $F(P_r; t)$  is at a constant value of 0. Intermediate values are as shown. Note that varying the value of  $k^{-2}$  has the effect of shifting the distribution curve along the  $P_r$  axis, while the shape of the curve is unaffected.

A manual method of curve fitting is chosen initially because of the relatively small amount of data available. Use of computerized curve fitting techniques is straight forward and would be worthwhile for evaluating a large number of paths or for achieving greater accuracy. First the distribution function of the received power is plotted for each path. Three examples of such plots are shown in

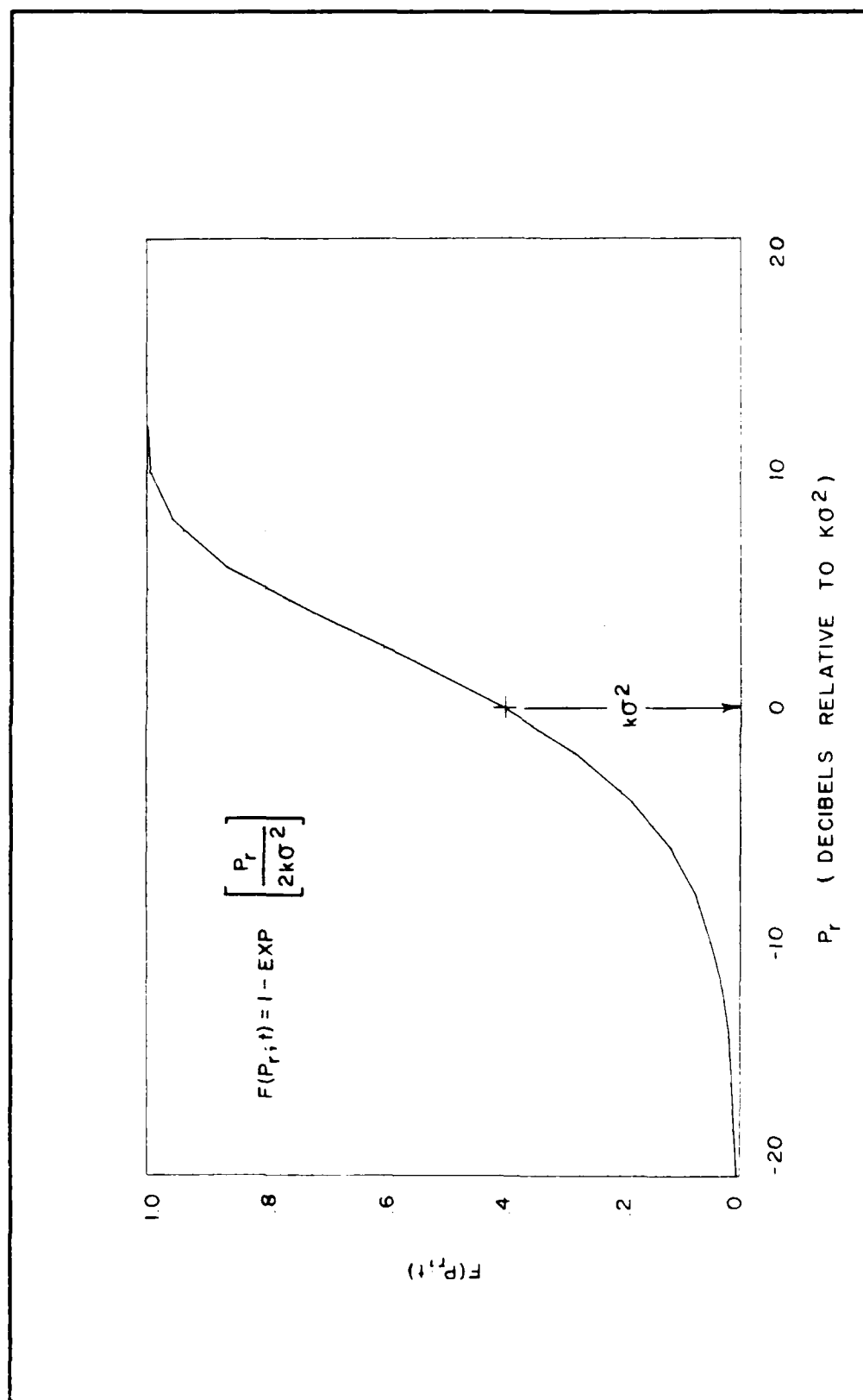


Figure 4. The Received Power Distribution Function,  $F(P_r; t)$

EXERCISE: LOCAL (5 CMBTCG)      DATES: 8-12 SEP 77  
 CIRCUIT: —      RCV TERM: MT VERNON (FROM SMART FIELD)      RCVR NR: —

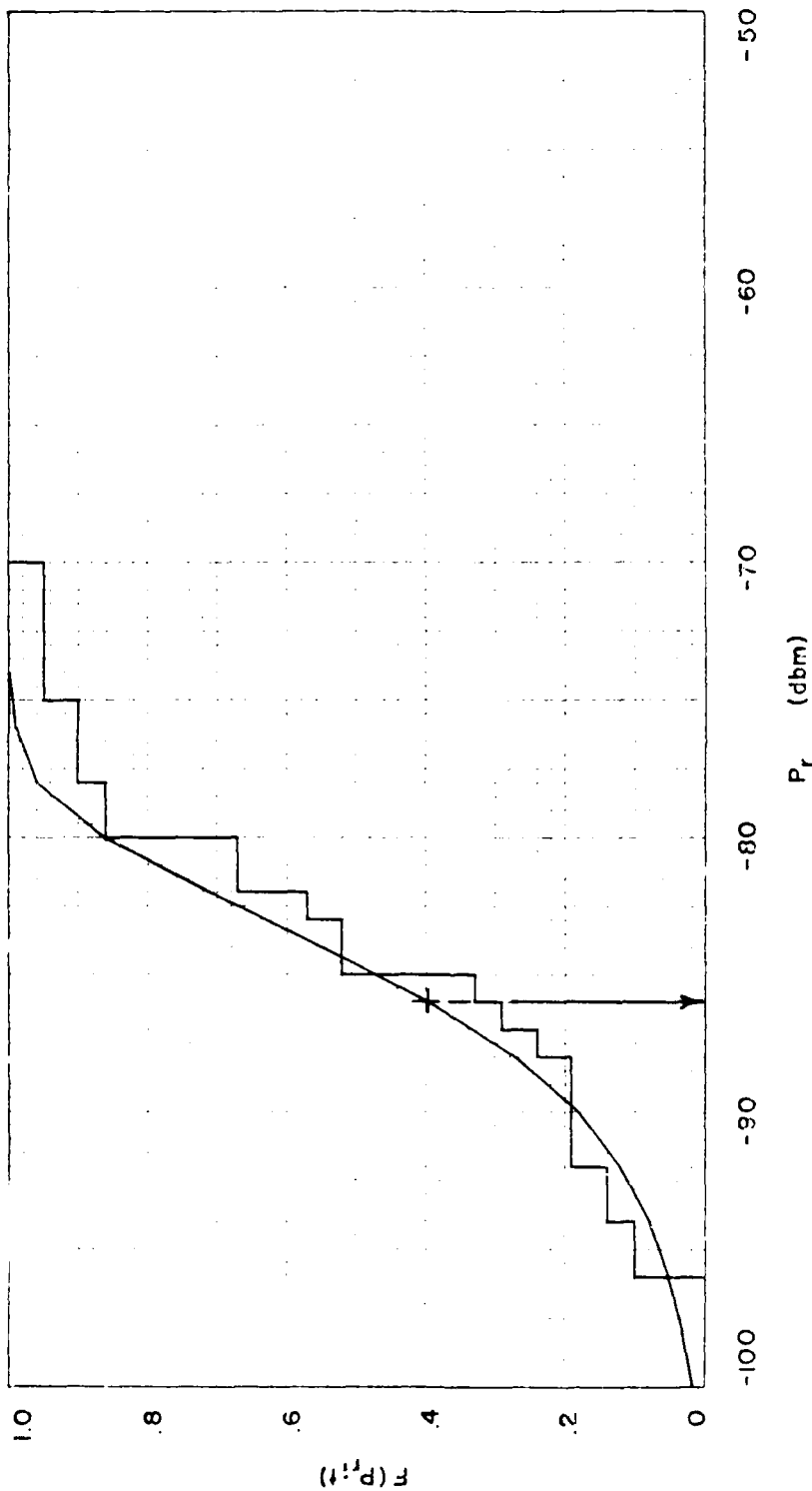


Figure 5. Comparison of Observed Data with the Assumed Power Distribution Function  
 (Sheet 1 of 3)

EXERCISE: SOLID SHIELD 77 DATES: 30 APR - 22 MAY 77  
 CIRCUIT: AF-562 RCV TERM: FT BRAGG RCVR NR: 1

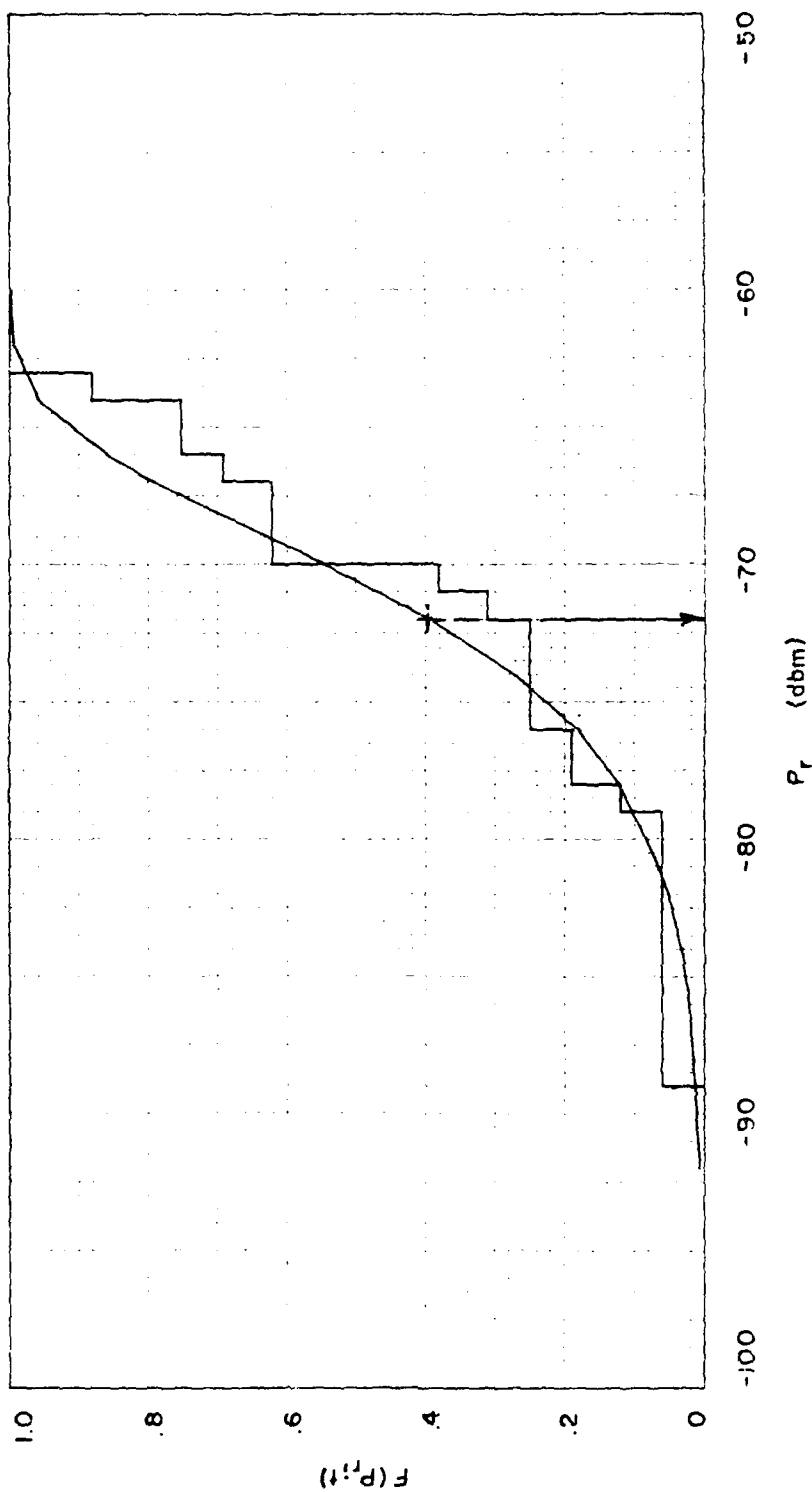


Figure 5. Comparison of Observed Data with the Assumed Power Distribution Function  
 (Sheet 2 of 3)

EXERCISE: BRAVE SHIELD XV DATES: 1-17 OCT 76

CIRCUIT: OP-11 RCV TERM: EGLIN AFB RCV NR: AVG

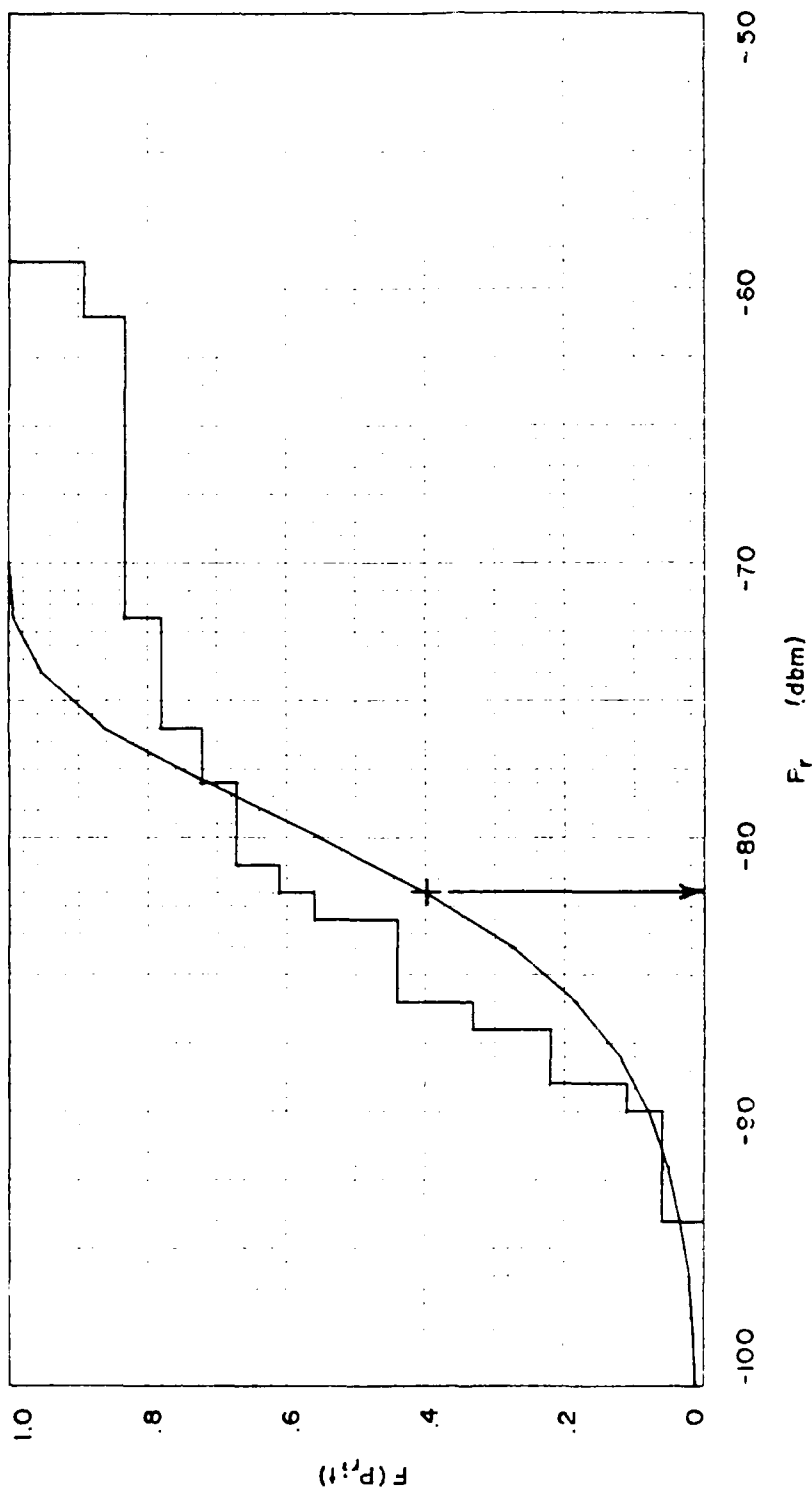


Figure 5. Comparison of Observed Data with the Assumed Power Distribution Function  
(Sheet 3 of 3)

Figure 5. Next the power distribution curve of Figure 4 is transferred to a piece of transparent acetate. The curve is then superimposed on the measured distribution plot in such a way as to give the best fit with the data. The value of  $k_0^2$  for each plot is also recorded for later use. Note that  $k_0^2$  is the value of  $P_r$  which corresponds to approximately  $F(P_r; t) = 0.4$ . Three superimposed power distribution curves and the resulting values of  $k_0^2$  are illustrated in Figure 5. The results of applying this procedure to each path are summarized in Table IV where a value of  $k_0^2$  is given to each distinct radio path. Note that in troposcatter propagation the path does not necessarily behave the same way in both directions, and the received power at one end of a link is not generally the same as the received power at the other end. Also, each TRC-97A has two receivers for diversity reception. Therefore, it is possible to associate up to four different sets of data with each radio link. Fewer sets of reported data indicate either incomplete observations or averaging of observations.

Several conclusions can be drawn from this manual curve fitting. First, the general shape of the distribution curves is enough like that of the assumed power distribution to support the existence of some correlation between the two. However, the correlation is obviously less than perfect, and more sophisticated statistical techniques would be required to quantify the degree of correlation. In many cases, the observed power distribution has a more gentle

slope than does the curve of Figure 4. The curves of Figure 5 are typical examples chosen from the paths in Table IV. They illustrate the range from good to poor correlation with the power distribution function of Eq (60).

Consider next the relationship between the received power distribution and the parameters of the proposed regression equation (Eq (69)). One would expect the received power, and therefore  $kr^2$ , to vary with some or all of the variables  $f$ ,  $d$ ,  $\theta$ , and  $N_s$ . For the most part, the available path data does not reflect specific operating frequencies and refractivity data is provided for only a few paths. Also information about the path geometry is generally not provided in sufficient detail to allow calculation of the scattering angle. The path length is available for each path, however, and  $kr^2$  is plotted as a function of path length for each of the paths in Table IV. The results are shown in Figure 6. It is now necessary to determine whether Figure 6 represents a reasonable relationship between  $kr^2$  and  $d$ . For this purpose, consider the relationship between  $L_s$  and  $d$  given by Eq (49). The path length appears in three terms of this expression. For typical values of  $\theta$  and  $d$  (see Appendix A), the factor  $\exp(-\theta d/40)$  remains very close to unity. Table III illustrates the range of values of the quantities  $(-10 \log d)$  and  $.33 \theta d$  for the paths in Appendix A. Clearly,  $(-10 \log d)$  is the dominant term, indicating that  $L_s$  (and therefore  $kr^2$ ) would decrease at a rate of



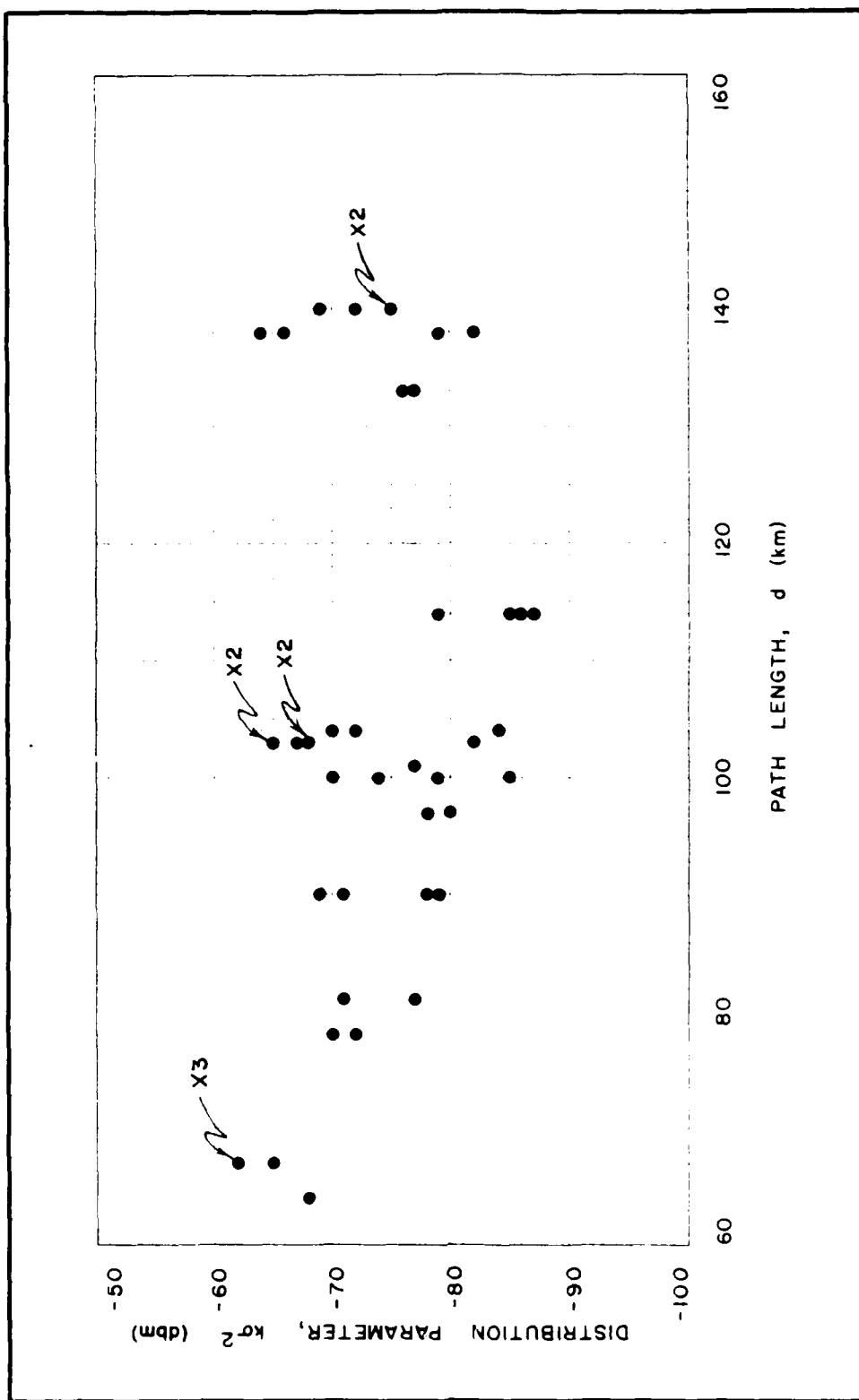


Figure 6. The Distribution Parameter  $k_0^2$  as a Function of Path Length

3 db/octave. This slope would obviously change for a different choice of the coefficient of the  $(\log d)$  term ( $a_2$  of Eq (69)). Such a regression line may well be contained within the data of Figure 6. Again, however, more sophisticated statistical methods are required to quantify the relationship between  $ko^2$  and  $d$ .

In summary, the path data presently available is not adequate to support further analysis. The correlation between observed data and the expected power distribution function (Eq (60)) cannot be conclusively stated. Further, sufficient information about  $f$ ,  $\theta$ , and  $N_g$  is not available to complete the regression analysis of Eq (69). The two obvious sources of this lack of correlation are the expected power distribution function and the data itself. The development of the power distribution assumes an underlying Rayleigh distribution for the envelope of the received signal voltage. Any deviation from a Rayleigh envelope would be reflected in the resulting power distribution. Regarding the data, some shortfall in the degree to which it represents the path would not be surprising. Measurement of received power levels in the field by operational units is usually undertaken to provide a general measure of system performance and not to support research activities. Measurements are taken infrequently, typically twice daily, and the duration of a particular radio link seldom exceeds a few weeks. Also, variations in measurement technique such as averaging between receivers at the same terminal, or

averaging between terminals would be expected to affect the results.

Two other possible causes for lack of correlation between Eq (60) and the data are anomalous propagation and mixed mode propagation. The path models developed here do not attempt to account for either of these phenomena. Anomalous propagation modes, such as ducting, are not uncommon and were almost certainly a factor in some of these paths. Also, propagation via obstacle gain diffraction may occur simultaneously with the troposcatter propagation mode. The diffraction mode requires a favorable path geometry, but is not uncommon over relatively short transhorizon paths.

One further shortcoming of the available data has surfaced during this analysis. Earlier in this section it was explained that  $L_s(t)$  is not directly observable, but could be derived from observations of  $P_r(t)$  by evaluating the remaining terms in the path model (see Eq (67), (68)). However the path data made available for this research does not contain enough detail about the path geometry and equipment configuration to evaluate  $b'$ .

### VIII. CONCLUSIONS

-----

This research began with an extremely general problem statement: current troposcatter prediction techniques are not always sufficiently accurate when applied to short range tactical troposcatter systems. Subsequent analysis has refined this into a very specific area of study which shows promise of improving path loss predictions. First, a general path model was developed based on the physical considerations of the troposcatter path. The general path model was then tailored to the AN/TRC-97A by a succession of comparisons with existing classical models and observed TRC-97A performance. Significant in this development has been the analysis of the importance of the various components in the path model. It has been concluded that inadequate modeling of the scattering loss,  $L_s(t)$ , is the most probable cause of inaccuracies in the overall path model. As a result, a modified scattering loss model was developed and a regression experiment was proposed to derive the coefficients in the model. After some evaluation of the available path data however, it was concluded that the data was not sufficient to support the regression analysis. Therefore, completion of the modified scattering loss model is not presently possible due to lack of suitable experimental data.

As a final note, inability of the data to fully support this research should not be taken as a criticism of the data

or its source. The path data made available for this study was collected during tactical training exercises for the purpose of field evaluation of radio system performance. The data is inherently sparse and not intended to support a research effort. It is possible that data suitable for the completion of this study can be made available only through a specific data collection effort.

## IX. RECOMMENDATIONS

The primary recommendation resulting from this research is that suitable path data be collected to verify the power distribution and complete the proposed regression analysis. The data provided for the current research was collected by tactical units on normal training exercises. Such data has the advantage of being representative of a variety of climatic regions and path profiles. However these tactical systems are seldom established for more than a few weeks at a time and the path data normally collected is inherently sparse. An alternate source of path data would be an organization which operates similar equipment in a research and development environment, such as the Air Force's Electronic Systems Division.

In order to complete the proposed regression analysis, data is required on both the received signal and the path geometry. Continuous recording of received signal level would be considerably more representative of the path than discrete measurements. Path geometry information must be in sufficient detail to permit calculation of the parameters of the regression equation ( $f$ ,  $d$ ,  $\theta$ ,  $R_s$ , and  $V(a_p)$ ) as well as the other loss components (e.g.,  $H_o$ ,  $A_d$ , etc.) If Data Sheet B-5 (AFCSP 100-61, Vol II) were completed for each path, the required geometry information would be available.

Several other recommendations for further investigation are also offered. First, present predictions estimate

refractivity from a chart of minimum monthly mean values. Incorporation of refractivity data more specific to a given path should produce more accurate path predictions. Second, current methods are based on values of surface refractivity, from which the refractivity within the scattering volume is extrapolated by a simple formula. The accuracy of this extrapolation at low altitudes (typical of the scattering volume for a short troposcatter path) may warrant further study. Also, it may be worthwhile to treat the refractivity as a quantity which varies throughout the scattering volume rather than considering only its value at the center of the scattering volume.

# BIBLIOGRAPHY

1. AFCSP 100-61, Volume II. Tactical Communications System Performance Standards and Assessment. Richards Gebaur AFB, Missouri: Air Force Communications Service, 1 September 1972 (Change 1 - 1 June 1973).
2. Bello, Phillip A. "A Troposcatter Channel Model," IEEE Transactions on Communications Technology, COM-17: 130-137 (April 1969).
3. Booker, H.G. and W.E. Gordon. "A Theory of Radio Scattering in the Troposphere," Proceedings of the IRE, 38: 401-412 (April 1950).
4. Norton, Kenneth A. "Point-to-Point Radio Relaying via the Scatter Mode of Tropospheric Propagation," IRE Transactions on Communications Systems, CS-4: 39-49 (March 1956).
5. Panter, Philip F. Communication Systems Design: Line-of-Sight and Tropo-Scatter Systems. New York: McGraw-Hill Book Company, 1972.
6. Papoulis, Athanasios. Probability, Random Variables, and Stochastic Processes. New York: McGraw-Hill Book Company, 1965.
7. Pusone, E. A Predictive Model Based on Physical Considerations for Troposcatter Communications Links. Technical Memorandum STC-TM-589. The Hague, Netherlands: SHAPE Technical Centre, November 1958/78. (AD B033 183)
8. Recommendations and Reports of the CCIR, 1978. XIV Plenary Assembly, Kyoto (Japan), Volume V, Propagation in Non-ionized Media. Geneva, Switzerland: International Radio Consultative Committee (CCIR) of the International Telecommunications Union (ITU), 1978. (PB 298 025/5GA)
9. Rice, P.L., A.G. Longley, K.A. Norton, and A.P. Baris. Transmission Loss Predictions for Tropospheric Communication Circuits. NBS Technical Note 101, Volume I. Boulder, Colorado: Environmental Science Services Administration, 7 May 1965 (Revised 1 January 1967). (AD 687 320)



10. Rice, P.H., A.G. Longley, K.A. Norton, and A.P. Barsis. Transmission Loss Predictions for Tropospheric Communication Circuits. NBS Technical Note 101, Volume II. Boulder, Colorado: Environmental Science Services Administration, 7 May 1965 (Revised 1 January 1967). (AD 687 821)
11. Rider, G.C. "Median Signal Level Prediction for Tropospheric Scatter," The Marconi Review, Third Quarter: 203-210 (1962).
12. Technical Order 31R5-2TRC97-12. Applications Manual - Radio Set, Type AN/TRC-97. Washington, D.C.: Department of the Air Force, 15 April 1969 (Change 3 - 1 February 1980).
13. Wozencraft, John M. and Irwin M. Jacobs. Principles of Communication Engineering. New York: John Wiley and Sons, 1965.
14. Yeh, Leang P. "Simple Methods for Designing Troposcatter Circuits," IRE Transactions on Communications Systems, CS-8: 193-198 (September 1960).

AD-A100 826

AIR FORCE INST OF TECH WRIGHT-PATTERSON AFB OH SCH00--ETC F/6 17/2.1  
TRANSMISSION LOSS PREDICTION FOR THE AN/TRC-97A OVER A TROPOSPH--ETC(U)  
DEC 80 H S STORY  
AFIT/GE/EE/80D-40

UNCLASSIFIED

NL

2 OF 2  
AD A  
100826

END  
DATE  
FILMED  
7-81  
DTIC

## Appendix A

### AFCSP 100-61 Path Loss Predictions for

#### ----- Eight Hypothetical Path Cases -----

This appendix contains the calculation of selected path parameters for eight hypothetical troposcatter paths. The eight paths are intended to represent the range of typical values expected from an AN/TRC-97A radio system under certain simplifying constraints. The paths consider the eight possible combinations of maximum and minimum operating frequency (4.4 - 5.0 Ghz), maximum and minimum path length (60 - 160 km), and maximum and minimum surface refractivity (290 - 390). In all cases, the OA-7160A/TRC-97A parabolic antenna is assumed (8-foot diameter, 15-foot height to center). Rather than attempt to account for an infinite number of terrain configurations, smooth earth is assumed. The procedures used are from AFCSP 100-61, Vol II.

DATA SHEET		SITE NO. 1 (TX)		DATE
B-5: TROPOSCATTER PATH CALCULATIONS		SITE NO. 2 (RX)		LINE NO.
ITEM NO.	PERFORMANCE FACTOR	VALUE	UNITS	REMARKS
1	Terminal Elevation Above Sea Level, TX, $h_{t1}$	0	km	From Path Profile
2	Terminal Elevation Above Sea Level, RX, $h_{t2}$	0	km	From Path Profile
3	Antenna Elevation Above Sea Level, TX, $h_{a1}$	.005	km	From Path Profile
4	Antenna Elevation Above Sea Level, RX, $h_{a2}$	.005	km	From Path Profile
5	Radio Horizon Elevation Above Sea Level, TX, $h_{L1}$	0	km	From Path Profile
6	Radio Horizon Elevation Above Sea Level, RX, $h_{L2}$	0	km	From Path Profile
7	Distance to Radio Horizon, TX, $d_{L1}$	8.7	km	From Path Profile
8	Distance to Radio Horizon, RX, $d_{L2}$	8.7	km	From Path Profile
9	Path Length, $d$	60	km	From Path Profile
10	Average Elevation of Radio Horizons, $h_{a1}$	0	km	(Item 5 + Item 6)/2
11	Average Elevation of Terminals, $h_{a2}$	0	km	(Item 1 + Item 2)/2
12	Average Elevation of Refracting Surface, $h_0$	0	km	Minimum (Item 10, Item 11)
13	Mean Refractivity, $N_0$	--		See Figure 4-1
14	Refractivity at Refracting Surface, $N_0$	290		(Item 13) exp $(-0.10 \times 7 \times \text{Item 12})$
15	Effective Earth's Radius, $a$	8320	km	See Figure 4-2
16	Mean Elevation, TX Terminal to TX Radio Horizon, $h_1$	0	km	From Path Profile
17	Mean Elevation, RX Terminal to RX Radio Horizon, $h_2$	0	km	From Path Profile
18	Effective Antenna Height, TX, $h_{te}$	.005	km	If Item 16 > Item 1; Item 3 - Item 1 If Item 16 < Item 1; Item 3 - Item 16
19	Effective Antenna Height, RX, $h_{re}$	.005	km	If Item 17 > Item 2, Item 4 - Item 2 If Item 17 < Item 2, Item 4 - Item 17
20	Antenna Elevation Angle, TX, $\theta_{e1}$	-.001098	rad	$\frac{\text{Item 5} - \text{Item 3}}{\text{Item 7}} - \frac{\text{Item 7}}{2 \times \text{Item 15}}$
21	Antenna Elevation Angle, RX, $\theta_{e2}$	-.001098	rad	$\frac{\text{Item 6} - \text{Item 4}}{\text{Item 8}} - \frac{\text{Item 8}}{2 \times \text{Item 15}}$
22	$\alpha_0$	+.002508	rad	$\frac{\text{Item 6}}{2 \times \text{Item 15}} - \text{Item 20} + \frac{\text{Item 3} - \text{Item 4}}{\text{Item 9}}$
23	$\beta_0$	+.002508	rad	$\frac{\text{Item 9}}{2 \times \text{Item 15}} + \text{Item 21} + \frac{\text{Item 4} - \text{Item 3}}{\text{Item 9}}$
24	Scatter Angle, $\theta_0$	+.005016	rad	Item 22 + Item 23
25	Path Asymmetry Parameter, $s$	1		Item 22/Item 23
26	$\theta_d$	--	km	Item 24 x Item 9

AFCS FORM 709 OCT 74 REVISED

RPT PAGE NO.

PAGE 1 OF 5 PAGES

Figure A1. Case 1 Troposcatter Path Calculation  
(Sheet 1 of 2)

ITEM NO.	PERFORMANCE FACTOR	VALUE	UNITS	REMARKS
27	Attenuation Function, $F(\theta d)$	--	dB	$\theta d \leq 10$ , See Figure 5-3 $\theta d > 10$ , See Figures 5-3 thru 5-5 If $s > 1$ , use $1/s$
28	Operating Frequency, $f$	4.4	GHz	Link Specifications
29	$r_1$	8.69		$6.3006 \times \text{Item 9} \times \text{Item 28} \times \text{Item 18}$
30	$r_2$	8.69		$6.3006 \times \text{Item 9} \times \text{Item 28} \times \text{Item 19}$
31	$h_0$ NOTE: If $r_1$ and $r_2 > 15$ , set $h_0 = 0$	.07524	km	$\frac{(\text{Item 25}) \times (\text{Item 9}) / (\text{Item 24})}{(1 + \text{Item 25})^2}$
32	Normalized Height of Horizon Ray Crossover, $n_0$	.0356		See Figure 5-6
33	NOTE: If $n_0 \geq 1$ , Use Items 34 - 37 Otherwise go to Step 38	--		$\frac{\text{Item 30}}{(\text{Item 29}) \times (\text{Item 25})}$
34	$H_0(r_1)$	--	dB	See Figure 5-7 If $n_0 > 5$ , use 5
35	$H_0(r_2)$	--	dB	See Figure 5-7 If $n_0 > 5$ , use 5
36	$\Delta H_0$	--	dB	See Figure 5-8
37	Frequency Gain Function, $H_0$ NOTE: If $n_0 < 1$ , use Items 38 - 43	--	dB	$1/2 \times (\text{Item 34} + \text{Item 35}) + \text{Item 36}$
38	$H_0(r_1)$	1.40	dB	See Figure 5-7. Use $n_0 = 1$
39	$H_0(r_2)$	1.40	dB	See Figure 5-7. Use $n_0 = 1$
40	$\Delta H_0$	0	dB	See Figure 5-8 Use $n_0 = 1$
41	Frequency Gain Function, $H_0$ , $n_0 = 1$	1.40	dB	$1/2 \times (\text{Item 38} + \text{Item 39}) + \text{Item 40}$
42	Frequency Gain Function, $H_0$ , $n_0 = 0$	1.20	dB	See Figure 5-9 Use $n_0 = 0$
43	Frequency Gain Function, $H_0$	1.21	dB	Item 42 + Item 32 (Item 41 - Item 42)
44	Frequency Gain Function, $H_0$	1.21	dB	Item 37 or Item 43
45	Atmospheric Absorption, $A_a$	--	dB	See Figure 4-7
46	Basic Transmission Loss for a Scatter Path, $L_{bsr}$	--	dB	$30 \log (\text{Item 28}) - 10 \log (\text{Item 9}) + \text{Item 27} + \text{Item 44} + \text{Item 45} + 90$
47	$d_{s1}$	18.41	km	$65(0.1/\text{Item 28})^{1/3}$
48	$d_L$	18.43	km	$130.3d \sqrt{\text{Item 18}} + \sqrt{\text{Item 19}}$
49	Effective Distance, $d_e$	153	km	If Item 9 $\leq$ Item 47 + Item 48, $130 \times \text{Item 9} / (\text{Item 47} + \text{Item 48})$ If Item 9 $>$ Item 47 + Item 48, $130 + \text{Item 9} - \text{Item 47} - \text{Item 48}$
50	Long Term Fading Parameter for Climatic Region n, $Y_n(50, d_e)$	--	dB	See Figure 4-8
51	Long Term Fading Parameter for Climatic Region n, $Y_n(1/2, 9, d_e)$	--	dB	See Figures 4-9 through 4-25

RPT PAGE NO.

PAGE 2 OF 3 PAGES

Figure A1. Case 1 Troposcatter Path Calculation  
(Sheet 2 of 2)

DATA SHEET				SITE NO. 1 (Tx)	DATE
B-5: TROPOSCATTER PATH CALCULATIONS				SITE NO. 2 (Rx)	LINE NO.
ITEM NO.	PERFORMANCE FACTOR	VALUE	UNITS	REMARKS	
1	Terminal Elevation Above Sea Level, TX, $h_{tg}$	0	km	From Path Profile	
2	Terminal Elevation Above Sea Level, RX, $h_{rg}$	0	km	From Path Profile	
3	Antenna Elevation Above Sea Level, TX, $h_{ts}$	.005	km	From Path Profile	
4	Antenna Elevation Above Sea Level, RX, $h_{rs}$	.005	km	From Path Profile	
5	Radio Horizon Elevation Above Sea Level, TX, $h_{Lt}$	0	km	From Path Profile	
6	Radio Horizon Elevation Above Sea Level, RX, $h_{Lr}$	0	km	From Path Profile	
7	Distance to Radio Horizon, TX, $d_{Lt}$	9.9	km	From Path Profile	
8	Distance to Radio Horizon, RX, $d_{Lr}$	9.9	km	From Path Profile	
9	Path Length, $d$	60	km	From Path Profile	
10	Average Elevation of Radio Horizons, $h_{a1}$	0	km	(Item 5 + Item 6)/2	
11	Average Elevation of Terminals, $h_{a2}$	0	km	(Item 1 + Item 2)/2	
12	Average Elevation of Refracting Surface, $h_s$	0	km	Minimum (Item 10, Item 11)	
13	Mean Refractivity, $N_0$	--		See Figure 4-1	
14	Refractivity at Refracting Surface, $N_s$	390		(Item 13) exp $(-0.10 \cdot 7 \times \text{Item 12})$	
15	Effective Earth's Radius, $a$	10,820	km	See Figure 4-2	
16	Mean Elevation, TX Terminal to TX Radio Horizon, $h_{t1}$	0	km	From Path Profile	
17	Mean Elevation, RX Terminal to RX Radio Horizon, $h_{r1}$	0	km	From Path Profile	
18	Effective Antenna Height, TX, $h_{te}$	.005	km	If Item 16 > Item 1, Item 3 - Item 1 If Item 16 < Item 1, Item 3 - Item 16	
19	Effective Antenna Height, RX, $h_{re}$	.005	km	If Item 17 > Item 2, Item 4 - Item 2 If Item 17 < Item 2, Item 4 - Item 17	
20	Antenna Elevation Angle, TX, $\theta_{et}$	-.000963	rad	$\frac{\text{Item 5} - \text{Item 3}}{\text{Item 7}} - \frac{\text{Item 7}}{2 \times \text{Item 15}}$	
21	Antenna Elevation Angle, RX, $\theta_{er}$	-.000963	rad	$\frac{\text{Item 6} - \text{Item 4}}{\text{Item 8}} - \frac{\text{Item 8}}{2 \times \text{Item 15}}$	
22	$\alpha_0$	+.001810	rad	$\frac{\text{Item 9}}{2 \times \text{Item 15}} + \text{Item 20} + \frac{\text{Item 3} - \text{Item 4}}{\text{Item 9}}$	
23	$\beta_0$	+.001810	rad	$\frac{\text{Item 9}}{2 \times \text{Item 15}} + \text{Item 21} + \frac{\text{Item 4} - \text{Item 3}}{\text{Item 9}}$	
24	Scatter Angle, $\theta_0$	+.003619	rad	Item 22 + Item 23	
25	Path Asymmetry Parameter, $s$	1		Item 22/Item 23	
26	$\theta_d$	--	km	Item 24 $\times$ Item 9	

AFCS FORM 709 OCT 74 REVISED

RPT PAGE NO.

PAGE 1 OF 3 PAGES

Figure A2. Case 2 Troposcatter Path Calculation  
(Sheet 1 of 2)

ITEM NO.	PERFORMANCE FACTOR	VALUE	UNITS	REMARKS
*27	Attenuation Function, $F(\theta d)$	--	dB	$\theta d \leq 10$ , See Figure 5-3 $\theta d > 10$ , See Figures 5-2 thru 5-5 If $s > 1$ , use $1/s$
28	Operating Frequency, $f$	4.4	GHz	Link Specifications
*29	$r_1$	8.69		$6.5808 \times \text{Item 9} \times \text{Item 28} \times \text{Item 16}$
*30	$r_2$	8.69		$6.5808 \times \text{Item 9} \times \text{Item 28} \times \text{Item 19}$
31	$h_0$ NOTE: If $r_1$ and $r_2 > 15$ , set $h_0 = 0$	.05428	km	$\frac{(\text{Item 25}) \times (\text{Item 9})(\text{Item 24})}{(1 + \text{Item 25})^2}$
32	Normalized Height of Horizon Ray Crossover, $n_s$	.0304		See Figure 5-6
33	NOTE: If $n_s \geq 1$ , Use Items 34 - 37 Otherwise go to Step 38	--		$\frac{\text{Item 30}}{(\text{Item 29}) \times (\text{Item 25})}$
34	$H_0(r_1)$	--	dB	See Figure 5-7 If $n_s > 5$ , use 5
35	$H_0(r_2)$	--	dB	See Figure 5-7 If $n_s > 5$ , use 5
36	$\Delta H_0$	--	dB	See Figure 5-8
37	Frequency Gain Function, $H_0$ NOTE: If $n_s < 1$ , use Items 38 - 43	--	dB	$1/2 \times (\text{Item 34} + \text{Item 35}) + \text{Item 36}$
38	$H_0(r_1)$	1.40	dB	See Figure 5-7. Use $n_s = 1$
39	$H_0(r_2)$	1.40	dB	See Figure 5-7. Use $n_s = 1$
40	$\Delta H_0$	0	dB	See Figure 5-8 Use $n_s = 1$
41	Frequency Gain Function, $H_0$ , $n_s = 1$	1.40	dB	$1/2 \times (\text{Item 38} + \text{Item 39}) + \text{Item 40}$
42	Frequency Gain Function, $H_0$ , $n_s = 0$	1.20	dB	See Figure 5-9 Use $n_s = 0$
43	Frequency Gain Function, $H_0$	1.21	dB	$\text{Item 42} + \text{Item 32} (\text{Item 41} - \text{Item 42})$
44	Frequency Gain Function, $H_0$	1.21	dB	Item 37 or Item 43
45	Atmospheric Absorption, $A_a$	--	dB	See Figure 4-7
46	Basic Transmission Loss for a Scatter Path, $L_{bsr}$	--	dB	$30 \log (\text{Item 28}) - 20 \log (\text{Item 9}) + \text{Item 27} + \text{Item 44} + \text{Item 45} + 90$
47	$d_{e1}$	18.41	km	$65(0.1/\text{Item 28})^{1/3}$
*48	$d_L$	18.43	km	$130.3 \sqrt{\text{Item 18} + \sqrt{\text{Item 19}}}$
49	Effective Distance, $d_e$	153	km	If $\text{Item 9} \leq \text{Item 47} + \text{Item 48}$ : $130 \times \text{Item 9}/(\text{Item 47} + \text{Item 48})$ If $\text{Item 9} > \text{Item 47} + \text{Item 48}$ : $130 + \text{Item 9} - \text{Item 47} - \text{Item 48}$
50	Long Term Fading Parameter for Climatic Region n, $V_n(50, d_e)$	--	dB	See Figure 4-8
51	Long Term Fading Parameter for Climatic Region n, $V_n(99.9, d_e)$	--	dB	See Figures 4-9 through 4-25

RPT PAGE NO.

PAGE 2 OF 8 PAGES

Figure A2. Case 2 Troposcatter Path Calculation  
(Sheet 2 of 2)

DATA SHEET		SITE NO. 1 (TA)		DATE
B.5: TROPOSCATTER PATH CALCULATIONS		SITE NO. 2 (RB)		LINK NO.
ITEM NO.	PERFORMANCE FACTOR	VALUE	UNITS	REMARKS
1	Terminal Elevation Above Sea Level, TX, $h_{t1}$	0	km	From Path Profile
2	Terminal Elevation Above Sea Level, RX, $h_{r1}$	0	km	From Path Profile
3	Antenna Elevation Above Sea Level, TX, $h_{t2}$	.005	km	From Path Profile
4	Antenna Elevation Above Sea Level, RX, $h_{r2}$	.005	km	From Path Profile
5	Radio Horizon Elevation Above Sea Level, TX, $h_{L1}$	0	km	From Path Profile
6	Radio Horizon Elevation Above Sea Level, RX, $h_{L2}$	0	km	From Path Profile
7	Distance to Radio Horizon, TX, $d_{L1}$	8.7	km	From Path Profile
8	Distance to Radio Horizon, RX, $d_{L2}$	8.7	km	From Path Profile
9	Path Length, $d$	160	km	From Path Profile
10	Average Elevation of Radio Horizons, $h_{a1}$	0	km	(Item 5 + Item 6)/2
11	Average Elevation of Terminals, $h_{a2}$	0	km	(Item 1 + Item 2)/2
12	Average Elevation of Refracting Surfaces, $h_s$	0	km	Minimum (Item 10, Item 11)
13	Mean Refractivity, $N_0$	--		See Figure 4-1
14	Refractivity at Refracting Surface, $N_s$	290		(Item 13) exp $(-0.10 \times 7 \times \text{Item 12})$
15	Effective Earth's Radius, $a$	8320	km	See Figure 4-2
16	Mean Elevation, TX Terminal to TX Radio Horizon, $\bar{h}_t$	0	km	From Path Profile
17	Mean Elevation, RX Terminal to RX Radio Horizon, $\bar{h}_r$	0	km	From Path Profile
18	Effective Antenna Height, TX, $h_{te}$	.005	km	If Item 16 > Item 1, Item 3 - Item 1 If Item 16 < Item 1, Item 3 - Item 16
19	Effective Antenna Height, RX, $h_{re}$	.005	km	If Item 17 > Item 2, Item 4 - Item 2 If Item 17 < Item 2, Item 4 - Item 17
20	Antenna Elevation Angle, TX, $\theta_{et}$	-.001098	rad	$\frac{\text{Item 5} - \text{Item 3}}{\text{Item 7}} = \frac{\text{Item 7}}{2 \times \text{Item 15}}$
21	Antenna Elevation Angle, RX, $\theta_{er}$	-.001098	rad	$\frac{\text{Item 6} - \text{Item 4}}{\text{Item 8}} = \frac{\text{Item 8}}{2 \times \text{Item 15}}$
22	$\alpha_0$	+.008517	rad	$\frac{\text{Item 9}}{2 \times \text{Item 15}} + \text{Item 20} + \frac{\text{Item 3} - \text{Item 4}}{\text{Item 9}}$
23	$\beta_0$	+.008517	rad	$\frac{\text{Item 6}}{2 \times \text{Item 15}} + \text{Item 21} + \frac{\text{Item 4} - \text{Item 3}}{\text{Item 9}}$
24	Scatter Angle, $\theta_0$	+.017035	rad	Item 22 + Item 23
25	Path Asymmetry Parameter, $s$	1		Item 22/Item 23
26	$\theta_d$	--	km	Item 24 $\times$ Item 9

AFCS FORM 709 REVISED

RPT PAGE NO.

PAGE 1 OF 3 PAGES

Figure A3. Case 3 Troposcatter Path Calculation  
(Sheet 1 of 2)



ITEM NO.	PERFORMANCE FACTOR	VALUE	UNITS	REMARKS
*27	Attenuation Function, $F(\theta d)$	--	dB	$\theta d \leq 10$ , See Figure 5-3 $\theta d > 10$ , See Figures 5-2 thru 5-5 If $s > 1$ , use $1/s$
28	Operating Frequency, $f$	4.4	GHz	Link Specifications
*29	$r_1$	23.16		$6.5608 \times \text{Item 9} \times \text{Item 28} \times \text{Item 18}$
*30	$r_2$	23.16		$6.5608 \times \text{Item 9} \times \text{Item 28} \times \text{Item 19}$
31	$h_0$ NOTE: If $r_1$ and $r_2 > 15$ , set $h_0 = 0$	--	km	$\frac{(\text{Item 25}) \times (\text{Item 9})(\text{Item 24})}{(1 + \text{Item 25})^2}$
32	Normalized Height of Horizon Ray Crossover, $n_s$	--		See Figure 5-6
33	$q$ NOTE: If $n_s \geq 1$ , Use Items 34 - 37 Otherwise go to Step 38	--		$\frac{\text{Item 30}}{(\text{Item 29}) \times (\text{Item 25})}$
34	$H_0(r_1)$	--	dB	See Figure 5-7 If $n_s > 5$ , use 5
35	$H_0(r_2)$	--	dB	See Figure 5-7 If $n_s > 5$ , use 5
36	$\Delta H_0$	--	dB	See Figure 5-8
37	Frequency Gain Function, $H_0$ NOTE: If $n_s < 1$ , use Items 38 - 43	--	dB	$1/2 \times (\text{Item 34} + \text{Item 35}) + \text{Item 36}$
38	$H_0(r_1)$	--	dB	See Figure 5-7. Use $n_s = 1$
39	$H_0(r_2)$	--	dB	See Figure 5-7. Use $n_s = 1$
40	$\Delta H_0$	--	dB	See Figure 5-8 Use $n_s = 1$
41	Frequency Gain Function, $H_0$ , $n_s = 1$	--	dB	$1/2 \times (\text{Item 38} + \text{Item 39}) + \text{Item 40}$
42	Frequency Gain Function, $H_0$ , $n_s = 0$	--	dB	See Figure 5-9 Use $n_s = 0$
43	Frequency Gain Function, $H_0$	0	dB	Item 42 + Item 32 (Item 41 - Item 42)
44	Frequency Gain Function, $H_0$	0	dB	Item 37 or Item 43
45	Atmospheric Absorption, $A_a$	--	dB	See Figure 4-7
46	Basic Transmission Loss for a Scatter Path, $L_{bst}$	--	dB	$30 \log (\text{Item 28}) - 20 \log (\text{Item 9}) + \text{Item 27} + \text{Item 44} + \text{Item 45} + 90$
47	$d_{01}$	18.41	km	$65(0.1/\text{Item 28})^{1/3}$
*48	$d_L$	18.43	km	$126.34 \sqrt{\sqrt{\text{Item 18}} + \sqrt{\text{Item 19}}}$
49	Effective Distance, $d_e$	253	km	If Item 9 $\leq$ Item 47 + Item 48, $130 \times \text{Item 9}/(\text{Item 47} + \text{Item 48})$ If Item 9 $>$ Item 47 + Item 48, $130 + \text{Item 9} - \text{Item 47} - \text{Item 48}$
50	Long Term Fading Parameter for Climatic Region n, $V_n(40, d_e)$	--	dB	See Figure 4-8
51	Long Term Fading Parameter for Climatic Region n, $Y_n(99.9, d_e)$	--	dB	See Figures 4-9 through 4-25

RPT PAGE NO.

PAGE 2 OF 6 PAGES

Figure A3. Case 3 Troposcatter Path Calculation  
(Sheet 2 of 2)

DATA SHEET			SITE NO. 1 (TX)	DATE
B-5: TROPOSCATTER PATH CALCULATIONS			SITE NO. 2 (RX)	LINK NO.
ITEM NO.	PERFORMANCE FACTOR	VALUE	UNITS	REMARKS
1	Terminal Elevation Above Sea Level, TX, $h_{t1}$	0	km	From Path Profile
2	Terminal Elevation Above Sea Level, RX, $h_{r1}$	0	km	From Path Profile
3	Antenna Elevation Above Sea Level, TX, $h_{t2}$	.005	km	From Path Profile
4	Antenna Elevation Above Sea Level, RX, $h_{r2}$	.005	km	From Path Profile
5	Radio Horizon Elevation Above Sea Level, TX, $h_{L1}$	0	km	From Path Profile
6	Radio Horizon Elevation Above Sea Level, RX, $h_{L2}$	0	km	From Path Profile
7	Distance to Radio Horizon, TX, $d_{L1}$	9.9	km	From Path Profile
8	Distance to Radio Horizon, RX, $d_{L2}$	9.9	km	From Path Profile
9	Path Length, $d$	160	km	From Path Profile
10	Average Elevation of Radio Horizons, $h_{s1}$	0	km	(Item 5 + Item 6)/2
11	Average Elevation of Terminals, $h_{s2}$	0	km	(Item 1 + Item 2)/2
12	Average Elevation of Refracting Surface, $h_s$	0	km	Minimum (Item 10, Item 11)
13	Mean Refractivity, $N_0$	--		See Figure 4-1
14	Refractivity at Refracting Surface, $N_s$	390		(Item 13) exp $(-0.30 \times 7 \times \text{Item 12})$
15	Effective Earth's Radius, $a$	10,820	km	See Figure 4-2
16	Mean Elevation, TX Terminal to TX Radio Horizon, $\bar{h}_1$	0	km	From Path Profile
17	Mean Elevation, RX Terminal to RX Radio Horizon, $\bar{h}_2$	0	km	From Path Profile
18	Effective Antenna Height, TX, $h_{te}$	.005	km	If Item 16 > Item 1, Item 3 - Item 1 If Item 16 < Item 1, Item 3 - Item 16
19	Effective Antenna Height, RX, $h_{re}$	.005	km	If Item 17 > Item 2, Item 4 - Item 2 If Item 17 < Item 2, Item 4 - Item 17
20	Antenna Elevation Angle, TX, $\theta_{et}$	-.000963	rad	$\frac{\text{Item 5} - \text{Item 3}}{\text{Item 7}} = \frac{\text{Item 7}}{2 \times \text{Item 15}}$
21	Antenna Elevation Angle, RX, $\theta_{er}$	-.000963	rad	$\frac{\text{Item 6} - \text{Item 4}}{\text{Item 8}} = \frac{\text{Item 8}}{2 \times \text{Item 15}}$
22	$\alpha_0$	+.006431	rad	$\frac{\text{Item 4}}{2 \times \text{Item 15}} + \text{Item 20} + \frac{\text{Item 3} - \text{Item 4}}{\text{Item 9}}$
23	$\beta_0$	+.006431	rad	$\frac{\text{Item 6}}{2 \times \text{Item 15}} + \text{Item 21} + \frac{\text{Item 4} - \text{Item 3}}{\text{Item 9}}$
24	Scatter Angle, $\theta_s$	+.012861	rad	Item 22 + Item 23
25	Path Asymmetry Parameter, $s$	1		Item 22/Item 23
26	$\theta_d$	--	km	Item 24 x Item 9

AFC3 FORM 709 OCT 74 REVISED

RPT PAGE NO.

PAGE 1 OF 5 PAGES

Figure A4. Case 4 Troposcatter Path Calculation  
(Sheet 1 of 2)

ITEM NO.	PERFORMANCE FACTOR	VALUE	UNITS	REMARKS
*27	Attenuation Function, $F(\theta d)$	--	dB	$\theta d \leq 10$ , See Figure 5-3 $\theta d > 10$ , See Figures 5-3 thru 5-5 If $s > 1$ , use $1/s$
28	Operating Frequency, $f$	1.4	GHz	Link Specifications
*29	$r_1$	23.16		$6.3008 \times \text{Item 9} \times \text{Item 28} \times \text{Item 18}$
*30	$r_2$	23.16		$6.3008 \times \text{Item 9} \times \text{Item 28} \times \text{Item 19}$
31	$h_0$ NOTE: If $r_1$ and $r_2 > 15$ , set $h_0 = 0$	--	km	$\frac{(\text{Item 25}) \times (\text{Item 9}) / (\text{Item 24})}{(1 + \text{Item 25})^2}$
32	Normalized Height of Horizon Ray Crossover, $n_s$	--		See Figure 5-6
33	NOTE: If $n_s \geq 1$ , Use Items 34 - 37 Otherwise go to Step 38	--		$\frac{\text{Item 30}}{(\text{Item 29}) \times (\text{Item 25})}$
34	$H_0(r_1)$	--	dB	See Figure 5-7 If $n_s > 5$ , use 5
35	$H_0(r_2)$	--	dB	See Figure 5-7 If $n_s > 5$ , use 5
36	$\Delta H_0$	--	dB	See Figure 5-8
37	Frequency Gain Function, $H_0$ NOTE: If $n_s < 1$ , use Items 38 - 43	--	dB	$1/2 \times (\text{Item 34} + \text{Item 35}) + \text{Item 36}$
38	$H_0(r_1)$	--	dB	See Figure 5-7. Use $n_s = 1$
39	$H_0(r_2)$	--	dB	See Figure 5-7. Use $n_s = 1$
40	$\Delta H_0$	--	dB	See Figure 5-8. Use $n_s = 1$
41	Frequency Gain Function, $H_0$ , $n_s = 1$	--	dB	$1/2 \times (\text{Item 38} + \text{Item 39}) + \text{Item 40}$
42	Frequency Gain Function, $H_0$ , $n_s = 0$	--	dB	See Figure 5-9. Use $n_s = 0$
43	Frequency Gain Function, $H_0$	--	dB	Item 42 + Item 32 (Item 41 - Item 42)
44	Frequency Gain Function, $H_0$	0	dB	Item 37 or Item 43
45	Atmospheric Absorption, $A_a$	--	dB	See Figure 4-7
46	Basic Transmission Loss for a Scatter Path, $L_{bst}$	--	dB	$30 \log (\text{Item 28}) - 20 \log (\text{Item 9}) + \text{Item 27} + \text{Item 44} + \text{Item 45} + 90$
47	$d_{s1}$	18.41	km	$65(0.1/\text{Item 28})^{1/3}$
*48	$d_L$	18.43	km	$130.34 \sqrt{\text{Item 18} + \sqrt{\text{Item 18}}}$
49	Effective Distance, $d_e$	253	km	If Item 9 $\leq$ Item 47 + Item 48, $130 \times \text{Item 9} / (\text{Item 47} + \text{Item 48})$ If Item 9 $>$ Item 47 + Item 48, $130 \times \text{Item 9} - \text{Item 47} - \text{Item 48}$
50	Long Term Fading Parameter for Climatic Region n, $\gamma_n(40, d_e)$	--	dB	See Figure 4-8
51	Long Term Fading Parameter for Climatic Region n, $\gamma_n(99.9, d_e)$	--	dB	See Figures 4-9 through 4-23

RPT PAGE NO.

PAGE 2 OF 8 PAGES

Figure A4. Case 4 Troposcatter Path Calculation  
(Sheet 2 of 2)

DATA SHEET		SITE NO. 1 (TX)		DATE
B-5: TROPOSCATTER PATH CALCULATIONS		SITE NO. 2 (RX)		LINE NO.
ITEM NO.	PERFORMANCE FACTOR	VALUE	UNITS	REMARKS
1	Terminal Elevation Above Sea Level, TX, $h_{Tg}$	0	km	From Path Profile
2	Terminal Elevation Above Sea Level, RX, $h_{Rg}$	0	km	From Path Profile
3	Antenna Elevation Above Sea Level, TX, $h_{Tg}$	.005	km	From Path Profile
4	Antenna Elevation Above Sea Level, RX, $h_{Rg}$	.005	km	From Path Profile
5	Radio Horizon Elevation Above Sea Level, TX, $h_{L1}$	0	km	From Path Profile
6	Radio Horizon Elevation Above Sea Level, RX, $h_{L2}$	0	km	From Path Profile
7	Distance to Radio Horizon, TX, $d_{L1}$	8.7	km	From Path Profile
8	Distance to Radio Horizon, RX, $d_{L2}$	8.7	km	From Path Profile
9	Path Length, $d$	60	km	From Path Profile
10	Average Elevation of Radio Horizons, $h_{s1}$	0	km	(Item 5 + Item 6)/2
11	Average Elevation of Terminals, $h_{s2}$	0	km	(Item 1 + Item 2)/2
12	Average Elevation of Refracting Surface, $h_s$	0	km	Minimum (Item 10, Item 11)
13	Mean Refractivity, $N_0$	--		See Figure 4-1
14	Refractivity at Refracting Surface, $N_s$	290		(Item 13) exp $(-0.107 \times \text{Item 12})$
15	Effective Earth's Radius, $a$	8320	km	See Figure 4-2
16	Mean Elevation, TX Terminal to TX Radio Horizon, $h_{T1}$	0	km	From Path Profile
17	Mean Elevation, RX Terminal to RX Radio Horizon, $h_{R1}$	0	km	From Path Profile
18	Effective Antenna Height, TX, $h_{Te}$	.005	km	If Item 16 > Item 1: Item 3 - Item 1 If Item 16 < Item 1: Item 3 - Item 16
19	Effective Antenna Height, RX, $h_{Re}$	.005	km	If Item 17 > Item 2: Item 4 - Item 2 If Item 17 < Item 2: Item 4 - Item 17
20	Antenna Elevation Angle, TX, $\theta_{et}$	-.001098	rad	$\frac{\text{Item 5} - \text{Item 3}}{\text{Item 7}} = \frac{\text{Item 7}}{2 \times \text{Item 15}}$
21	Antenna Elevation Angle, RX, $\theta_{er}$	-.001098	rad	$\frac{\text{Item 6} - \text{Item 4}}{\text{Item 8}} = \frac{\text{Item 8}}{2 \times \text{Item 15}}$
22	$\alpha_0$	+.002508	rad	$\frac{\text{Item 9}}{2 \times \text{Item 15}} + \text{Item 20} + \frac{\text{Item 3} - \text{Item 4}}{\text{Item 9}}$
23	$\beta_0$	+.002508	rad	$\frac{\text{Item 9}}{2 \times \text{Item 15}} + \text{Item 21} + \frac{\text{Item 4} - \text{Item 3}}{\text{Item 9}}$
24	Scatter Angle, $\theta_0$	+.005016	rad	Item 22 + Item 23
25	Path Asymmetry Parameter, $a$	1		Item 22/Item 23
26	$\theta_d$	--	km	Item 24 $\times$ Item 9

AFCS FORM 709 REVISED

RPT PAGE NO.

PAGE 1 OF 3 PAGES

Figure A5. Case 5 Troposcatter Path Calculation  
(Sheet 1 of 2)

ITEM NO.	PERFORMANCE FACTOR	VALUE	UNITS	REMARKS
*27	Attenuation Function, $F(\theta d)$	--	dB	$\theta d \leq 10$ , See Figure 5-3 $\theta d > 10$ , See Figures 5-2 thru 5-5 If $s > 1$ , use $1/s$
28	Operating Frequency, $f$	5.0	GHz	Link Specifications
*29	$r_1$	9.87		$6.3808 \times \text{Item 9} \times \text{Item 28} \times \text{Item 18}$
*30	$r_2$	9.87		$6.3808 \times \text{Item 9} \times \text{Item 28} \times \text{Item 19}$
31	$h_0$ NOTE: If $r_1$ and $r_2 > 15$ , set $h_0 = 0$	.07524	km	$\frac{(\text{Item 25}) \times (\text{Item 9})(\text{Item 24})}{(1 + \text{Item 25})^2}$
32	Normalized Height of Horizon Ray Crossover, $n_0$	.0356		See Figure 5-6
33	NOTE: If $n_0 \geq 1$ , Use Items 34 - 37 Otherwise go to Step 38	--		$\frac{\text{Item 30}}{(\text{Item 29}) \times (\text{Item 25})}$
34	$H_0(r_1)$	--	dB	See Figure 5-7 If $n_0 > 5$ , use 5
35	$H_0(r_2)$	--	dB	See Figure 5-7 If $n_0 > 5$ , use 5
36	$\Delta H_0$	--	dB	See Figure 5-8
37	Frequency Gain Function, $H_0$ NOTE: If $n_0 < 1$ , use Items 38 - 42	--	dB	$1/2 \times (\text{Item 34} + \text{Item 35}) + \text{Item 36}$
38	$H_0(r_1)$	1.10	dB	See Figure 5-7. Use $n_0 = 1$
39	$H_0(r_2)$	1.10	dB	See Figure 5-7. Use $n_0 = 1$
40	$\Delta H_0$	0	dB	See Figure 5-8. Use $n_0 = 1$
41	Frequency Gain Function, $H_0$ , $n_0 = 1$	1.10	dB	$1/2 \times (\text{Item 38} + \text{Item 39}) + \text{Item 40}$
42	Frequency Gain Function, $H_0$ , $n_0 = 0$	1.00	dB	See Figure 5-9. Use $n_0 = 0$
43	Frequency Gain Function, $H_0$	1.00	dB	$\text{Item 42} + \text{Item 32} (1.00 - \text{Item 41})$
44	Frequency Gain Function, $H_0$	1.00	dB	Item 37 or Item 43
45	Atmospheric Absorption, $A_a$	--	dB	See Figure 4-7
46	Basic Transmission Loss for a Scatter Path, $L_{bst}$	--	dB	$30 \log (\text{Item 28}) - 20 \log (\text{Item 9}) + \text{Item 27} + \text{Item 44} + \text{Item 45} + 90$
47	$d_{s1}$	17.64	km	$65(0.1/\text{Item 28})^{1/3}$
*48	$d_L$	18.45	km	$130.34(\sqrt{\text{Item 18}} + \sqrt{\text{Item 19}})$
49	Effective Distance, $d_e$	155	km	If $\text{Item 9} \leq \text{Item 47} + \text{Item 48}$ , $130 \times \text{Item 9}/(\text{Item 47} + \text{Item 48})$ If $\text{Item 9} > \text{Item 47} + \text{Item 48}$ , $130 + \text{Item 9} - \text{Item 47} - \text{Item 48}$
50	Long Term Fading Parameter for Climatic Region n, $V_n(50, d_e)$	--	dB	See Figure 4-8
51	Long Term Fading Parameter for Climatic Region n, $Y_n(99.9, d_e)$	--	dB	See Figures 4-9 through 4-25

RPT PAGE NO.

PAGE 2 OF 8 PAGES

Figure A5. Case 5 Troposcatter Path Calculation  
(Sheet 2 of 2)

DATA SHEET		SITE NO. 1 (Tx)		DATE
B-5: TROPOSCATTER PATH CALCULATIONS		SITE NO. 2 (Rx)		LINE NO
ITEM NO.	PERFORMANCE FACTOR	VALUE	UNITS	REMARKS
1	Terminal Elevation Above Sea Level, TX, $h_{1g}$	0	km	From Path Profile
2	Terminal Elevation Above Sea Level, RX, $h_{2g}$	0	km	From Path Profile
3	Antenna Elevation Above Sea Level, TX, $h_{1s}$	.005	km	From Path Profile
4	Antenna Elevation Above Sea Level, RX, $h_{2s}$	.005	km	From Path Profile
5	Radio Horizon Elevation Above Sea Level, TX, $h_{1L}$	0	km	From Path Profile
6	Radio Horizon Elevation Above Sea Level, RX, $h_{2L}$	0	km	From Path Profile
7	Distance to Radio Horizon, TX, $d_{1L}$	9.9	km	From Path Profile
8	Distance to Radio Horizon, RX, $d_{2L}$	9.9	km	From Path Profile
9	Path Length, $d$	60	km	From Path Profile
10	Average Elevation of Radio Horizons, $h_{a1}$	0	km	(Item 5 + Item 6)/2
11	Average Elevation of Terminals, $h_{a2}$	0	km	(Item 1 + Item 2)/2
12	Average Elevation of Refracting Surface, $h_s$	0	km	Minimum (Item 10, Item 11)
13	Mean Refractivity, $N_0$	--		See Figure 4-1
14	Refractivity at Refracting Surface, $N_s$	390		(Item 13) exp $(-0.10 \cdot 7 \times \text{Item 12})$
15	Effective Earth's Radius, $a$	10,820	km	See Figure 4-2
16	Mean Elevation, TX Terminal to TX Radio Horizon, $h_r$	0	km	From Path Profile
17	Mean Elevation, RX Terminal to RX Radio Horizon, $h_r$	0	km	From Path Profile
18	Effective Antenna Height, TX, $h_{1e}$	.005	km	If Item 16 > Item 1, Item 3 - Item 1 If Item 16 < Item 1, Item 3 - Item 16
19	Effective Antenna Height, RX, $h_{2e}$	.005	km	If Item 17 > Item 2, Item 4 - Item 2 If Item 17 < Item 2, Item 4 - Item 17
20	Antenna Elevation Angle, TX, $\theta_{et}$	-.000963	rad	$\frac{\text{Item 5} - \text{Item 3}}{\text{Item 7}} = \frac{\text{Item 7}}{2 \times \text{Item 15}}$
21	Antenna Elevation Angle, RX, $\theta_{er}$	-.000963	rad	$\frac{\text{Item 6} - \text{Item 4}}{\text{Item 8}} = \frac{\text{Item 8}}{2 \times \text{Item 15}}$
22	$\alpha_0$	+.001810	rad	$\frac{\text{Item 6}}{2 \times \text{Item 15}} + \text{Item 20} = \frac{\text{Item 3} - \text{Item 4}}{\text{Item 9}}$
23	$\beta_0$	+.001810	rad	$\frac{\text{Item 6}}{2 \times \text{Item 15}} + \text{Item 21} = \frac{\text{Item 4} - \text{Item 3}}{\text{Item 9}}$
24	Scatter Angle, $\theta_0$	-.003619	rad	Item 22 + Item 23
25	Path Asymmetry Parameter, $s$	1		Item 22/Item 23
26	$\theta_0$	--	km	Item 24 x Item 9

AFC5 FORM 709 OCT 74 REVISED

RPT PAGE NO.

PAGE 1 OF 5 PAGES

Figure A6. Case 6 Troposcatter Path Calculation  
(Sheet 1 of 2)

ITEM NO.	PERFORMANCE FACTOR	VALUE	UNITS	REMARKS
*27	Attenuation Function, $F(\theta d)$	--	dB	$\theta d \leq 10$ : See Figure 5-3 $\theta d > 10$ : See Figures 5-2 thru 5-5 If $s > 1$ , use $1/s$
28	Operating Frequency, $f$	5.0	GHz	Link Specifications
*29	$r_1$	9.87		$6.5808 \times \text{Item 9} \times \text{Item 28} \times \text{Item 18}$
*30	$r_2$	9.87		$6.5808 \times \text{Item 9} \times \text{Item 28} \times \text{Item 19}$
31	$h_0$ NOTE: If $r_1$ and $r_2 > 15$ , set $h_0 = 0$	.05428	km	$\frac{(\text{Item 25}) \times (\text{Item 9})(\text{Item 24})}{(1 + \text{Item 25})}$
32	Normalized Height of Horizon Ray Crossover, $n_s$	.0304		See Figure 5-6
33	NOTE: If $n_s \geq 1$ , Use Items 34 - 37 Otherwise go to Step 38	--		$\frac{\text{Item 30}}{(\text{Item 29}) \times (\text{Item 25})}$
34	$H_0(r_1)$	--	dB	See Figure 5-7 If $n_s > 5$ , use 5
35	$H_0(r_2)$	--	dB	See Figure 5-7 If $n_s > 5$ , use 5
36	$\Delta H_0$	--	dB	See Figure 5-8
37	Frequency Gain Function, $H_0$ NOTE: If $n_s < 1$ , use Items 38 - 43	--	dB	$1/2 \times (\text{Item 34} + \text{Item 35}) + \text{Item 36}$
38	$H_0(r_1)$	1.10	dB	See Figure 5-7. Use $n_s = 1$
39	$H_0(r_2)$	1.10	dB	See Figure 5-7. Use $n_s = 1$
40	$\Delta H_0$	0	dB	See Figure 5-8. Use $n_s = 1$
41	Frequency Gain Function, $H_0$ , $n_s = 1$	1.10	dB	$1/2 \times (\text{Item 38} + \text{Item 39}) + \text{Item 40}$
42	Frequency Gain Function, $H_0$ , $n_s = 0$	1.00	dB	See Figure 5-9. Use $n_s = 0$
43	Frequency Gain Function, $H_0$	1.00	dB	$\text{Item 42} + \text{Item 32} (\text{Item 41} - \text{Item 42})$
44	Frequency Gain Function, $H_0$	1.00	dB	Item 37 or Item 43
45	Atmospheric Absorption, $A_a$	--	dB	See Figure 4-7
46	Basic Transmission Loss for a Scatter Path, $L_{bst}$	--	dB	$30 \log (\text{Item 28}) - 10 \log (\text{Item 9}) + \text{Item 27} + \text{Item 44} + \text{Item 45} + 90$
47	$d_{s1}$	17.64	km	$65(0.1/\text{Item 28})^{1/3}$
*48	$d_L$	18.43	km	$130.3d \sqrt{\text{Item 18} + \sqrt{\text{Item 19}}}$
49	Effective Distance, $d_e$	153	km	If $\text{Item 9} \leq \text{Item 47} + \text{Item 48}$ , $130 \times \text{Item 9}/(\text{Item 47} + \text{Item 48})$ If $\text{Item 9} > \text{Item 47} + \text{Item 48}$ , $130 + \text{Item 9} - \text{Item 47} - \text{Item 48}$
50	Long Term Fading Parameter for Climatic Region n, $Y_n(50, d_e)$	--	dB	See Figure 4-8
51	Long Term Fading Parameter for Climatic Region n, $Y_n(99.9, d_e)$	--	dB	See Figures 4-9 through 4-23

RPT PAGE NO.

PAGE 2 OF 8 PAGES

Figure A6. Case 6 Troposcatter Path Calculation  
(Sheet 2 of 2)

DATA SHEET			SITE NO. 1 (TX)		DATE
B-5: TROPOSCATTER PATH CALCULATIONS			SITE NO. 2 (RX)		LINE NO
ITEM NO.	PERFORMANCE FACTOR	VALUE	UNITS	REMARKS	
1	Terminal Elevation Above Sea Level, TX, $h_{1g}$	0	km	From Path Profile	
2	Terminal Elevation Above Sea Level, RX, $h_{2g}$	0	km	From Path Profile	
3	Antenna Elevation Above Sea Level, TX, $h_{1s}$	.005	km	From Path Profile	
4	Antenna Elevation Above Sea Level, RX, $h_{2s}$	.005	km	From Path Profile	
5	Radio Horizon Elevation Above Sea Level, TX, $h_{1r}$	0	km	From Path Profile	
6	Radio Horizon Elevation Above Sea Level, RX, $h_{2r}$	0	km	From Path Profile	
7	Distance to Radio Horizon, TX, $d_{L1}$	8.7	km	From Path Profile	
8	Distance to Radio Horizon, RX, $d_{L2}$	8.7	km	From Path Profile	
9	Path Length, $d$	160	km	From Path Profile	
10	Average Elevation of Radio Horizons, $h_{a1}$	0	km	(Item 5 + Item 6)/2	
11	Average Elevation of Terminals, $h_{a2}$	0	km	(Item 1 + Item 2)/2	
12	Average Elevation of Refracting Surface, $h_s$	0	km	Minimum (Item 10, Item 11)	
13	Mean Refractivity, $N_0$	--		See Figure 4-1	
14	Refractivity at Refracting Surface, $N_s$	.290		(Item 13) exp $(-0.10 \cdot 7 \times \text{Item 12})$	
15	Effective Earth's Radius, $a$	8320	km	See Figure 4-2	
16	Mean Elevation, TX Terminal to TX Radio Horizon, $h_1$	0	km	From Path Profile	
17	Mean Elevation, RX Terminal to RX Radio Horizon, $h_2$	0	km	From Path Profile	
18	Effective Antenna Height, TX, $h_{1e}$	.005	km	If Item 16 > Item 1, Item 3 - Item 1 If Item 16 < Item 1, Item 3 - Item 16	
19	Effective Antenna Height, RX, $h_{2e}$	.005	km	If Item 17 > Item 2, Item 4 - Item 2 If Item 17 < Item 2, Item 4 - Item 17	
20	Antenna Elevation Angle, TX, $\theta_{et}$	-.001098	rad	$\frac{\text{Item 5} - \text{Item 3}}{\text{Item 7}} = \frac{\text{Item 7}}{2 \times \text{Item 15}}$	
21	Antenna Elevation Angle, RX, $\theta_{er}$	-.001098	rad	$\frac{\text{Item 6} - \text{Item 4}}{\text{Item 8}} = \frac{\text{Item 8}}{2 \times \text{Item 15}}$	
22	$\alpha_0$	+.008517	rad	$\frac{\text{Item 6}}{2 \times \text{Item 15}} + \text{Item 20} + \frac{\text{Item 3} - \text{Item 4}}{\text{Item 9}}$	
23	$\beta_0$	+.008517	rad	$\frac{\text{Item 5}}{2 \times \text{Item 15}} + \text{Item 21} + \frac{\text{Item 4} - \text{Item 3}}{\text{Item 9}}$	
24	Scatter Angle, $\theta_0$	+.017035	rad	Item 22 + Item 23	
25	Path Asymmetry Parameter, $a$	1		Item 22/Item 23	
26	$\theta_d$	--	km	Item 24 $\times$ Item 9	

AFCS FORM 709 revised OCT 74

RPT PAGE NO.

PAGE 1 OF 5 PAGES

Figure A7. Case 7 Troposcatter Path Calculation  
(Sheet 1 of 2)



ITEM NO.	PERFORMANCE FACTOR	VALUE	UNITS	REMARKS
*27	Attenuation Function, $F(\theta d)$	--	dB	$\theta d \leq 10$ , See Figure 5-3 $\theta d > 10$ , See Figures 5-2 thru 5-3 If $s > 1$ , use $1/s$
28	Operating Frequency, $f$	5.0	GHz	Link Specifications
*29	$r_1$	26.32		$6.3008 \times \text{Item 9} \times \text{Item 28} \times \text{Item 18}$
*30	$r_2$	26.32		$6.3008 \times \text{Item 9} \times \text{Item 28} \times \text{Item 19}$
31	$h_0$ NOTE: If $r_1$ and $r_2 > 15$ , set $h_0 = 0$	--	km	$\frac{(\text{Item 25}) \times (\text{Item 9})(\text{Item 24})}{(1 + \text{Item 25})^2}$
32	Normalized Height of Horizon Ray Crossover, $n_s$	--		See Figure 5-6
33	$n$ NOTE: If $n_s \geq 1$ , Use Items 34 - 37 Otherwise go to Step 38	--		$\frac{\text{Item 30}}{(\text{Item 29}) \times (\text{Item 25})}$
34	$H_0(r_1)$	--	dB	See Figure 5-7 If $n_s > 5$ , use 5
35	$H_0(r_2)$	--	dB	See Figure 5-7 If $n_s > 5$ , use 5
36	$\Delta H_0$	--	dB	See Figure 5-8
37	Frequency Gain Function, $H_0$ NOTE: If $n_s < 1$ , use Items 38 - 43	--	dB	$1/2 \times (\text{Item 34} + \text{Item 35}) + \text{Item 36}$
38	$H_0(r_1)$	--	dB	See Figure 5-7. Use $n_s = 1$
39	$H_0(r_2)$	--	dB	See Figure 5-7. Use $n_s = 1$
40	$\Delta H_0$	--	dB	See Figure 5-8 Use $n_s = 1$
41	Frequency Gain Function, $H_0$ , $n_s \geq 1$	--	dB	$1/2 \times (\text{Item 38} + \text{Item 39}) + \text{Item 40}$
42	Frequency Gain Function, $H_0$ , $n_s \geq 0$	--	dB	See Figure 5-9 Use $n_s = 0$
43	Frequency Gain Function, $H_0$	--	dB	Item 42 + Item 32 (Item 41 - Item 42)
44	Frequency Gain Function, $H_0$	0	dB	Item 37 or Item 43
45	Atmospheric Absorption, $A_0$	--	dB	See Figure 4-7
46	Basic Transmission Loss for a Scatter Path, $L_{bst}$	--	dB	$30 \log (\text{Item 28}) - 10 \log (\text{Item 9}) + \text{Item 27} + \text{Item 44} + \text{Item 45} + 90$
47	$d_{s1}$	17.64	km	$65(0.1/\text{Item 28})^{1/3}$
*48	$d_L$	18.45	km	$130.24 \sqrt{\text{Item 18} \times \sqrt{\text{Item 19}}}$
49	Effective Distance, $d_0$	253	km	If Item 9 $\leq$ Item 47 + Item 48, $130 \times \text{Item 9}/(\text{Item 47} + \text{Item 48})$ If Item 9 $>$ Item 47 + Item 48, $130 + \text{Item 9} - \text{Item 47} - \text{Item 48}$
50	Long Term Fading Parameter for Climatic Region n, $V_n(50, d_0)$	--	dB	See Figure 4-8
51	Long Term Fading Parameter for Climatic Region n, $V_n(99.9, d_0)$	--	dB	See Figures 4-9 through 4-25

RPT PAGE NO.

PAGE 2 OF 6 PAGES

Figure A7. Case 7 Troposcatter Path Calculation  
(Sheet 2 of 2)

DATA SHEET				SITE NO. 1 (Tx)		DATE	
B-5: TROPOSCATTER PATH CALCULATIONS				SITE NO. 2 (Rx)		LINE NO.	
ITEM NO.	PERFORMANCE FACTOR	VALUE	UNITS	REMARKS			
1	Terminal Elevation Above Sea Level, TX, $h_{t1}$	0	km	From Path Profile			
2	Terminal Elevation Above Sea Level, RX, $h_{r2}$	0	km	From Path Profile			
3	Antenna Elevation Above Sea Level, TX, $h_{t1}$	.005	km	From Path Profile			
4	Antenna Elevation Above Sea Level, RX, $h_{r2}$	.005	km	From Path Profile			
5	Radio Horizon Elevation Above Sea Level, TX, $h_{L1}$	0	km	From Path Profile			
6	Radio Horizon Elevation Above Sea Level, RX, $h_{L2}$	0	km	From Path Profile			
7	Distance to Radio Horizon, TX, $d_{L1}$	9.9	km	From Path Profile			
8	Distance to Radio Horizon, RX, $d_{L2}$	9.9	km	From Path Profile			
9	Path Length, $d$	160	km	From Path Profile			
10	Average Elevation of Radio Horizons, $h_{s1}$	0	km	(Item 5 + Item 6)/2			
11	Average Elevation of Terminals, $h_{s2}$	0	km	(Item 1 + Item 2)/2			
12	Average Elevation of Refracting Surface, $h_s$	0	km	Minimum (Item 10, Item 11)			
13	Mean Refractivity, $N_0$	--		See Figure 4-1			
14	Refractivity at Refracting Surface, $N_s$	390		(Item 13) exp $(-0.10 \cdot 7 \times \text{Item 12})$			
15	Effective Earth's Radius, $a$	10,820	km	See Figure 4-2			
16	Mean Elevation, TX Terminal to TX Radio Horizon, $\bar{h}_1$	0	km	From Path Profile			
17	Mean Elevation, RX Terminal to RX Radio Horizon, $\bar{h}_2$	0	km	From Path Profile			
18	Effective Antenna Height, TX, $h_{te}$	.005	km	If Item 16 > Item 1, Item 3 - Item 1 If Item 16 < Item 1, Item 3 - Item 16			
19	Effective Antenna Height, RX, $h_{re}$	.005	km	If Item 17 > Item 2, Item 4 - Item 2 If Item 17 < Item 2, Item 4 - Item 17			
20	Antenna Elevation Angle, TX, $\theta_{e1}$	-.000963	rad	$\frac{\text{Item 5} - \text{Item 3}}{\text{Item 7}} = \frac{\text{Item 7}}{2 \times \text{Item 15}}$			
21	Antenna Elevation Angle, RX, $\theta_{e2}$	-.000963	rad	$\frac{\text{Item 6} - \text{Item 4}}{\text{Item 8}} = \frac{\text{Item 8}}{2 \times \text{Item 15}}$			
22	$\alpha_0$	+.006431	rad	$\frac{\text{Item 6}}{2 \times \text{Item 15}} + \text{Item 20} + \frac{\text{Item 3} - \text{Item 4}}{\text{Item 9}}$			
23	$\beta_0$	+.006431	rad	$\frac{\text{Item 9}}{2 \times \text{Item 15}} + \text{Item 21} + \frac{\text{Item 4} - \text{Item 3}}{\text{Item 9}}$			
24	Scatter Angle, $\theta_0$	+.012861	rad	Item 22 + Item 23			
25	Path Asymmetry Parameter, $s$	1		Item 22/Item 23			
26	$\theta_d$	--	km	Item 24 $\times$ Item 9			

AFCS FORM 709 revised OCT 74 RPT PAGE NO. PAGE 1 OF 5 PAGES

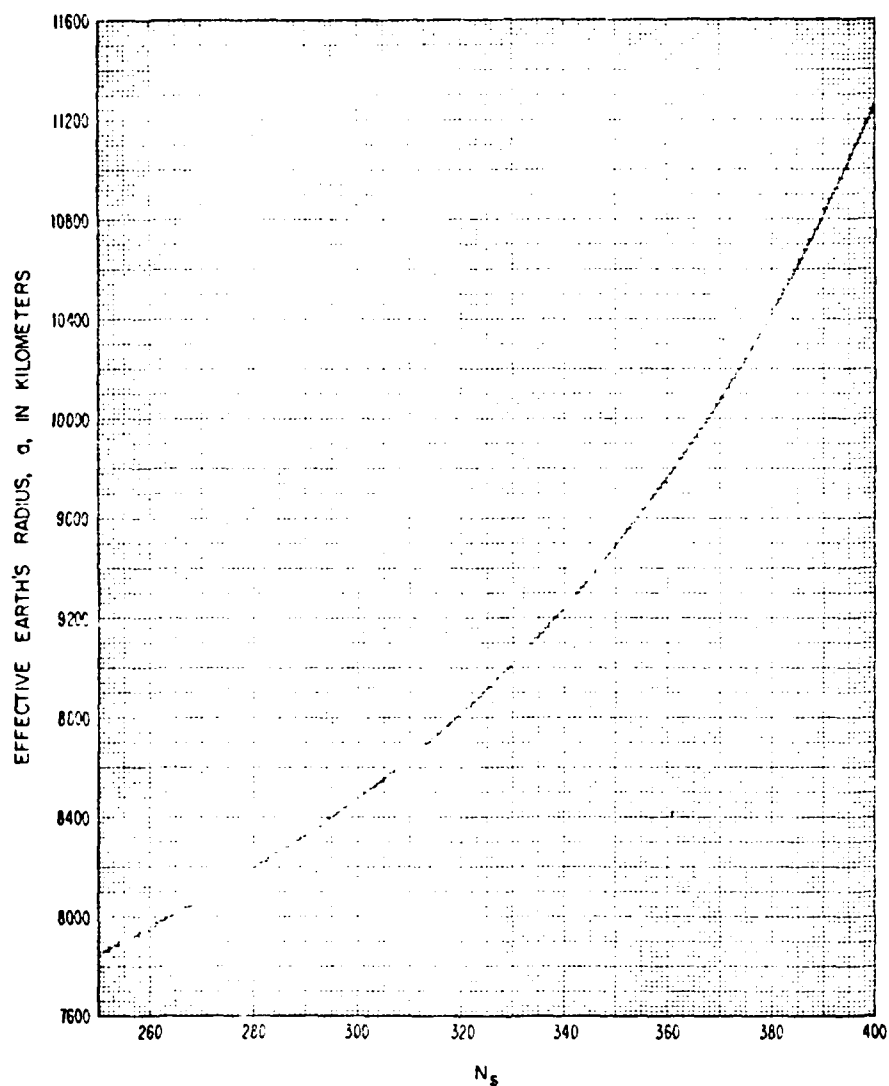
Figure A8. Case 8 Troposcatter Path Calculation  
(Sheet 1 of 2)

ITEM NO.	PERFORMANCE FACTOR	VALUE	UNITS	REMARKS
*27	Attenuation Function, $F(\theta d)$	--	dB	$\theta d \leq 10$ , See Figure 5-3 $\theta d > 10$ , See Figures 5-3 thru 5-5 If $s > 1$ , use $1/s$
28	Operating Frequency, $f$	5.0	GHz	Link Specifications
*29	$r_1$	26.32		$6.808 \times \text{Item 9} \times \text{Item 28} \times \text{Item 16}$
*30	$r_2$	26.32		$6.808 \times \text{Item 9} \times \text{Item 28} \times \text{Item 16}$
31	$h_0$ NOTE: If $r_1$ and $r_2 > 15$ , set $h_0 = 0$	--	km	$\frac{(\text{Item 25}) \times (\text{Item 9})(\text{Item 24})}{(1 + \text{Item 25})^2}$
32	Normalized Height of Horizon Ray Crossover, $n_s$	--		See Figure 5-6
33	NOTE: If $n_s \geq 1$ , Use Items 34 - 37 Otherwise go to Step 38	--		$\frac{\text{Item 30}}{(\text{Item 29}) \times (\text{Item 25})}$
34	$H_0(r_1)$	--	dB	See Figure 5-7 If $n_s > 5$ , use 5
35	$H_0(r_2)$	--	dB	See Figure 5-7 If $n_s > 5$ , use 5
36	$\Delta H_0$	--	dB	See Figure 5-8
37	Frequency Gain Function, $H_0$ NOTE: If $n_s < 1$ , use Items 38 - 43	--	dB	$1/2 \times (\text{Item 34} + \text{Item 35}) + \text{Item 36}$
38	$H_0(r_1)$	--	dB	See Figure 5-7. Use $n_s = 1$
39	$H_0(r_2)$	--	dB	See Figure 5-7. Use $n_s = 1$
40	$\Delta H_0$	--	dB	See Figure 5-8. Use $n_s = 1$
41	Frequency Gain Function, $H_0$ , $n_s = 1$	--	dB	$1/2 \times (\text{Item 38} + \text{Item 39}) + \text{Item 40}$
42	Frequency Gain Function, $H_0$ , $n_s = 0$	--	dB	See Figure 5-9. Use $n_s = 0$
43	Frequency Gain Function, $H_0$	--	dB	Item 42 + Item 32 (Item 41 - Item 42)
44	Frequency Gain Function, $H_0$	0	dB	Item 37 or Item 43
45	Atmospheric Absorption, $A_a$	--	dB	See Figure 4-7
46	Basic Transmission Loss for a Scatter Path, $L_{bpr}$	--	dB	$30 \log (\text{Item 28}) - 20 \log (\text{Item 9}) + \text{Item 27} + \text{Item 44} + \text{Item 45} + 90$
47	$d_{s1}$	17.64	km	$65(0.1/\text{Item 28})^{1/3}$
*48	$d_L$	18.43	km	$130.34(\sqrt{\text{Item 18}} + \sqrt{\text{Item 19}})$
49	Effective Distance, $d_e$	253	km	If Item 9 $\leq$ Item 47 + Item 48, $130 \times \text{Item 9}/(\text{Item 47} + \text{Item 48})$ If Item 9 $>$ Item 47 + Item 48, $130 + \text{Item 9} - \text{Item 47} - \text{Item 48}$
*50	Long Term Fading Parameter for Climatic Region n, $V_n(50, d_e)$	--	dB	See Figure 4-8
51	Long Term Fading Parameter for Climatic Region n, $V_n(99.9, d_e)$	--	dB	See Figures 4-9 through 4-25

RPT PAGE NO.

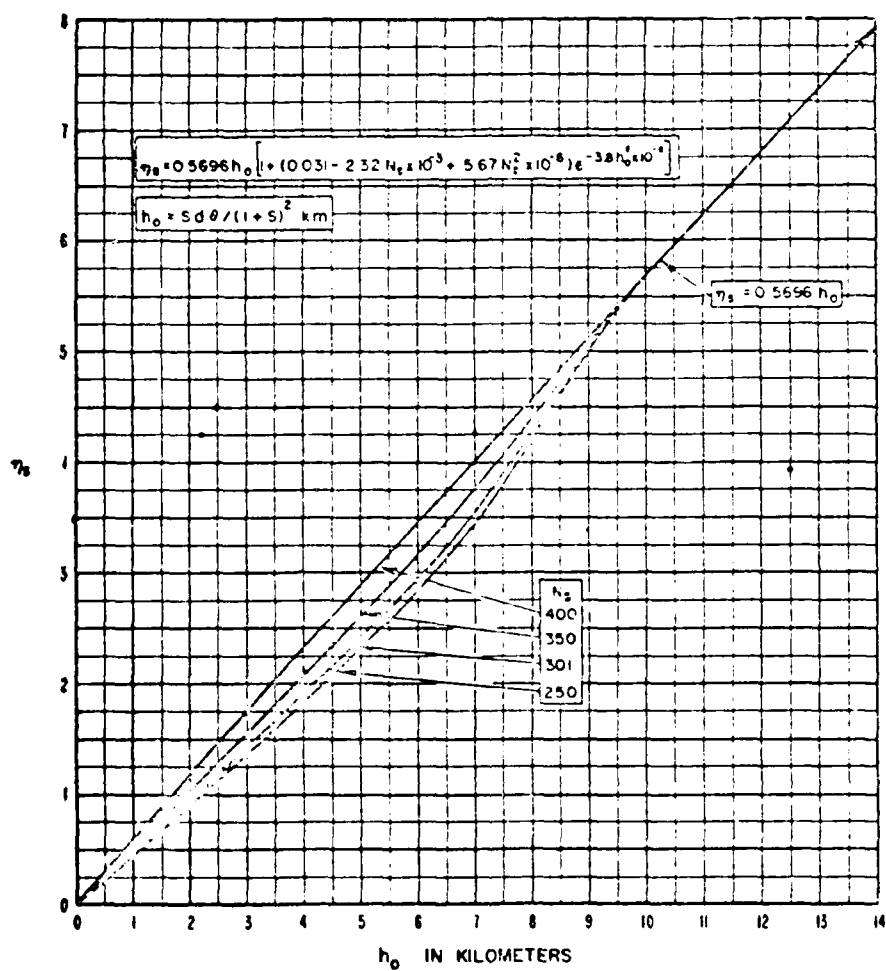
PAGE 2 OF 8 PAGES

Figure A8. Case 8 Troposcatter Path Calculation  
(Sheet 2 of 2)



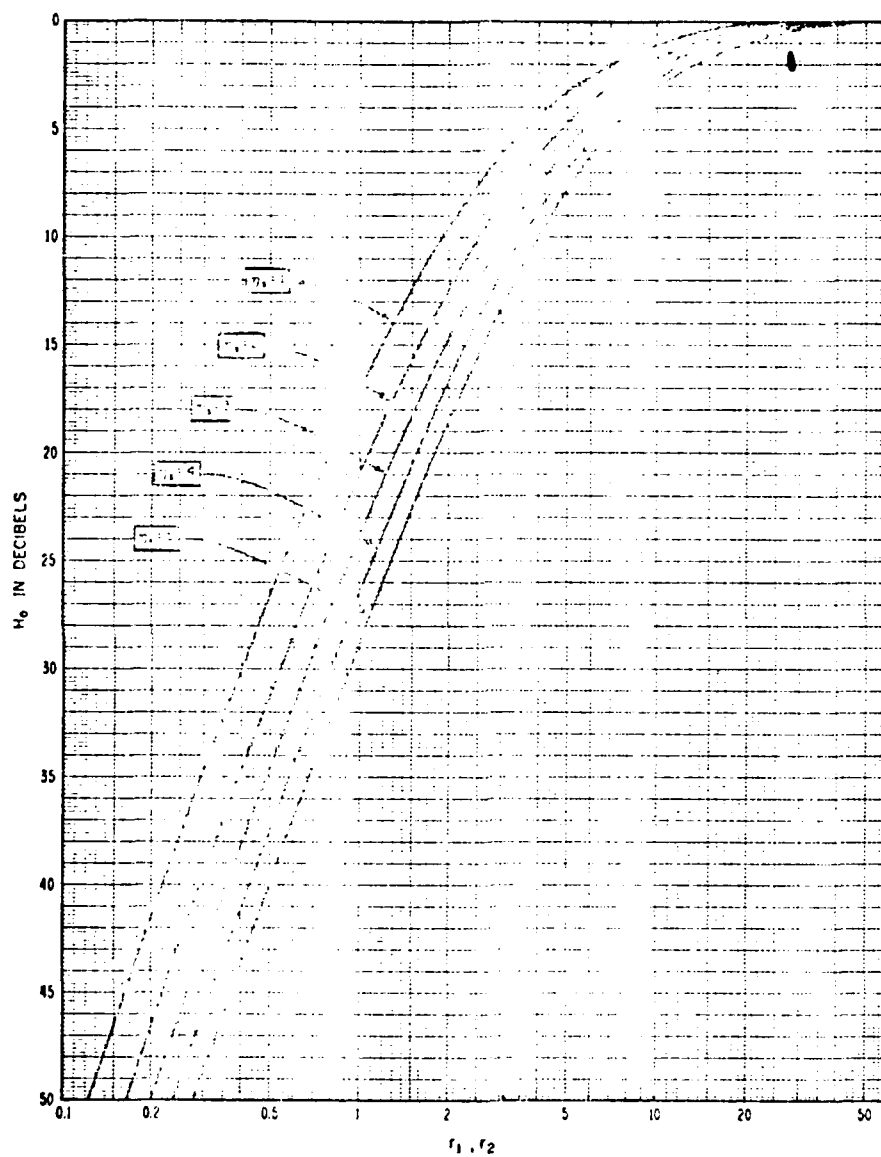
Effective Earth's Radius,  $a$ , Versus Surface Refractivity,  $N_s$

Figure A9. Effective Earth's Radius,  $a$   
(Ref 1: Figure 4-2)



The Parameter  $\eta_s(h_0)$ , Used to Compute  $H_0(r_1, r_2, S, \eta_s)$

Figure A10. Normalized Height of Horizon Ray Crossover,  $\eta_s$  (Ref 1: Figure 5-6)



The Frequency Gain Function,  $H_0$

Figure A11. Frequency Gain Function,  $H_0$ , for  $n_s \geq 1$   
(Ref 1: Figure 5-7)

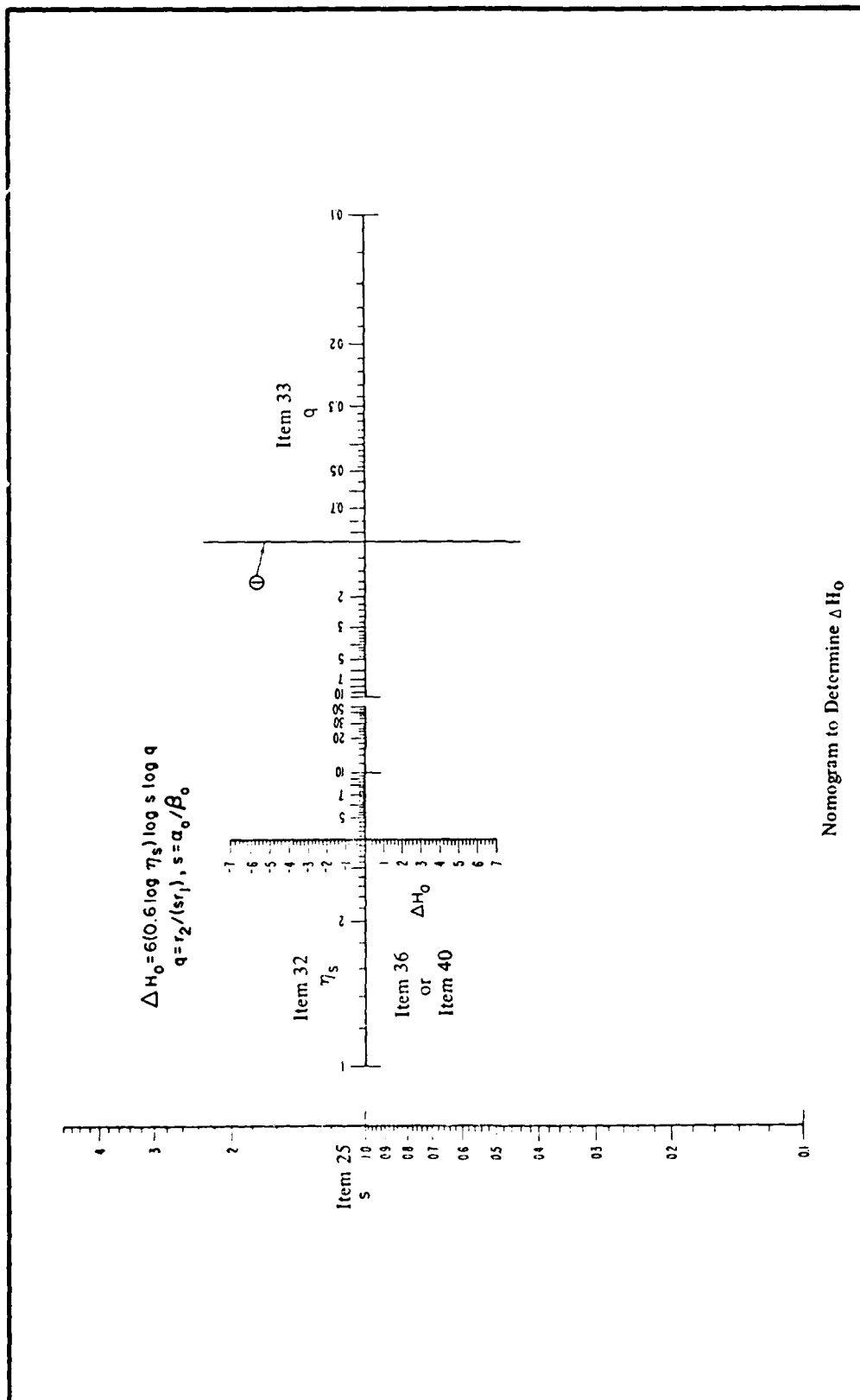


Figure A12. Frequency Gain Assymetry Function,  $\Delta H_0$  (Ref 1: Figure 5-8)

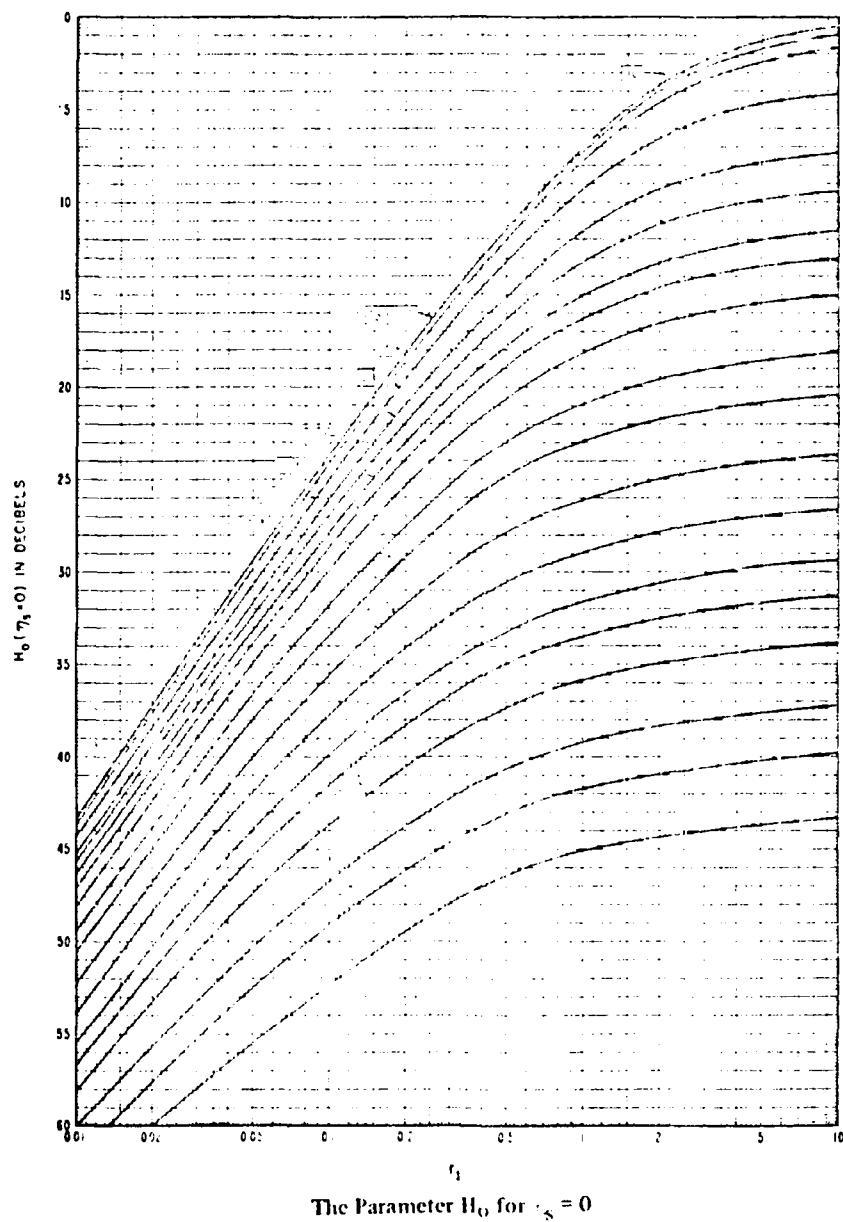
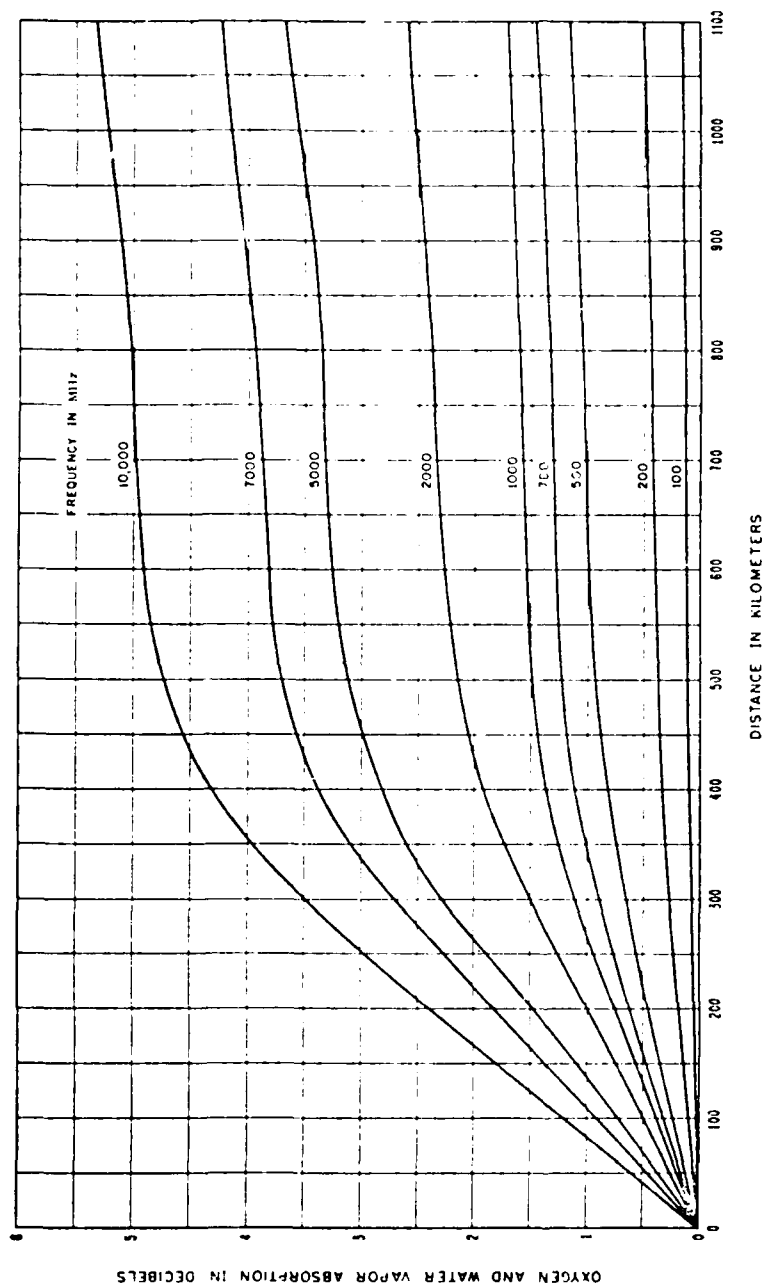


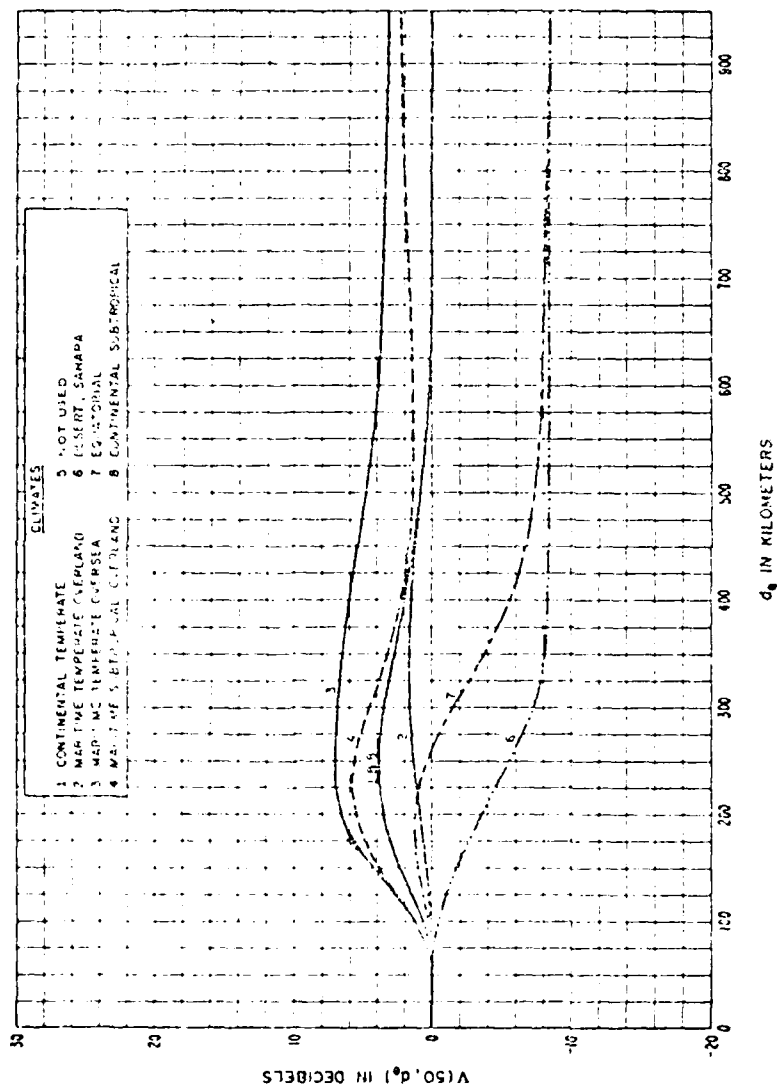
Figure A13. Frequency Gain Function,  $H_0$ , for  $\eta_s = 0$   
(Ref 1: Figure 5-9)





Estimate of Median Oxygen and Water Vapor Absorption from August Data, Washington, D.C.

Figure A14. Atmospheric Absorption,  $A_a$  (Ref 1: Figure 4-7)



The Function  $V(50, d_e)$  for 8 Climatic Regions  $L(50) = L_{cr} - V(50, d_e)$  db

Figure A15. The Climatological Function,  $V(d_e)$  (Ref 1: Figure 4-8)

VITA

----

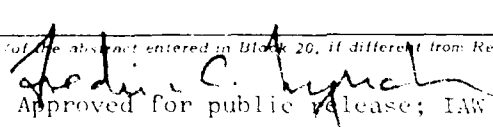
H. Stephen Story was born in Denver, Colorado on 17 January 1948. The son of an Air Force officer, he grew up in many different places, graduating from high school in Wheatland, California in 1965. In June 1970 he received the degree of Bachelor of Science in Electrical Engineering from Virginia Polytechnic Institute and an Air Force commission via ROTC. Entering active duty in July 1970, his military assignments have included the 727th Tactical Control Squadron, Bergstrom AFB, Texas; 1st Combat Communications Squadron, Lindsey AS, Germany; and the Tactical Air Forces Interoperability Group, Langley AFB, Virginia. In June 1979 he was assigned to the Air Force Institute of Technology to pursue a masters degree in electrical engineering.

Permanent Address:

3434 South Akron Street  
Denver, Colorado 80231

UNCLASSIFIED

SECURITY CLASSIFICATION OF THIS PAGE (When Data Entered)

REPORT DOCUMENTATION PAGE		READ INSTRUCTIONS BEFORE COMPLETING FORM
1. REPORT NUMBER	2. GOVT ACCESSION NO.	3. RECIPIENT'S CATALOG NUMBER
AFIT GE EE 80D-40	AD-A166 826	
4. TITLE (and Subtitle)	5. TYPE OF REPORT & PERIOD COVERED	
TRANSMISSION LOSS PREDICTION FOR THE AN/TRC-97A OVER A TROPOSPHERIC SCATTER PATH	MS Thesis	
	6. PERFORMING ORG. REPORT NUMBER	
7. AUTHOR(s)	8. CONTRACT OR GRANT NUMBER(s)	
H. Stephen Story Captain USAF		
9. PERFORMING ORGANIZATION NAME AND ADDRESS	10. PROGRAM ELEMENT, PROJECT, TASK AREA & WORK UNIT NUMBERS	
Air Force Institute of Technology (AFIT/EN) Wright-Patterson AFB, Ohio 45433		
11. CONTROLLING OFFICE NAME AND ADDRESS	12. REPORT DATE	
	12 December 1980	
	13. NUMBER OF PAGES	
	120	
14. MONITORING AGENCY NAME & ADDRESS (if different from Controlling Office)	15. SECURITY CLASS. of this report.	
	Unclassified	
	15a. DECLASSIFICATION/DOWNGRADING SCHEDULE	
16. DISTRIBUTION STATEMENT (of this Report)		
Approved for public release; distribution unlimited.		
17. DISTRIBUTION STATEMENT (of the abstract entered in Block 20, if different from Report)		
 Approved for public release; IAW AFR 190-17 Frederick C. Lynch, Major, USAF Director of Public Affairs		
18. SUPPLEMENTARY NOTES		
19. KEY WORDS (Continue on reverse side if necessary and identify by block number)		
Tropospheric scatter communications		
20. ABSTRACT (Continue on reverse side if necessary and identify by block number)		
This research investigates transmission loss predictions for a short range tactical troposcatter radio system. The analysis is based on the AN/TRC-97A radio set, but the conclusions reached should apply to similar troposcatter systems operating at frequencies from 4.4 to 5.0 GHz and over distances of 160 km or less. A general analysis of the troposcatter path is performed to determine the sensitivity of the transmission loss to the various phenomena which contribute to the loss. That component of the loss which is unique to the		

DD FORM 1 JAN 73 1473

EDITION OF 1 NOV 65 IS OBSOLETE

UNCLASSIFIED

SECURITY CLASSIFICATION OF THIS PAGE (When Data Entered)

UNCLASSIFIED

SECURITY CLASSIFICATION OF THIS PAGE When Data Entered:

Block 20:

scattering process is studied in further detail and a modified scattering loss model is developed. A procedure for determining the coefficients of the scattering loss model based on observed transmission loss is described. A preliminary analysis of the path data available for this research is performed. It is found that the received power probability distribution for the observed paths does not agree with the theoretical distribution in all cases. Further, the available path data is seen to lack sufficiently detailed path geometry information to complete the analysis of the scattering loss model. Recommendations concerning data requirements and continued research are offered.

UNCLASSIFIED

SECURITY CLASSIFICATION OF THIS PAGE When Data Entered:

DATE  
FILMED  
-18-